


 Cite this: *Lab Chip*, 2026, 26, 3282

## Point-of-care SERS platforms: integrating microfluidics and machine learning for disease screening

 Biqing Chen, <sup>a</sup> Xiaohong Qiu<sup>\*a</sup> and Yang Li<sup>\*b</sup>

With the continuous advancement of research on life systems and disease mechanisms, analytical technologies are now moving toward the resolution of single molecules and individual genes. Among them, surface-enhanced Raman scattering (SERS) has garnered widespread interest because of its ultrahigh sensitivity, allowing even single-molecule detection. When integrated with microfluidics, SERS-based platforms combine the strengths of both techniques, offering complementary and synergistic effects. This integration enables rapid, non-invasive, ultrasensitive, and high-throughput analysis of biological samples, which is highly valuable for biomedical research and potential clinical applications. Consequently, this interdisciplinary approach has emerged as a major focus of current investigations. In this review, we outline recent developments and applications of microfluidic SERS systems in bioanalysis. The discussion first introduces the basic concepts and classifications of SERS–microfluidic strategies, such as continuous-flow, microarray, droplet-based, lateral flow assay (LFA), and digital formats. We then highlight their applications in biomolecular detection, cellular analysis, and disease diagnostics. Overall, the evidence suggests that microfluidic SERS platforms represent a powerful and promising tool for advancing bioanalytical science.

 Received 3rd March 2026,  
 Accepted 23rd April 2026

DOI: 10.1039/d6lc00202a

[rsc.li/loc](https://rsc.li/loc)

### 1. Introduction: from molecular fingerprinting to point-of-care diagnostics

Life processes are characterized by dynamic fluctuations of biomolecules and their surrounding microenvironments.<sup>1,2</sup> Tracking and analyzing these biomolecules is essential for understanding biological regulation and disease progression, and it forms the foundation for the development of reliable and ultrasensitive diagnostic as well as therapeutic approaches.<sup>3</sup> With ongoing advances in molecular biology, analytical techniques are steadily approaching single-molecule and single-gene resolution,<sup>4</sup> making the pursuit of higher precision in bioanalysis increasingly important. Conventional bioanalytical methods, including fluorescence assays, colorimetry, immunoassays, electrochemiluminescence (ECL), and polymerase chain reaction (PCR), are widely employed for genetic and protein biomarker detection.<sup>5–7</sup> However, these approaches often fall short in spatial resolution, sensitivity,

multiplexing ability, and single-cell or molecule-level analysis. Therefore, more advanced analytical strategies are urgently required.

Raman spectroscopy offers unique molecular fingerprint information and has been extensively applied across biomedical sciences, surface chemistry, molecular recognition, and trace detection.<sup>8–11</sup> The discovery of surface-enhanced Raman scattering (SERS) revolutionized the field by significantly increasing sensitivity and broadening the applicability of Raman spectroscopy, enabling single-cell and single-molecule level detection and addressing major drawbacks of traditional bioanalytical methods.<sup>12,13</sup> The SERS effect was first reported by Fleischmann *et al.* in the 1970s<sup>14</sup> and later independently validated by the groups of Van Duyne and Creighton in 1977.<sup>15,16</sup> These studies revealed that when molecules interact with roughened noble metal surfaces, their Raman signals are strongly amplified.<sup>17</sup> This breakthrough led to unprecedented Raman signal enhancement and the realization of single-molecule spectroscopy.<sup>18</sup> Importantly, SERS retains the inherent merits of Raman spectroscopy, such as fingerprint specificity, narrow spectral features, photostability, and non-contact, non-destructive *in situ* analysis, enabling wide application in biosensing and biomedical research.<sup>19–22</sup>

Two general strategies are commonly applied in SERS analysis: direct (label-free) and indirect detection.<sup>23,24</sup> Direct detection, one of the most distinctive advantages of SERS, identifies biomolecules based on their inherent vibrational

<sup>a</sup> Department of Gynaecology and Obstetrics, The Second Affiliated Hospital of Harbin Medical University, Harbin Medical University, Heilongjiang 150081, PR China. E-mail: qixiaohong@hrbmu.edu.cn

<sup>b</sup> Research Center for Innovative Technology of Pharmaceutical Analysis, College of Pharmacy, Harbin Medical University, Heilongjiang, 150081, China. E-mail: liy@hrbmu.edu.cn

fingerprints, without the need for external labeling.<sup>25</sup> Such spectra provide structural and conformational information of adsorbed biomolecules.<sup>26</sup> This approach has been successfully used for amino acids, proteins, nucleobases, nucleic acids, and cellular metabolites.<sup>27,28</sup> In cases where intrinsic signals are too weak or difficult to observe, indirect detection becomes essential. This strategy employs reporter-tagged SERS probes functionalized with recognition ligands, allowing detection of the target species through strong signals from the reporter.<sup>29</sup> Indirect SERS has been applied to analyze microenvironmental parameters such as pH, ROS, and temperature, as well as membrane proteins and other targets otherwise inaccessible to direct detection.<sup>30–32</sup> Although it sacrifices molecular fingerprint information, it provides high-intensity signals, rapid response, ultralow detection limits, and excellent multiplexing capabilities due to narrow spectral peaks.<sup>33</sup> Consequently, indirect SERS is widely used in protein/DNA analysis, live-cell imaging, cancer diagnostics, and other clinical applications.<sup>34–36</sup>

In recent years, integrating SERS with microfluidics has emerged as a promising strategy to enhance analytical reliability and functionality.<sup>37,38</sup> Microfluidic technology, often termed “lab-on-a-chip” (LoC), enables the miniaturization of sample pretreatment, detection, and data analysis into a single compact device.<sup>39–41</sup> Compared to conventional macroscale instrumentation, microfluidics offers reduced reagent consumption, improved efficiency, precise control, and portability. The incorporation of SERS into microfluidic chips provides several additional benefits: ultralow detection limits inside microchannels,<sup>42</sup> multiplexed detection through multi-channel designs,<sup>43</sup> and improved reproducibility by mitigating SERS signal fluctuations.<sup>44</sup> These fluctuations, typically arising from substrate heterogeneity and inconsistent molecule–substrate interactions,<sup>45</sup> can be effectively minimized by controlled microfluidic conditions. For instance, by tuning nanoparticle flow rates and concentrations within channels, uniform and stable SERS-active substrates can be generated *in situ*.<sup>46</sup> Similarly, well-designed channel geometries and mixing modules regulate reaction times and substrate–analyte ratios, thereby reducing peak variability and enhancing detection stability.<sup>47</sup> Although several recent reviews have addressed microfluidic SERS systems and optofluidic biosensing technologies, most of them primarily focus on device engineering, nanostructure design, or general analytical performance. In contrast, the present review places a stronger emphasis on the translational and clinical potential of microfluidic SERS platforms, particularly in the context of point-of-care testing (POCT). Specifically, this review highlights three distinguishing aspects. First, it systematically discusses how microfluidic SERS systems can be adapted for decentralized and portable diagnostic applications, bridging the gap between laboratory-based technologies and real-world clinical deployment. Second, it provides an in-depth analysis of machine learning-driven spectral interpretation, emphasizing the role of artificial intelligence in improving diagnostic accuracy, robustness, and scalability in complex biological

environments. Third, rather than focusing solely on device fabrication, this work integrates analytical strategies, application scenarios, and clinical validation considerations, offering a more comprehensive framework for understanding how microfluidic SERS can be translated into practical disease screening tools. Therefore, this review is positioned at the intersection of microfluidics, SERS, and intelligent data analysis, with a particular focus on point-of-care diagnostics and real-world biomedical applications.

Recent advances in the broader SERS field further highlight the rapid evolution of this area toward more integrated, intelligent, and application-oriented analytical systems. In particular, emerging substrate engineering strategies based on semiconductor-assisted or hybrid nanostructures have demonstrated new opportunities for improving sensitivity, stability, and interfacial control in SERS detection. For example, recent studies have explored advanced material platforms such as amorphous semiconductor monolayers and noble metal–semiconductor nanohybrids to enhance Raman signal generation through synergistic electromagnetic and charge-transfer effects, thereby expanding the analytical scope of SERS in trace detection and biodiagnostics. At the same time, newly published studies and reviews have increasingly emphasized the convergence of high-performance SERS substrates with intelligent data analysis, biomedical sensing, and translational applications.<sup>45,47,48</sup> These developments indicate that the field is moving beyond isolated proof-of-concept sensing demonstrations toward more robust, reproducible, and clinically relevant analytical systems. Against this background, integrating SERS with microfluidics is particularly attractive, as it provides not only ultrasensitive molecular detection but also controlled sample handling, automation, miniaturization, and compatibility with point-of-care workflows. The fusion of SERS and microfluidics thus creates a synergistic platform that not only expands the capabilities of each technology but also addresses their individual limitations. Although numerous reviews have covered SERS and microfluidics independently, systematic overviews specifically dedicated to SERS-based microfluidic bioanalytical methods remain relatively scarce.<sup>12,48</sup> The present review aims to fill this gap by summarizing the current progress and applications of SERS–microfluidic strategies in bioanalysis. It begins with an introduction to the fundamentals of SERS, microfluidics, and their integration, followed by a classification of existing SERS–microfluidic approaches.

Beyond their simple combination, microfluidics, SERS, and machine learning can be understood as three functionally complementary layers within an integrated analytical framework. In such a framework, microfluidics serves as the physical control layer, enabling precise manipulation of sample transport, mixing, separation, and reaction conditions; SERS functions as the molecular information layer, providing ultrasensitive and information-rich vibrational fingerprints; and machine learning acts as the computational decision layer, transforming complex spectral outputs into robust analytical or diagnostic conclusions. Importantly, the value of integrating

these three technologies lies not merely in assembling them into a single platform, but in the way each component addresses a fundamental limitation of the others. Microfluidics improves the reproducibility, automation, and throughput of SERS measurements by regulating analyte–substrate interactions under controlled conditions. SERS, in turn, provides chemically specific and highly sensitive readouts that are difficult to achieve with conventional microfluidic detection modules alone. Machine learning becomes particularly important because the spectral complexity, high dimensionality, and biological heterogeneity of SERS datasets often exceed the capacity of conventional manual or rule-based interpretation. As such, ML is not only a downstream analytical add-on, but increasingly a transformative component that enables the practical extraction of clinically relevant information from complex microfluidic-SERS workflows. From this perspective, the convergence of microfluidics, SERS, and machine learning should be viewed as the emergence of a closed-loop intelligent bioanalytical system, rather than a simple technological juxtaposition. This systems-level integration is especially relevant for point-of-care diagnostics, where sensitivity, automation, robustness, and decision support must all be achieved simultaneously within compact and deployable formats.

## 2. Microfluidic–SERS chips

Surface-enhanced Raman spectroscopy (SERS) leverages the plasmonic properties of nanostructured metals to amplify Raman scattering signals, greatly enhancing the vibrational modes of molecules adsorbed on or near metallic surfaces.<sup>49</sup> Because of its high sensitivity, ability to deliver molecular fingerprints, label-free detection, and minimal sample consumption, SERS has become an attractive tool in medical diagnostics and biological research.<sup>50–53</sup>

Lab-on-a-chip (LoC) devices integrate fluidic control elements such as inlets, outlets, channels, chambers, and valves into a miniaturized platform.<sup>54</sup> These systems allow rapid and precise handling of microliter- or nanoliter-scale samples, enabling efficient mixing, separation, and detection with reduced reagent use and improved reproducibility. Incorporating SERS substrates into LoC devices, coupled with portable Raman readers, has accelerated the emergence of compact sensing systems capable of detecting trace biomolecules quickly, reproducibly, and with high sensitivity.<sup>54</sup> Depending on substrate type, fluidic configuration (continuous or segmented), and mixing mechanism (active or passive), diverse LoC–SERS systems have been reported.<sup>55,56</sup>

One representative example is the centrifugal microfluidic (CM) device, which uses a compact disc (CD) with pre-patterned channels where centrifugal force drives liquid motion. The combination of CM and SERS referred to as CD–SERS offers improvements in portability, automation, and miniaturization.<sup>57,58</sup> Unlike pump-driven LoC systems, CD–SERS minimizes dead volume, ensures reproducible fluid control, and accommodates small sample sizes ranging from

tens to hundreds of microliters.<sup>47,59</sup> Moreover, CM platforms allow sample handling, pretreatment, and analysis to occur in parallel,<sup>60</sup> greatly streamlining analytical workflows. These designs have already been applied for sensitive detection of small molecules in analytical chemistry.<sup>61,62</sup>

For label-free SERS detection, biological samples often contain proteins and macromolecules that interfere with target signal acquisition. Thus, pretreatment is necessary to reach the required detection limits and improve quantification accuracy.<sup>63,64</sup> Common approaches include protein precipitation (PP), ultrafiltration (UF), liquid–liquid extraction, and solid-phase extraction (SPE).<sup>65</sup> Among them, SPE is widely used because it is rapid, efficient, and semi-selective, allowing the effective isolation of compounds from biological fluids, especially when combined with label-free SERS for simultaneous detection of multiple analytes.<sup>64,66</sup>

### 2.1 Design principles of microfluidic–SERS chips

Coupling microfluidics with SERS provides a powerful framework for optofluidic biosensing.<sup>52</sup> The high surface-to-volume ratio of microchannels accelerates molecular recognition events, such as antigen–antibody binding, thereby increasing response speed. In addition, the continuous flow within microchannels facilitates uniform mixing, efficient heat transfer, and reduced nonspecific adsorption of probes, which collectively improve detection reproducibility.<sup>67</sup> By controlling nanoparticle aggregation, particle size, and analyte distribution, microfluidic–SERS systems achieve higher sensitivity and quantitative precision.<sup>68,69</sup>

Strategies to reduce nonspecific adsorption in microfluidic–SERS chips include:

**Substrate engineering.** Nanostructured SERS substrates can be fabricated or modified *in situ* within microchannels using electrochemical deposition, ion etching, or electron-beam lithography. Surface modifications with passivating or biocompatible layers further reduce background adsorption.

**On-chip pretreatment.** Filtration modules or ligand-based screening units upstream of the detection zone selectively remove impurities, enhancing specificity.

**Flow regulation.** Precise control of sample flow rate and residence time in channels ensures specific interactions between analytes and detection sites, minimizing nonspecific binding.

### 2.2 Advantages of microfluidic–SERS chips

Integrating SERS into microfluidic systems offers multiple benefits:

**Improved sensitivity and specificity.** Optimized channel and substrate designs maximize analyte–substrate interactions, essential for detecting trace targets in clinical and environmental monitoring.

**Automated sample processing.** Pretreatment, mixing, and detection can be seamlessly integrated on-chip, reducing contamination risks and improving reproducibility.

**High-throughput capability.** Multiplexed or parallel designs enable simultaneous analysis of multiple samples, accelerating applications such as drug screening.

**Real-time monitoring.** Continuous sampling within microchannels allows dynamic monitoring of molecular or cellular processes with high temporal resolution.

Recent reports highlight the wide-ranging potential of SERS-based microfluidic devices in biosensing, environmental assays, and clinical diagnostics, including biomarker detection at ultralow concentrations, opening avenues for early disease detection and personalized medicine.

Reproducibility remains one of the most critical challenges limiting the practical application and clinical translation of SERS-based detection systems. Despite the ultrahigh sensitivity of SERS, signal variability often arises from nanoscale heterogeneity, stochastic hotspot distribution, and inconsistent analyte–substrate interactions. These factors can lead to significant spectral fluctuations, thereby reducing quantitative reliability and inter-sample comparability. From a mechanistic perspective, SERS reproducibility is primarily governed by four key factors: (i) hotspot distribution and electromagnetic field uniformity, (ii) nanoparticle size, morphology, and aggregation state, (iii) substrate fabrication consistency, and (iv) signal acquisition and data processing strategies. Addressing these factors requires a combination of materials engineering, microfluidic control, and computational approaches. Hotspot engineering plays a central role in improving reproducibility. The creation of uniformly distributed electromagnetic hotspots, such as through ordered nanostructures, lithographically defined arrays, or self-assembled nanogap architectures, can significantly reduce signal variability. In microfluidic environments, controlled flow conditions further help regulate nanoparticle aggregation and hotspot formation *in situ*, enabling more stable and reproducible SERS signals. Nanoparticle uniformity is another critical determinant. Variations in particle size, shape, and surface chemistry directly affect plasmonic resonance and enhancement factors. Microfluidic synthesis offers a powerful route to produce nanoparticles with narrow size distributions and controlled morphology, thereby improving batch-to-batch consistency compared with conventional bulk synthesis methods. Substrate fabrication control is equally important for ensuring reproducibility across measurements. Advanced fabrication techniques, including electron-beam lithography, nanoimprint lithography, and template-assisted assembly, enable precise control over nanostructure geometry and spacing. In addition, surface modification strategies, such as antifouling coatings or functional ligands, can reduce nonspecific adsorption and improve signal stability in complex biological matrices. In addition to material and device-level strategies, signal normalization and data processing approaches are essential for improving reproducibility at the analytical level. Internal standards, ratiometric SERS probes, and spectral calibration methods are widely used to compensate for signal fluctuations. Furthermore, machine learning-based approaches, including baseline correction, denoising, feature extraction, and

multivariate calibration, can enhance robustness by extracting reproducible spectral patterns from noisy datasets. Overall, achieving high reproducibility in microfluidic–SERS systems requires an integrated strategy that combines rational nanostructure design, precise fluidic control, standardized fabrication processes, and advanced data analysis. Continued progress in these areas will be essential for translating SERS technologies from proof-of-concept demonstrations to reliable clinical diagnostic tools.

### 2.3 Types of microfluidic–SERS chips

Microfluidic–SERS systems can generally be grouped into five categories: continuous-flow, droplet-based, microarray-based, digital, and lateral flow assay (LFA)-based platforms.<sup>70,71</sup>

**2.3.1 Continuous-flow platforms.** Reproducibility is a major obstacle in SERS quantification due to challenges in controlling nanoparticle aggregation and ensuring uniform analyte distribution.<sup>72–74</sup> Continuous-flow microchannels help overcome these issues by promoting efficient mixing of analytes with metal nanoparticles, leading to improved sensitivity and reproducibility.<sup>75</sup> Early studies emphasized micromixer designs that combine analytes and nanoparticles effectively.<sup>76,77</sup> As nanoparticles and analytes travel through channels, averaging effects across nanogaps further enhance reproducibility.<sup>78</sup>

**2.3.2 Droplet-based platforms.** Microfluidics can operate in continuous or segmented (droplet) modes. Continuous flow enables uniform mixing but suffers from “memory effects”, caused by nanoparticle deposition on channel walls, which reduces sensitivity and reproducibility.<sup>79–81</sup> To address this, segmented two-phase droplet systems were introduced.<sup>82,83</sup> Droplet-based SERS avoids memory effects by confining analytes within nanoliter droplets suspended in an immiscible carrier fluid, with Raman signals measured in rapidly moving droplets.<sup>84,85</sup> Droplet manipulation (*e.g.*, merging, splitting, sorting, incubation) supports precise biological assays with high throughput.<sup>86,87</sup>

**2.3.3 Microarray-based platforms.** Advances in nanofabrication have enabled arrays with nanogaps below 10 nm, giving rise to microarray-based SERS devices.<sup>88,89</sup> These combine microarray technology, often used in DNA/protein assays, with SERS to achieve multiplex, high-throughput detection that is difficult with LFAs or conventional LoC chips.<sup>90–92</sup> Multiplexed nanostructures within microarrays allow simultaneous detection of multiple analytes.<sup>93–95</sup>

**2.3.4 Digital platforms.** Digital microfluidics (DMF) manipulates microliter-to-nanoliter droplets on electrode arrays using electrowetting-on-dielectric (EWOD). This allows droplet merging, mixing, splitting, and dispensing without pumps or valves.<sup>96</sup> SERS-enabled DMF platforms have been applied in bacterial detection, antibiotic resistance testing, and real-time cellular monitoring, offering high flexibility and minimal sample loss.

**2.3.5 Lateral flow assay (LFA)-based platforms.** Paper-based LFAs provide simple, low-cost diagnostic tools. Integrating SERS

into LFAs enables both visual colorimetric readouts and quantitative Raman-based measurements at test and control lines, significantly enhancing sensitivity. Nevertheless, challenges exist in achieving uniform biomarker distribution, maintaining biological activity during immobilization, and labor-intensive preparation of standard curves.<sup>97</sup> Automated programmable microfluidic channels that generate concentration gradients may help overcome these limitations, improving efficiency and assay accuracy.

#### 2.4 Comparative overview of major microfluidic-SERS platform types

Although microfluidic-SERS systems share the common goal of improving analytical sensitivity, reproducibility, and miniaturization, different platform architectures exhibit distinct operational strengths and limitations. Therefore, selecting an appropriate microfluidic-SERS format depends not only on analytical sensitivity, but also on practical considerations such as sample consumption, throughput, response time, multiplexing capability, automation level, and intended application scenario. In general, continuous-flow platforms are advantageous for stable signal acquisition, efficient mixing, and real-time monitoring, making them well suited for dynamic analysis and on-chip reaction control. Droplet-based systems, by contrast, offer ultralow sample consumption and high-throughput compartmentalization, which are particularly valuable for digital assays and single-entity analysis. Microarray-based platforms provide strong multiplexing capacity and are especially attractive for parallel biomarker screening. Digital microfluidic systems offer programmable droplet manipulation with high operational flexibility and minimal reagent waste, while lateral flow assay (LFA)-based SERS platforms remain highly promising for point-of-care testing due to their simplicity, portability, and low cost. To provide readers with a more practical framework for evaluating these formats, a comparative summary of the major microfluidic-SERS platform types is presented in Table 1, including their typical analytical characteristics, operational advantages, and representative biomedical applications.

### 3. Machine learning-driven intelligent spectral analysis

The integration of machine learning into SERS has significantly advanced data interpretation and classification accuracy. Traditional algorithms such as principal component analysis (PCA), partial least squares (PLS), and support vector machines (SVM) have been widely applied for spectral feature extraction, dimensionality reduction, and supervised classification, markedly enhancing the sensitivity and reliability of analyte detection.<sup>98–100</sup> In the context of microfluidic-SERS systems, machine learning should not be regarded solely as an auxiliary data-processing tool. Rather, it increasingly functions as an enabling component that

determines how spectral information is translated into actionable analytical or diagnostic outputs, thereby influencing the practical architecture and clinical utility of the overall sensing platform.

Artificial intelligence (AI) broadly refers to computational systems designed to emulate human cognitive processes, including learning, recognition, and decision-making. In spectroscopy particularly reflectance spectroscopy (RS) and surface-enhanced Raman scattering (SERS) AI has become indispensable for decoding complex spectral datasets.<sup>99,101</sup> These approaches are well-suited for handling large, high-dimensional, and heterogeneous datasets, enabling adaptive analysis, scalability, and improved interpretability. As such, the convergence of AI and SERS marks a transformative step in analytical and biomedical sciences.

Spectroscopic datasets typically contain thousands of variables, with overlapping peaks, background noise, and subtle biochemical variations. Manual interpretation is not only time-consuming but also subject to bias. AI methods, especially deep learning, overcome these limitations. Convolutional neural networks (CNNs), for example, can process one-dimensional spectral data as structured signals, automatically learning hierarchical features and enabling accurate classification, such as distinguishing malignant from normal tissues.<sup>102</sup> SVMs, in contrast, are powerful tools for high-dimensional supervised learning tasks, and have been effectively used for tumor subtype discrimination.<sup>103</sup>

One key advantage of CNNs is their ability to extract multi-level spectral features directly from raw input, avoiding the need for handcrafted preprocessing or manual feature engineering.<sup>104–106</sup> For visualization and simplification of complex datasets, dimensionality-reduction methods such as PCA<sup>107,108</sup> and t-distributed stochastic neighbor embedding (t-SNE)<sup>109,110</sup> are commonly applied to highlight the most informative features while reducing computational complexity.

Partial least squares discriminant analysis (PLS-DA) has also gained traction by linking spectral fingerprints to biological or clinical outcomes, including prediction of therapeutic responses. Ensemble-based methods such as random forests (RF) are particularly robust for noisy or heterogeneous datasets, offering reliable feature selection and classification. In addition, unsupervised models like autoencoders can compress and denoise spectral data, retaining diagnostically relevant patterns while enhancing interpretability.

Together, these AI-driven approaches mitigate long-standing challenges in SERS analysis such as spectral overlap, noise artifacts, and large-volume datasets thereby improving precision, efficiency, and scalability. The integration of AI with spectroscopy is reshaping biomedical analytics by delivering higher accuracy in spectral interpretation and enabling novel applications in disease monitoring, diagnosis, and personalized treatment.<sup>111–114</sup>

Although machine learning (ML) has significantly enhanced the analytical potential of SERS, its practical implementation in spectroscopic workflows remains

Table 1 Comparative overview of major microfluidic-SERS platform types

Platform type	Sensitivity (LOD level)	Signal-to-noise ratio (SNR)	Reproducibility	Sample consumption		Throughput time		Response	Major advantages	Main limitations	Typical applications
				Low to moderate ( $\mu\text{L}$ scale)	Moderate to high	Moderate to high	Fast to moderate				
Continuous-flow	High (typically nM-pM range; improved by controlled mixing)	Moderate to high (depends on flow stability and substrate uniformity)	High (due to controlled fluid dynamics and reduced hotspot variability)	Low to moderate ( $\mu\text{L}$ scale)	Moderate to high	Fast to moderate	Stable flow conditions, efficient mixing, real-time monitoring, reduced signal fluctuation	Possible channel fouling, memory effects, more complex fluidic control	Biomolecule detection, reaction monitoring, bacterial analysis, dynamic biochemical assays		
Droplet-based	Very high (often pM-fM; enhanced confinement effects)	High (isolated droplets reduce background noise and interference)	Moderate to high (depends on droplet uniformity and generation stability)	Very low (nL-pL scale)	High	Fast	Minimal sample/reagent use, reduced cross-contamination, high-throughput screening, single-entity analysis	Complex droplet control, interface instability, device integration challenges	mRNA detection, digital assays, single-cell analysis, pathogen screening		
Microarray-based	High (pM-fM depending on hotspot density)	High (uniform nanostructures provide stable signal enhancement)	High (well-defined nanofabrication ensures reproducibility)	Low to moderate	Very high	Fast after fabrication	Parallel detection, strong multiplexing, high-density hotspots	Expensive fabrication, limited flexibility after design	DNA/protein arrays, multiplex biomarker screening, high-throughput disease profiling		
Digital microfluidic (DMF)	High (nM-pM; depends on droplet manipulation precision)	Moderate to high (affected by electrode surface and droplet control)	Moderate (subject to electrode variability and droplet consistency)	Very low to low	Moderate to high	Fast	Pump-free, programmable control, automation-friendly, low reagent consumption	Electrode complexity, surface fouling, evaporation issues	Bacterial detection, antibiotic susceptibility testing, real-time cellular assays, hazardous analyte detection		
LFA-based	Moderate to high (typically nM-pM; enhanced vs. traditional LFA by SERS)	Moderate (background interference and signal variability exist)	Moderate to low (limited control over analyte distribution)	Very low	High	Very fast	Low cost, portable, easy to use, ideal for POCT	Lower quantitative accuracy, limited fluid control, standardization challenges	Infectious disease screening, nucleic acid testing, rapid biomarker detection, point-of-care diagnostics		

associated with several important challenges. In many cases, model performance is not determined solely by algorithm selection, but also by upstream spectral quality, dataset structure, and the interpretability of learned features. One of the most fundamental issues is spectral preprocessing. Raw SERS spectra are often affected by baseline drift, fluorescence background, shot noise, cosmic spikes, peak shifting, and intensity variation caused by experimental or substrate-related factors. Consequently, preprocessing steps such as baseline correction, smoothing, denoising, normalization, peak alignment, and outlier removal are often essential before model training. However, these procedures are not always standardized, and different preprocessing pipelines may substantially alter downstream model performance. This lack of harmonization remains a major obstacle to reproducibility and cross-study comparability. A second challenge is the limited size and heterogeneity of available datasets. In many biomedical SERS studies, the number of spectra or patient samples is relatively small, while the spectral dimensionality remains high. This imbalance can easily lead to model instability and poor generalization. In addition, datasets are often collected under highly controlled laboratory conditions, which may not adequately reflect real-world biological variability, instrument-to-instrument differences, or batch effects. As a result, models that perform well in proof-of-concept studies may fail to maintain accuracy in external or clinical validation settings. Model overfitting is therefore a particularly important concern in SERS-based machine learning. Complex models, especially deep learning architectures such as convolutional neural networks (CNNs), can achieve high apparent accuracy even when trained on limited or non-independent datasets. Without careful validation strategies such as external test cohorts, patient-level splitting, cross-platform validation, or prospective studies, model performance may be overestimated. This issue is especially relevant in SERS, where spectra collected from the same substrate batch, sample preparation run, or patient source may contain hidden correlations that artificially inflate classification performance. Interpretability is another critical consideration, particularly for biomedical and clinical applications. While traditional methods such as PCA, PLS-DA, and linear SVM often provide more transparent feature structures, deep learning models are frequently treated as “black boxes”, making it difficult to determine which spectral regions or biochemical features drive classification decisions. This lack of interpretability may hinder biological insight, clinician trust, and regulatory acceptance. Therefore, explainable AI strategies, including feature importance analysis, saliency mapping, SHAP-based interpretation, and peak-level attribution, are becoming increasingly important for translating ML-assisted SERS systems into clinically meaningful tools. Taken together, these considerations suggest that the future development of ML-assisted SERS should move beyond simply applying increasingly sophisticated algorithms. Greater emphasis should instead be placed on standardized preprocessing, rigorous validation,

dataset quality, and interpretable modeling frameworks to ensure robustness, reproducibility, and real-world translational value.

Importantly, the application of machine learning in SERS analysis must be interpreted in the context of the intrinsic physicochemical characteristics of SERS spectra. Unlike idealized spectral data, real SERS signals are often affected by baseline drift caused by fluorescence background, peak overlap arising from complex molecular mixtures, stochastic noise, and signal variability induced by heterogeneous hotspot distributions and microfluidic flow conditions. These factors significantly influence data quality and, consequently, model performance. From this perspective, machine learning does not operate independently of the underlying spectral physics. Instead, its effectiveness is closely linked to how well these physicochemical artifacts are addressed during preprocessing and feature extraction. For example, baseline correction and normalization are essential for compensating intensity variation, while dimensionality reduction techniques such as PCA help mitigate peak overlap and high-dimensional redundancy. In addition, advanced models such as convolutional neural networks (CNNs) can learn local spectral patterns and partially tolerate peak shifting or distortion; however, their performance remains sensitive to data quality and consistency. Therefore, understanding the physicochemical origin of spectral variability is critical for selecting appropriate machine learning strategies and avoiding misinterpretation of model outputs. In addition to spectral complexity, several methodological challenges must be carefully considered. Dataset bias is a common issue in SERS-based studies, where spectra are often collected under controlled laboratory conditions with limited sample diversity. As a result, trained models may capture experimental artifacts rather than true biochemical differences, leading to poor generalization in real-world applications. Similarly, overfitting remains a significant concern, particularly for deep learning models trained on small datasets with high spectral dimensionality. Model interpretability is another important limitation. While traditional statistical models offer more transparent relationships between spectral features and classification outcomes, complex models such as deep neural networks are often difficult to interpret in terms of underlying molecular signatures. This limitation may hinder biological insight and reduce confidence in clinical decision-making. Accordingly, integrating explainable AI approaches and feature-level analysis is increasingly important for ensuring reliable and interpretable SERS-based diagnostics. An important consideration is the extent to which machine learning can compensate for the inherent limitations of label-free SERS detection. Label-free approaches provide rich molecular fingerprint information but are often affected by spectral overlap, weak signal intensity, and biological variability, making direct interpretation challenging. In this context, machine learning can enhance classification performance by extracting subtle patterns from complex spectra; however, it

does not fundamentally eliminate the underlying signal variability or ambiguity. In contrast, indirect (label-based) SERS strategies generate stronger and more standardized signals through reporter molecules, thereby improving signal-to-noise ratio and analytical consistency. Consequently, these approaches may require less complex data-driven interpretation but sacrifice intrinsic molecular information. Therefore, the choice between label-free and indirect SERS should not be viewed solely as an experimental preference, but also as a data-analysis consideration. Systems relying on label-free detection often benefit more strongly from

advanced machine learning frameworks, whereas indirect SERS platforms may achieve robust performance with simpler analytical models. Understanding this interplay between signal generation and data interpretation is essential for designing effective microfluidic-SERS diagnostic systems.

## 4. In-depth analysis of microfluidic-SERS application scenarios

Before discussing specific application scenarios, it is important to distinguish between different functional roles

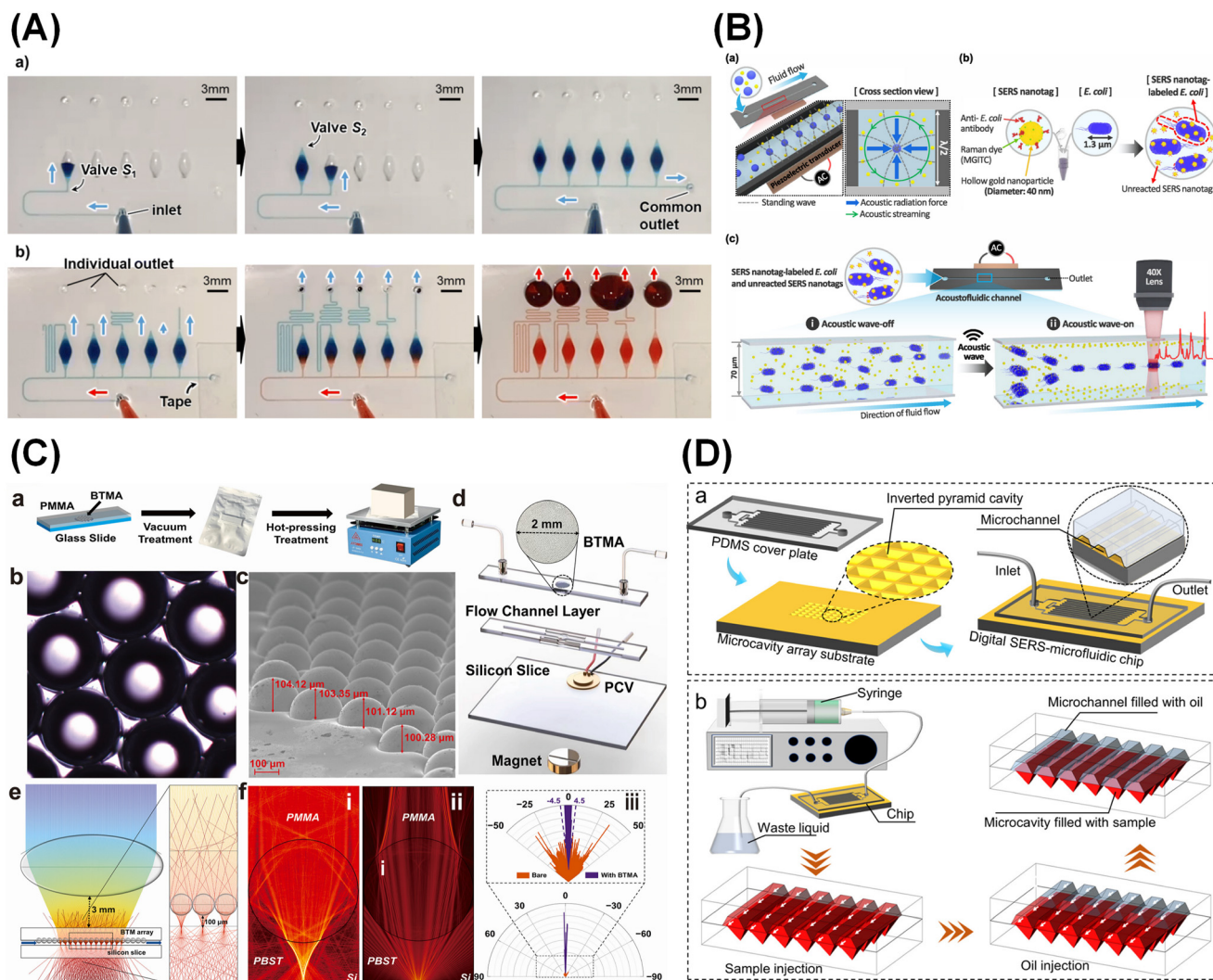


**Fig. 1** (A). Experimental results showing the liquid manipulation in the microfluidic device. (a) Sequentially dispensing of blue-coloured water into five microchambers. (b) Washing away the blue-coloured water and simultaneously replacing it with red-coloured water in all the microchamber at a constant flow rate.<sup>115</sup> (B). (a) Acoustic field-induced separation of large and small particles in a microfluidic channel. (b) Tagged bacteria generated by the reaction between SERS nanotags and bacteria in a microtube. (c) Behavior of bacteria and SERS nanotags after injecting tagged bacteria into the microfluidic channel in (i) acoustic wave-off and (ii) acoustic wave-on.<sup>117</sup> (C). Fabrication and Characterization of BTMA-SERS microfluidic chip.<sup>120</sup> (a) The process of the vacuum self-assembly hot-pressing method. (b) The microscopic view of BTMA embedded in PMMA layer. (c) The scanning electron microscope images of BTMA which shows the embedding depth of microspheres. (d) The structure of each part of BTMA-SERS microfluidic chip, which the 2 mm BTMA is embedded in the top cover of the flow channel. (e) The modeling of BTMA for the light focusing effect. (f) The light scattering mechanism of BTMA: (i) photonic nano-jets of BTMA; (ii) directional antenna effects of BTMA; (iii) the BTMA limits the Raman scattering emission angle to  $\pm 4.5^\circ$ . (D). (a) Schematic diagram of the digital SERS-microfluidic chip. (b) Operation procedure of the sample discretization.<sup>121</sup> Reproduced from ref. 115, 117, 120 and 121 with permission from Royal Society of Chemistry, American Chemical Society, Elsevier, and American Chemical Society, respectively; copyright 2024, 2025, 2024, and 2024.

of microfluidic–SERS systems in practical bioanalysis. In general, reported studies can be broadly categorized into two types: (i) systems that rely primarily on the intrinsic analytical capability of microfluidic–SERS platforms, and (ii) systems in which machine learning plays a critical role in enabling reliable interpretation of complex spectral data. In the first category, microfluidic control combined with optimized SERS substrates can provide sufficient signal intensity, specificity, and reproducibility to enable direct detection and quantitative analysis without advanced computational assistance. These systems are typically based on label-based strategies or well-defined target molecules with strong and distinguishable spectral signatures. In contrast, the second category includes applications where spectral complexity, biological variability, or weak signal features limit direct interpretation. In such cases, machine learning becomes essential for extracting meaningful patterns, enabling classification, or improving diagnostic accuracy. These systems are commonly associated with label-free detection of complex biological samples, such as cells, tissues, or biofluids. This distinction provides a useful framework for understanding the relative contributions of microfluidic design, SERS signal generation, and machine learning in different application contexts.

#### 4.1 Infectious diseases

**4.1.1 Viral infections.** Mostafa Kamal Masud and colleagues designed a microfluidic device capable of simultaneously detecting multiple SARS-CoV-2 antigens, including S1, RBD, and NCD. Their system offered multiplex detection, incorporated control groups, and simplified the experimental workflow by integrating the full detection process onto a single platform. The use of gold nanoparticle-based SERS nanotags (mAuNPs) removed the requirement for enzymatic amplification, while a portable Raman spectrometer enabled on-site measurements without sophisticated instruments or laboratory facilities<sup>115</sup> (Fig. 1A).

In another study, Jing Wang *et al.* developed a multivalent probe (MVP) strategy in which nanobodies served as protein-recognition ligands and gold–silver alloy nanocages were coated with Raman reporters. Coupled with a nano-mixing enhanced microfluidic chip, this MVP-based SERS immunoassay enabled detection of SARS-CoV-2 spike proteins and viral particles in clinical nasopharyngeal swabs. Testing across 39 infected patients and 39 healthy individuals showed an 84.6% agreement with RT-qPCR, underscoring the potential of MVP-assisted microfluidic SERS systems for pandemic diagnostics.<sup>116</sup>

**4.1.2 Bacterial infections.** Sohyun Park *et al.* reported an acoustofluidic SERS system for rapid bacterial detection. In their method, bacteria labeled with SERS nanotags were passed through a silicon channel, where acoustic waves generated by a piezoelectric transducer focused the labeled bacteria in the channel center while separating free nanotags toward the walls<sup>117</sup> (Fig. 1B). Similarly, Hugo Cortes-Cano *et al.* designed a polymer-based SERS microfluidic prototype to monitor surface processes, capturing dynamic deposition

of compounds on microchannel walls. This setup offered real-time surface assessment with reduced reagents and sample use, minimal environmental impact, and rapid bacterial detection within one hour.<sup>118</sup>

Hao Wang *et al.* compared conventional nanoparticle synthesis with microfluidic methods. Laminar-flow microfluidics allowed precise control over reagent mixing, producing nanoparticles with narrower size distributions, which were then used in SERS studies involving horseradish peroxidase (HRP) and *Escherichia coli*.<sup>119</sup> Zhenyong Dong *et al.* introduced a SERS microfluidic chip embedded with a barium titanate microsphere array (BTMA), fabricated through vacuum-assisted thermal pressing. Bacterial detection was achieved using immune magnetic enrichment combined with immune SERS tags<sup>120</sup> (Fig. 1C).

Ping Wen *et al.* developed a digital SERS microfluidic chip employing an inverted pyramid microcavity (IPM) array to isolate and purify microbes, enabling rapid microbial quantification. This approach demonstrated potential for detecting a wide variety of pathogens, including bacteria and viruses<sup>121</sup> (Fig. 1D). Yue Liu and collaborators created a ZnO/Ag nanostructured SERS microfluidic array, where zinc oxide nanoflowers decorated with silver nanoparticles enhanced sensitivity for efficient bacterial capture and detection.<sup>122</sup>

Lindong Shang *et al.* combined label-free SERS with optical tweezers in a microfluidic environment to analyze six industrial *Lactobacillus* strains. Machine learning models including support vector machine (SVM) and XGBoost classified Raman spectra with over 95% accuracy, highlighting the platform's robustness<sup>123</sup> (Fig. 2A). Chi-Yao Ku *et al.* proposed an air–liquid microfluidic SERS (ALM–SERS) system, using precise droplet manipulation to control sequential molecular adsorption, allowing selective analysis of bacterial secretions<sup>124</sup> (Fig. 2B).

Mehdi Feizpour *et al.* introduced a framework combining on-chip SERS with a two-dimensional convolutional neural network (2D-CNN) for bacterial identification. Direct laser writing was used to create SERS-active regions within the chip, enabling customizable hotspots and efficient *in situ* measurements<sup>125</sup> (Fig. 2C). Bingyang Huo *et al.* developed a co-recognition, enrichment, and sensing (CES) strategy, integrated with a modular microfluidic device and magnetically controlled sliding unit, which allowed seamless switching between magnetic loading and elution steps for high-specificity bacterial detection<sup>126</sup> (Fig. 2D).

Finally, Heera Jayan *et al.* designed a Y-shaped serpentine microfluidic SERS chip for the rapid, label-free detection of *E. coli* in food samples. This device demonstrated strong potential for food safety applications by providing sensitive, real-time pathogen screening<sup>127</sup> (Table 2).

#### 4.2 Liquid biopsy

**4.2.1 Circulating tumor cells (CTCs).** Renhao Ni *et al.* combined a single-cell trapping platform with tumor-targeted silver nanoprobe and tapered multimode optical fibers coupled to Raman spectroscopy. This approach enhanced

## Lab on a Chip

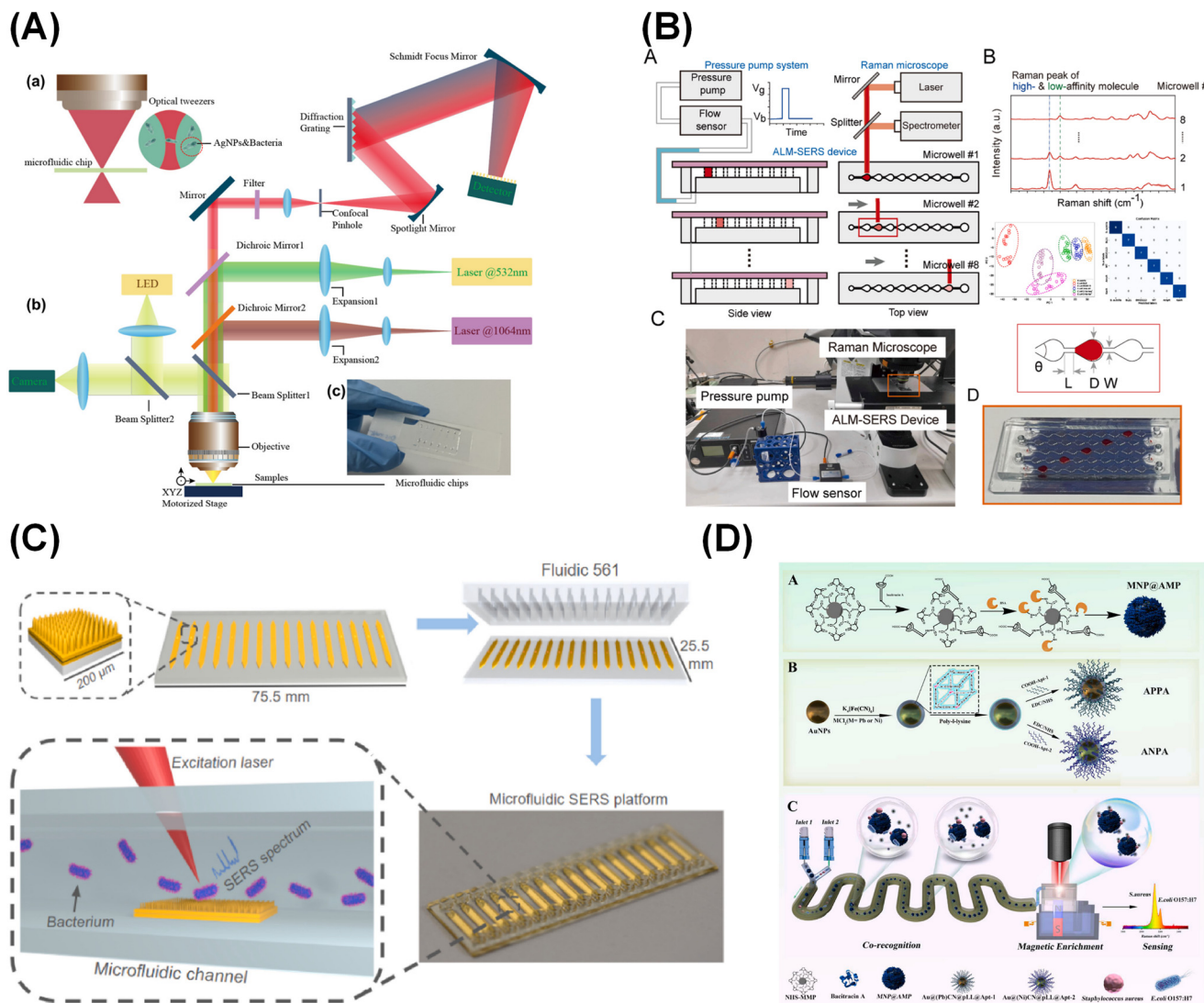


Fig. 2 (A). (a) Optical tweezers capture AgNPs and bacteria. (b) Optical tweezer Raman optical path diagram. (c) Microfluidic chips.<sup>123</sup> (B). (A) Schematic of the ALM-SERS system, consisting of (1) the air-liquid microfluidics attaching SERS substrate (ALM-SERS) device, (2) the pressure pump system, and (3) the Raman microscope. The dimensions of the microwell angle ( $\theta$ ), microwell diameter ( $D$ ), neck length ( $L$ ), and width ( $W$ ) are  $60^\circ$ , 2 mm, 1 mm, and 0.4 mm, respectively. (B) The series of SERS spectra at microwells #1 to #8 can be continuously acquired by integrating the motorized stage and Raman microscope and analyzed using data categorization methods (PCA or SVM). Photograph of (C) the ALM-SERS system and (D) the ALM-SERS device. Five red-colored food dye droplets were encapsulated in microwells.<sup>124</sup> (C). Schematic representation of SERS substrate integration and chip assembly. Fluidic 561 is a 16-channel commercial chip.<sup>125</sup> (D). Illustration of the detection of *S. aureus* and *E. coli* O157:H7 in CES method based on the MNP@AMP (A), silent region Raman probe APPA and ANPA (B), and CES Strategy coupling with integrated FM-MCS SERS platform (C).<sup>126</sup> Reproduced from ref. 123–126 with permission from American Chemical Society, Elsevier, Elsevier, and Elsevier, respectively; copyright 2023, 2025, 2025, and 2024.

Raman scattering intensity, minimized optical loss, and suppressed background interference. Their findings revealed strong associations between single-cell Raman spectral features and biological processes such as adhesion, migration, and extracellular matrix remodeling, offering a rapid and precise method for pancreatic cancer diagnosis and monitoring.<sup>128</sup>

Yujiao Xie *et al.* reported a cancer cell enrichment and identification system that integrated SERS-active bioprobes with a microfluidic spiral inertial separation chip. Cancer cells were effectively isolated from peripheral blood, and subsequent machine learning-assisted linear discriminant

analysis (LDA) differentiated three types of cancer cells from white blood cells with >90% accuracy<sup>38</sup> (Fig. 3A).

Ying Zhuo *et al.* presented a multifunctional microfluidic device for parallel isolation and detection of CTCs and prostate-specific antigen (PSA). A pagoda-like tiered chamber enabled sequential separation of CTCs with 87% capture efficiency, while functionalized magnetic beads were employed for PSA enrichment *via* sandwich immunoassay<sup>129</sup> (Fig. 3B).

Inspired by the structural behavior of CTCs, Changbiao Zhan *et al.* designed a coordinated microfluidic device (CMD) incorporating a nanowire forest trapping substrate (NFTS).

**Table 2** Summary of representative microfluidic-SERS applications for infectious disease detection

Category	Detection strategy	System design/key technique	Key performance/feature	Ref.
Viral infection	Label-based (SERS nanotags)	Multiplex microfluidic chip with AuNP nanotags + portable Raman	Multiplex detection of SARS-CoV-2 antigens; POCT-compatible system	115
Viral infection	Label-based (immunoassay)	MVP nanobody + Au-Ag nanocage reporters + nano-mixing microfluidics	Detection in clinical swabs; 84.6% agreement with RT-qPCR	116
Bacterial infection	Label-based	Acoustofluidic SERS focusing system with piezoelectric control	Rapid bacterial separation and detection with improved specificity	117
Bacterial infection	Label-free/surface monitoring	Polymer-based microfluidic SERS chip	Real-time surface process monitoring; detection within ~1 h	118
Bacterial infection	Label-based	Microfluidic-controlled nanoparticle synthesis for SERS probes	Improved nanoparticle uniformity and detection reproducibility	119
Bacterial infection	Label-based	BTMA-based SERS chip + immune magnetic enrichment	High-specificity bacterial detection	120
Bacterial infection	Label-based/digital SERS	Digital microfluidic chip with IPM array	Rapid microbial quantification; broad pathogen applicability	121
Bacterial infection	Label-based	ZnO/Ag nanoflower SERS microfluidic array	Enhanced bacterial capture and sensitivity	122
Bacterial infection	Label-free	Optical tweezers + microfluidic SERS	>95% classification accuracy for bacterial strains	123
Bacterial infection	Label-free (controlled adsorption)	Air-liquid microfluidic SERS (ALM-SERS) system	Selective analysis of bacterial secretions	124
Bacterial infection	Label-free	On-chip SERS + 2D-CNN + laser-written hotspots	ML-enabled bacterial identification	125
Bacterial infection	Label-based	CES strategy + magnetic-controlled microfluidics	Integrated enrichment and high-specificity detection	126
Bacterial infection	Label-free	Serpentine microfluidic SERS chip	Rapid <i>E. coli</i> detection in food samples	127

This platform enabled dual-mode recognition and real-time phenotypic profiling of CTCs directly from whole blood, ensuring efficient capture and analysis<sup>130</sup> (Fig. 3C).

Emtiaz Ahmed *et al.* established a mesoporous gold biosensor that allowed the SERS-based evaluation of immune checkpoint protein (ICP) heterogeneity within individual CTCs from lung cancer samples. The platform enabled high-specificity capture and analysis of proteins such as PD-L1, B7H4, CD276, and CD80.<sup>131</sup> Amin Hassanzadeh-Barforoushi *et al.* developed a high-throughput CTC manipulation system integrated with multiplexed Raman-based analysis modules, demonstrating its suitability for *in vitro* cancer diagnostics<sup>132</sup> (Fig. 3D).

Youqiang Zhou *et al.* fabricated a PMMA-triangular column nanoarray (PMMA-TCNA) microfluidic chip embedded with gold films as functional SERS substrates. This chip successfully enriched PC3 cells and simultaneously achieved sensitive Raman-based identification, suggesting potential utility in early prostate cancer detection<sup>133</sup> (Fig. 3E).

#### 4.2.2 Nucleic acid detection

**RNA detection.** Diogo Costa *et al.* employed a microfluidic device to monitor localized surface plasmon resonance (LSPR) by continuously introducing probe solutions, enabling real-time observation of thiolated oligonucleotide-sensor interactions.<sup>134</sup> Researchers from Politecnico di Torino combined an automated microfluidic platform with a portable Raman spectrometer for detecting miR-214, using a multi-chamber chip with a hybridization assay for functionalization.<sup>135</sup> Yang Lu *et al.* constructed a SERS-active microcone array substrate (MCASS) microchip for miR-141 detection, providing enhanced Raman

sensitivity and large modification areas for DNA probes<sup>136</sup> (Fig. 4A).

Xiaohui Lu *et al.* created a barcoded microfluidic SERS system capable of multiplex miRNA imaging. Encoded nanorod aggregates were positioned at patterned nanogaps of vertically aligned nanorod arrays, generating strong electromagnetic enhancement. A dovetail-shaped micromixer further accelerated probe hybridization and capture<sup>137</sup> (Fig. 4B). Jin Qian *et al.* integrated rolling circle amplification (RCA) with microdroplet-based SERS detection to quantify miRNA-21 and miRNA-155 in idiopathic pulmonary fibrosis serum samples. This strategy achieved single-nucleotide resolution and significantly improved reproducibility<sup>138</sup> (Fig. 4C and D).

Ka Wai Ng *et al.* proposed a lateral flow assay (LFA)-based test for hsa-miR-17-5p, applying DNA hairpin probes for selectivity and SERS nanoprobe for sensitive signal readout, enabling early pregnancy biomarker screening.<sup>139</sup>

**DNA detection.** Yeru Wang *et al.* designed a DNA-derived dynamic hydrogel scaffold (DDHS) integrated into a microfluidic chip to capture exosomes *via* CD63 recognition, achieving an ultra-low detection limit of 2.63 particles per  $\mu\text{L}$ <sup>140</sup> (Fig. 5A and B). Yayun Qian *et al.* presented a high-throughput SERS microfluidic chip using enzyme-assisted signal amplification (EASA) and catalytic hairpin assembly (CHA). This system applied hpDNA-modified Au nanocone arrays to detect circulating tumor DNA (ctDNA) in lung cancer mouse models.<sup>141</sup>

Lei Wu *et al.* developed a finger-actuated microfluidic chip with built-in filtration grooves for rapid ctDNA analysis from whole blood without amplification. The SERS platform allowed direct detection with high sensitivity.<sup>142</sup> Yan Su *et al.* introduced

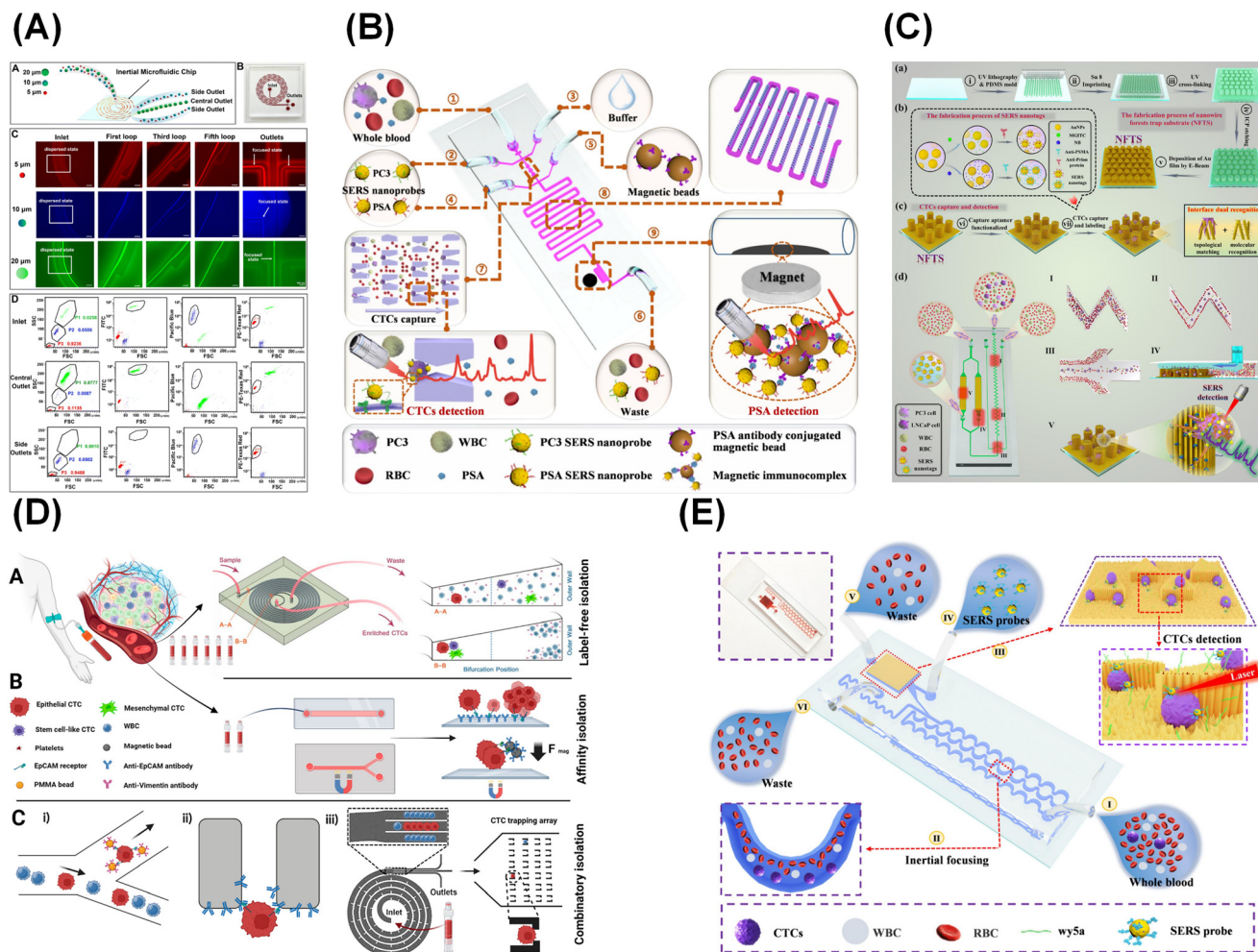


**Fig. 3** (A). Separation effect of fluorescent microspheres by inertial microfluidic chip. Separation diagram of mixture of three types of micro-particles with diameter of 5  $\mu\text{m}$ , 10  $\mu\text{m}$  and 20  $\mu\text{m}$  (A); photograph of inertial microfluidic chip with inlet, spiral channel, and outlets (B), fluorescent pictures of particles' trajectories in inlet, first loop, third loop, fifth loop and outlets (C), comparison of fluorescent intensity and proportion of particles in collected liquid sample from inlet, central outlet and both side outlets (D).<sup>38</sup> (B). Schematic of simultaneous separation and SERS detections of CTCs and PSA in an integrated microfluidic chip.<sup>129</sup> (C). (a) Schematic illustration of the NFTS fabrication process. (b) Sequential process for preparing two different types of antibody-conjugated SERS nanotags; (c) Schematic illustration of the modification of capture aptamers on NFTS and subsequent CTCs capture process. (d) The workflow of multistage capture and *in situ* single-cell phenotype analysis with SERS measurement for PCa CTCs on CMD.<sup>130</sup> (D). Microfluidic CTC isolation technologies. (A) Label-free, (B) affinity-based, and (C) combinatory isolation.<sup>132</sup> (E). Schematic diagram of CTCs captures and SERS detections on microfluidic chip.<sup>133</sup> Reproduced from ref. 38, 129, 130, 132 and 133 with permission from Royal Society of Chemistry, Elsevier, Elsevier, American Chemical Society, and Elsevier, respectively; copyright 2024, 2025, 2025, 2024, and 2025.

enzymatic recycling (ER) reactions in microdroplets for isothermal amplification, enabling single-molecule level sensitivity without thermal cycling, achieving results within 20 minutes<sup>143</sup> (Fig. 5C).

**4.2.3 Exosome detection.** Xin Wang *et al.* established a SERS-integrated microfluidic chip for analyzing exosome secretion at the single-cell level, successfully distinguishing breast cancer subtypes and monitoring drug response with machine learning.<sup>144</sup> Quan Zhou *et al.* developed EV-GLYPH, a SERS-based microfluidic approach for multiplex glycoprotein profiling of sEVs in non-small cell lung cancer, differentiating malignant from benign nodules<sup>145</sup> (Fig. 6A).

Weiming Lin *et al.* designed a serpentine-channel chip with multiplexed SERS tags to profile multiple tumor biomarkers on

extracellular vesicles (EVs), eliminating manual processing steps<sup>146</sup> (Fig. 6B). Hui Chen *et al.* reported a deep learning-assisted chip that enriched exosomes with gold nanocube-anti-CD9 conjugates (PACD) and enabled Raman-based subtype analysis of NSCLC<sup>147</sup> (Fig. 6C).

Ying Jin *et al.* applied a size-based microfluidic chip combined with tangential flow filtration for osteosarcoma exosome isolation, achieving 82% recovery and >93% diagnostic accuracy with machine learning<sup>148</sup> (Fig. 6D). Huakun Jia *et al.* fabricated a cactus-like nanostructured SERS array for detecting prostate cancer-derived exosomes with enhanced sensitivity<sup>149</sup> (Fig. 7A).

Wenbo Dong *et al.* combined digital microfluidics with Raman spectroscopy for serum exosome analysis, enabling portable and real-time monitoring<sup>150</sup> (Fig. 7B and C). Xingya

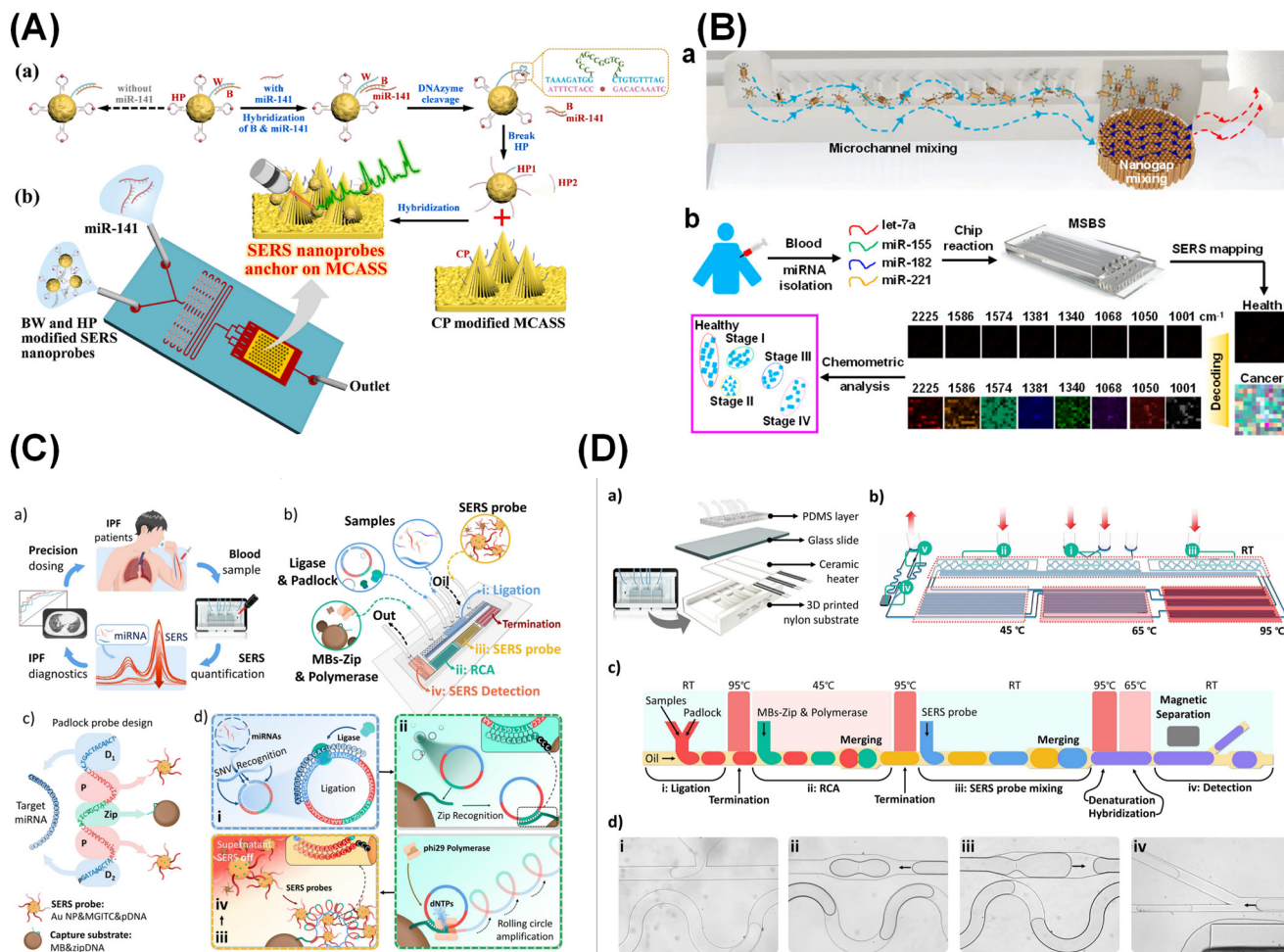


**Fig. 4** (A). Schematic diagram of miRNA recognition and SERS detection on microfluidic chip.<sup>136</sup> (B). Schematic of the proposed microfluidic-SERS barcoding system (MSBS) for multiplexed detection of miRNAs and early cancer diagnosis.<sup>137</sup> (C). a) Principle of the SERS-RCA-microfluidic biosensor for detecting ipf-related miRNA. b) design of the microfluidic chip. i: Target miRNA recognition and ligation. ii: RCA initiation, where streptavidin-coated MB&zipDNA, DNA polymerase, DTT, dNTP, and buffer are introduced. iii: Au NPs coupling area, where Au NPs&MGITC&pDNA are introduced. iv: SERS signal detection area, where a magnet is placed to capture MB-RCA-Au NPs complexes and separate the supernatant. (c) Design of the padlock probe and functional descriptions of the D1, D2, P, and zip regions. (d) RCA initiation. (iii and iv) SERS signal output, where RCA products are connected to Au NPs in iii, and MB-RCA-Au NPs complexes are magnetically captured and subjected to SERS detection in iv.<sup>138</sup> (D). Comprehensive representation and functionality of the microfluidic system.<sup>138</sup> Reproduced from ref. 136–138 with permission from Elsevier, American Chemical Society, and Elsevier, respectively; copyright 2023, 2023, and 2024.

Chen *et al.* developed a seven-channel chip (S-MMEV) to simultaneously analyze multiple sEV biomarkers and accurately differentiate ovarian cancer patients from healthy controls.<sup>151</sup> Kwun Hei Willis Ho *et al.* demonstrated a droplet microfluidic-SERS aptasensor for HER2-positive exosome detection from breast cancer cells, achieving high sensitivity through nanoparticle aggregation hotspots<sup>152</sup> (Fig. 7D).

**4.2.4 Detection of other biomarkers.** Marika Niihori *et al.* fabricated a glass-based Au nanoparticle monolayer sensor incorporating iron(III) sensitizers to detect dopamine at nanomolar levels with amplified SERS effects.<sup>153</sup> Xiaoyan Xue *et al.* synthesized AuNPs/MoS<sub>2</sub> composites *via* microfluidic-assisted nanomaterial growth for adenine and cytosine detection.<sup>154</sup> Lili Cong *et al.* developed AgNP-doped hydrogel microbeads using *in situ* polymerization, allowing selective entry of small molecules for alkaline phosphatase (ALP) SERS detection.<sup>155</sup>

Ksenia Maleeva *et al.* introduced a plasmonic polymer-embedded Au nanoparticle film, providing robust SERS signals across pH ranges (3–9) and elevated temperatures (~150 °C), enabling amino acid analysis.<sup>156</sup> Javier Plou *et al.* utilized paper-based capillary pumps to simplify SERS analysis of cell secretions<sup>157</sup> (Fig. 8A). Ziteng Zhang *et al.* designed a nanostructured SERS microfluidic biosensor for simultaneous quantification of serotonin, dopamine, and cortisol three biomarkers linked to emotional states.<sup>158</sup>

Jiwon Yoon *et al.* produced SERS-active cylindrical microgels through photo-crosslinking, enabling stable detection of small molecules without preprocessing<sup>159</sup> (Fig. 8B). Kaibin Yao *et al.* developed plasmonic cellulose microfibrils coated with AgNPs for urea detection in microchannels, with deep learning algorithms applied for automated recognition.<sup>160</sup> Francesca Toffanello *et al.* fabricated inkjet-printed AuNP films on

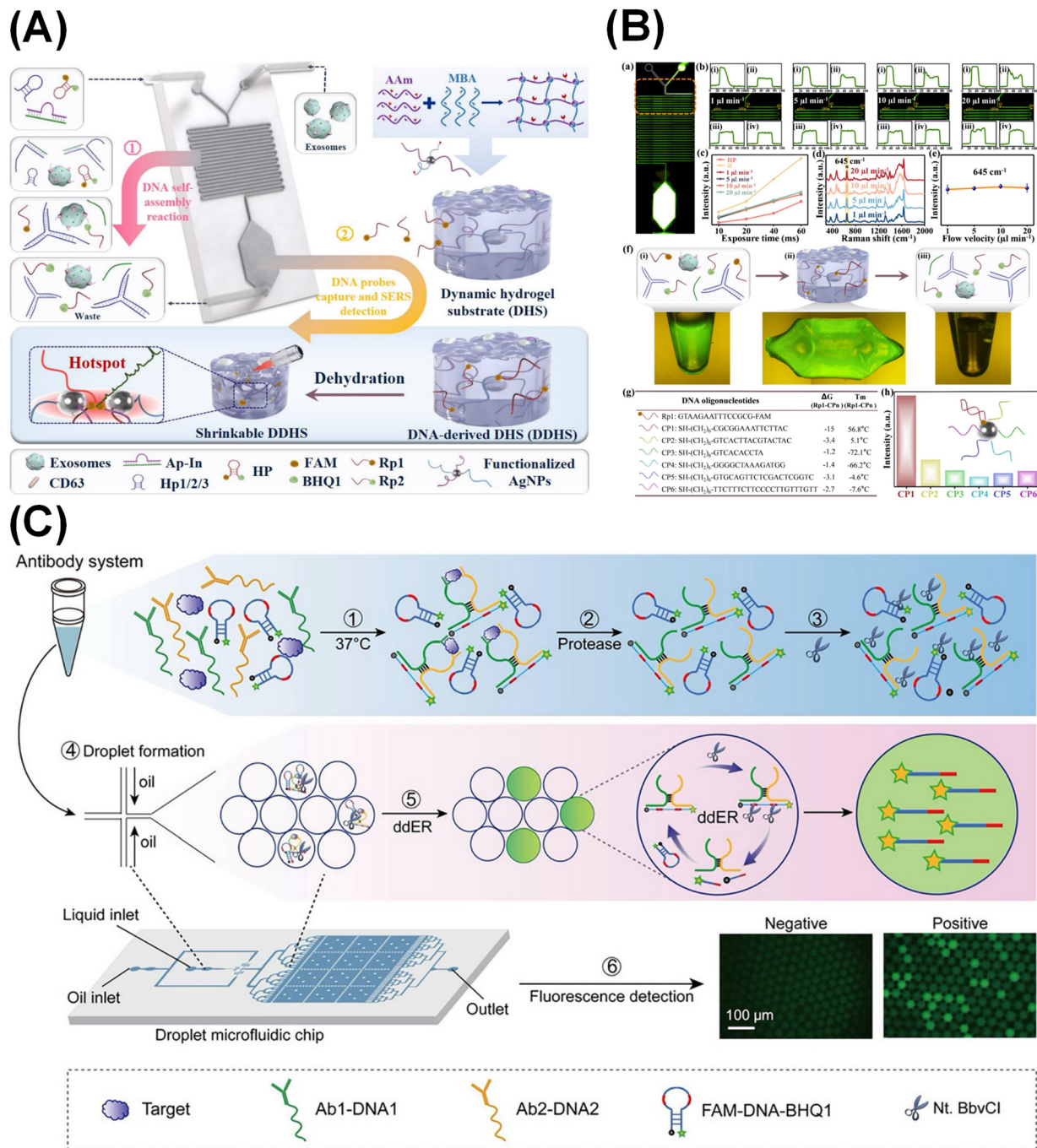


**Fig. 5** (A) Schematic of SERS-based microfluidic chip on the synergy between DDHS and DNA self-assembly technology for exosome detection.<sup>140</sup> (B) (a) Fluorescent image of the entire microfluidic channels. (b) Corresponding fluorescence intensity profiles at locations indicated by dotted frame under various flow rates (1/5/10/20  $\mu\text{L min}^{-1}$ ). X and Y axes denote the channel width and the relative fluorescence intensity, respectively. (c) The line drawing of the HP recovered fluorescent intensity by DNA self-assembly against the flow rate. SERS spectra (d) and plotting of the  $645\text{ cm}^{-1}$  peak intensity values (e) of FAM detection on detection chamber corresponded to the rates of 1, 5, 10, 20  $\mu\text{L min}^{-1}$  respectively. (f) Schematic of FAM-labeled Rp1 locked in DDHS, and the fluorescent microscopy images of DDHS (ii) and DNA reporter probes capture step which before (i) and after (iii) flowing through DDHS. (g) The DNA sequences and hybridization information of Rp1 and CPn. (h) The SERS measurement results in DDHS which modified CPn.<sup>140</sup> (C) Scheme of antibody-based digital droplet enzyme recycling single-molecule homogeneous immunoassay (ddER-SiMHoI). The workflow consists of six major steps: step 1, target and reaction reagents (two affinity probes and a molecular beacon) are incubated at 37 °C to form an immune complex; step 2, protease is added to degrade the target and terminates the reaction; step 3, an endonuclease is introduced for subsequent reaction; step 4, the reaction reagents serve as aqueous phase in a bi-phase microfluidic chip to generate water-in-oil droplets; step 5, the endonuclease acts on the reaction products, and triggers an in-droplet enzymatic recycling reaction at 50 °C to accumulate unquenched FAM fragments; step 6, using a fluorescence microscopy to digitalize the illuminated droplets. Under an excitation wavelength of 494 nm, no apparent fluorescence signals can be observed from negative samples, while clear green fluorescence signals can be observed from positive samples.<sup>143</sup> Reproduced from ref. 140 and 143 with permission from Elsevier and Wiley-VCH, respectively; copyright 2024 and 2025.

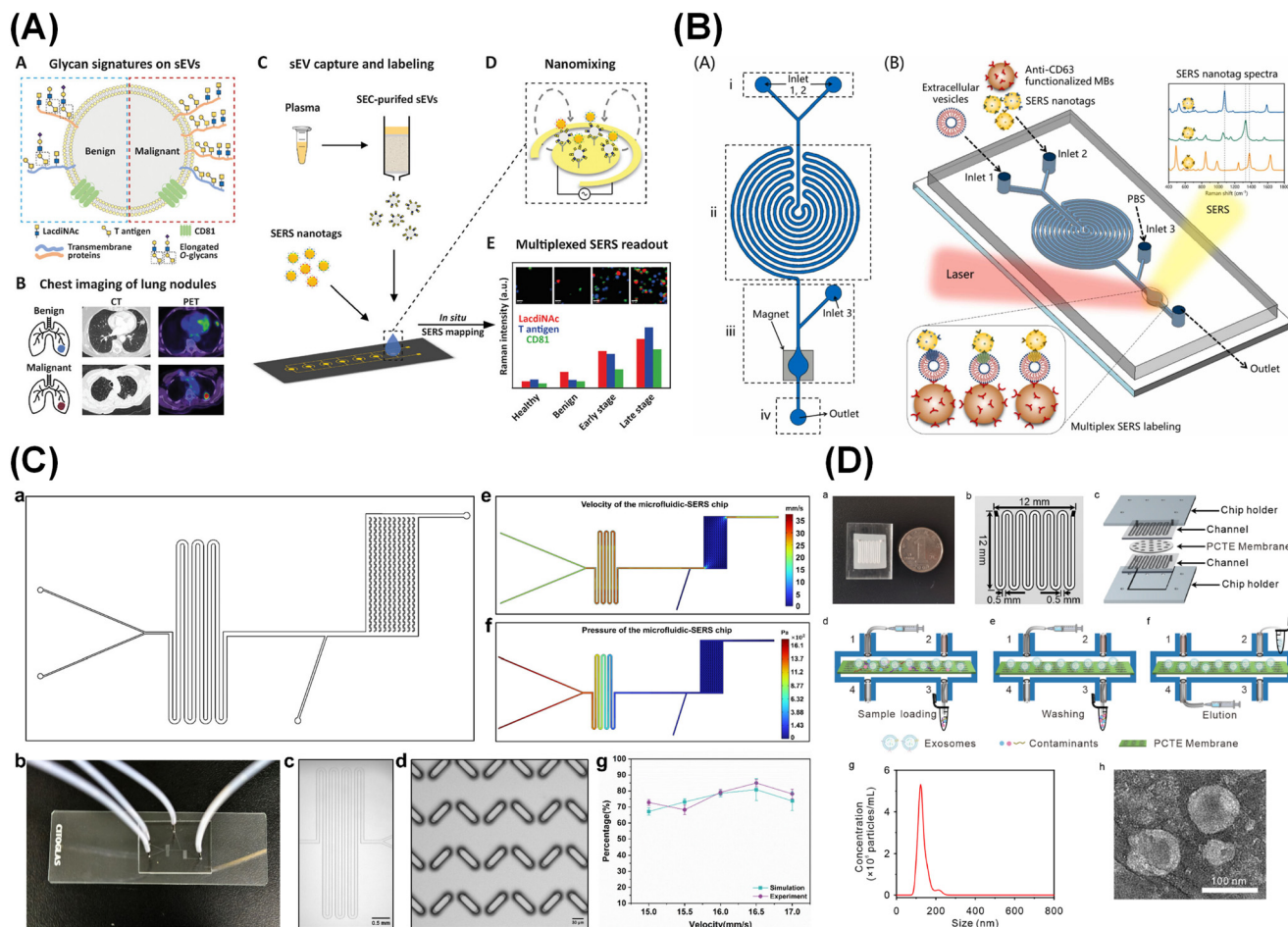


**Fig. 6** (A). Principle of EV-GLYPH assay for early-stage NSCLC identification.<sup>145</sup> (B). (A) Schematic structure and (B) working principle of the on-chip SERS-based EV phenotyping platform, including (i) sample inlet ports, (ii) a serpentine microstructure for mixing and immunoreaction, (iii) a zone for magnetic enrichment, washing, and SERS detection, and (iv) a sample outlet port.<sup>146</sup> (C). (a) CAD diagram of the microfluidic-SERS chip. (b) A prototype of the microfluidic-SERS chip. (c) Mixing chamber of the chip. (d) Trapping chamber of the chip. (e) Velocity distribution map of the microfluidic-SERS chip. (f) Pressure distribution map of the microfluidic-SERS chip. (g) Trapping efficiency of the chip.<sup>147</sup> (D). The rapid separation and purification of exosomes through a size-dependent microfluidic chip employing tangential flow filtration.<sup>148</sup> Reproduced from ref. 145–148 with permission from Wiley-VCH, Elsevier, American Chemical Society, and Elsevier, respectively; copyright 2024, 2023, 2025, and 2025.

aluminum foils within microfluidic chips, facilitating SERS-based monitoring of biomimetic reaction kinetics<sup>161</sup> (Fig. 8C).

Bingfang Zou *et al.* introduced magneto-plasmonic nanostirrers carrying Raman reporters as capture carriers to improve microfluidic biosensor reproducibility, demonstrated using interleukin-6.<sup>162</sup> Changbiao Zhan *et al.* designed 3D AuNP-based hydrogel microparticles with hierarchical nanostructures, allowing simultaneous SERS detection of alpha-fetoprotein (AFP) and alpha-fucosidase (AFU).<sup>46</sup> Yongxiang Hu *et al.* used femtosecond laser nanoparticle array implantation to integrate gold nanostructures into flexible microfluidic films for online SERS monitoring of oxidation reactions<sup>163</sup> (Fig. 8D) (Table 3).

### 4.3 Gas detection

To bridge the gap in real-time sensing and monitoring of neurotoxic gases for emergency response, durable and reusable SERS-enabled microfluidic chips have been

designed. Marta Lafuente *et al.* incorporated a three-dimensional photonic metal framework, consisting of mesoporous silica (MCM48) nanospheres densely decorated with gold nanoparticles (MCM48@Au), into a silicon microfluidic chip for trace gas enrichment and label-free detection. The amplification effect achieved through mesoporous silica preconcentration was benchmarked against denser silica structures (Stöber@Au), showing superior performance.<sup>164</sup>

In another study, Yanyan Lu *et al.* developed a bifunctional composite SERS substrate for trace volatile detection. This system combined a gold/silica enhancement layer with a porous  $\text{Cu}(\text{OH})_2$  adsorption layer, fabricated *via* a microfluidic-assisted gas-liquid interface self-assembly process. The platform successfully tracked temporal changes in benzaldehyde signals and enabled specific recognition of volatile organic compounds (VOCs), including benzene, xylene, styrene, and nitrobenzene. Their work highlights a

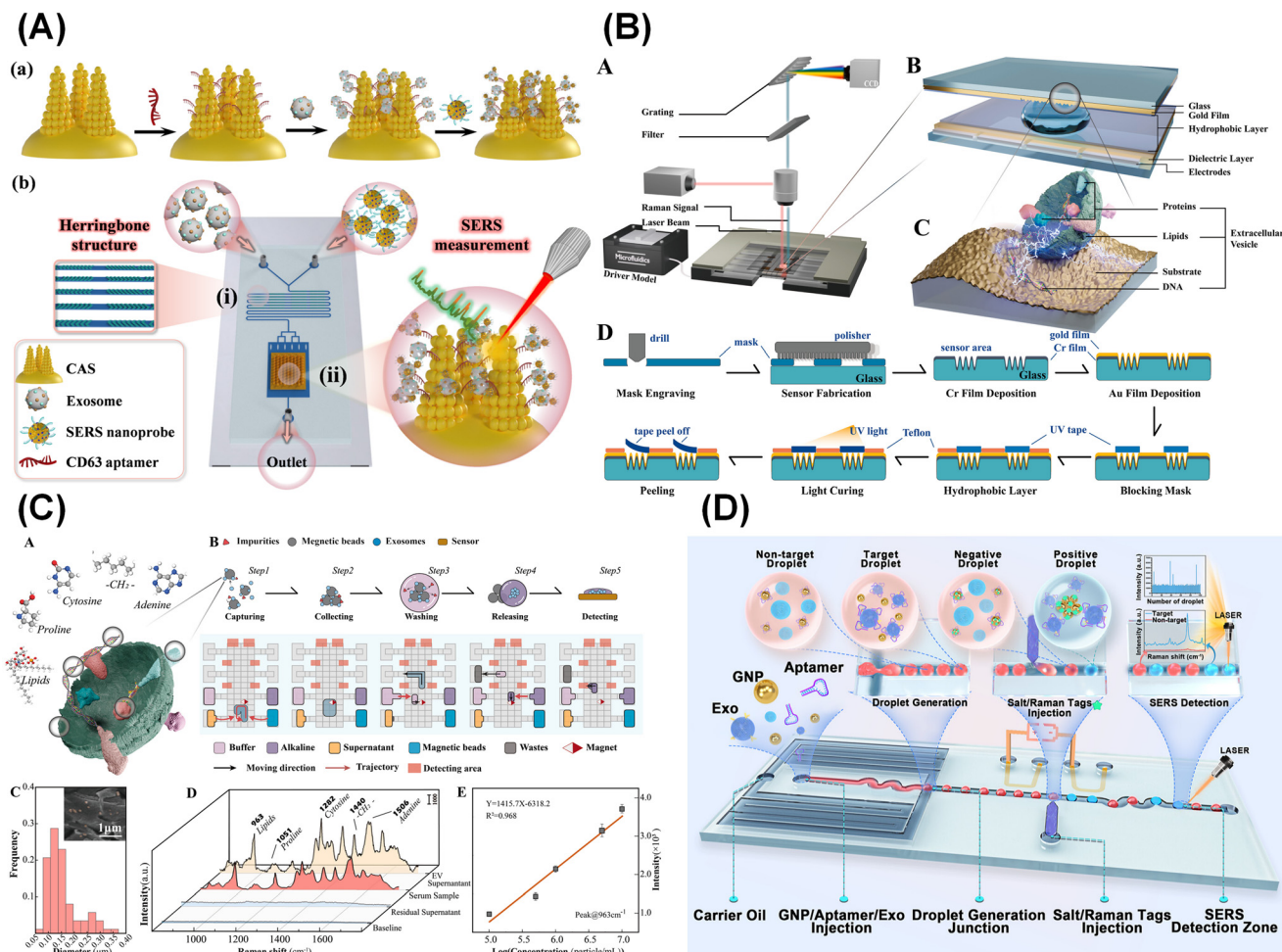


**Fig. 7** (A) (a) Formation steps of the 'sandwich' immunocomplexes on CAS. (b) Schematic illustration of the SERS-based microfluidic aptamer chip for exosome detection (i) The mixing channel of each sample; (ii) Rectangular detection chamber embedded with the CAS substrate.<sup>149</sup> (B) Integrated system that combines Raman spectroscopy with DMF for biochemical analysis. (A) The schematic of DMF based *in situ* Raman measurement system. (B) The structure of the DMF device with the TRES sensor. (C) The system allows for both on-chip enrichment and detection of exosomes. (D) The schematic process of fabricating the TRES sensor onto the DMF top plate.<sup>150</sup> (C). On-chip enrichment and detection of exosome sample.<sup>150</sup> (D). Illustration of the process of SERS-based droplet microfluidic platform for detecting HER2-positive exosomes.<sup>152</sup> Reproduced from ref. 149, 150 and 152 with permission from MDPI, Elsevier, and American Chemical Society, respectively; copyright 2024, 2025, and 2024.

straightforward and efficient approach for the SERS-based detection of trace-level gaseous VOCs.<sup>165</sup>

#### 4.4 Drug analysis

Nguyen La Ngoc Tran *et al.* employed microfluidic sensor devices to quantify dopamine in solution.<sup>166</sup> Siyue Xiong *et al.* designed a pump-free microfluidic chip integrated with a solid-state SERS-active substrate for detecting trace levels of cortisol in body fluids *via* immunoassay. The method utilized a competitive binding reaction between cortisol molecules and SERS-tagged cortisol antigens anchored on nanostructured gold, with dual detection channels serving as controls to enhance accuracy and efficiency.<sup>167</sup> Similarly, Fuqi Yao *et al.* introduced a microfluidic synthesis platform capable of producing uniform core-shell nanocubes within 15 minutes, which were subsequently applied as SERS

substrates for detecting methylene blue and the antibiotic sulfadiazine.<sup>168</sup>

Jingyu Xiao *et al.* reported a noninvasive wearable plasmonic microfluidic sensor designed for sweat sampling and concurrent monitoring of acetaminophen. The system incorporated a gold nanosphere-cone array as the SERS-active element, enabling sensitive and real-time identification of acetaminophen fingerprints.<sup>169</sup> Laura Seriola *et al.* developed a compact benchtop SERS detection system that integrates sample preparation, rapid sensing, and machine learning-based data interpretation. Using methotrexate (MTX) as a model drug in serum, the platform allowed simultaneous preparation of up to eight samples within five minutes and SERS mapping at a throughput of one test every five minutes<sup>170</sup> (Fig. 9A).

Automation was further advanced by Gohar Soufi *et al.*, who combined micro solid-phase extraction ( $\mu$ SPE) with a

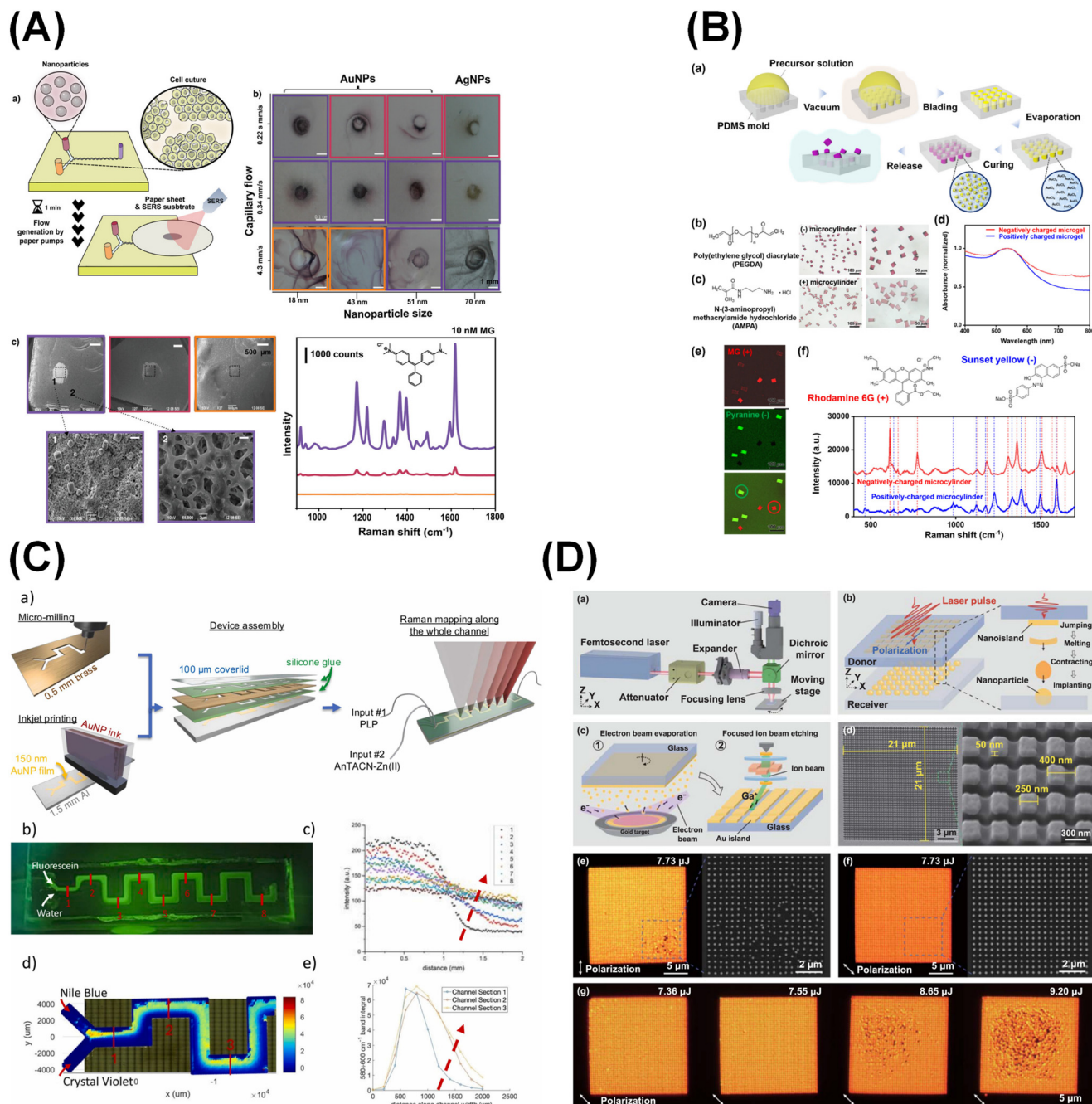


**Fig. 8** (A). a) Scheme of the custom-made device with one inlet for cell culture and another for addition of NPs. The double role of the paper sheet (as the pump and support for nanoparticles), speeds up sample collection and SERS substrate preparation, thus reducing waiting time down to ca. 1 min. b) Influence of paper capillary action and NP diameter on SERS substrate formation. In general, three different substrate qualities can be distinguished. Higher speed yielded disparate substrates (orange boxes), whereas lower velocities led to more homogeneous SERS substrates, created around the area in contact with the microfluidic outlet (violet boxes). Nanoparticles with larger sizes present restricted diffusion through the paper, resulting in a dense accumulation of NPs over heterogeneous small areas (red boxes). c) Representative SEM images of substrates with different nanoparticle distributions and their corresponding SERS spectra averaged over the indicated squared area, upon incubation with 10 nM malachite green (MG). Higher magnification images show general features of paper with (1) or without (2) NP accumulation.<sup>157</sup> (B). Production of SERS-active microcylinders with a single compartment.<sup>159</sup> (C). (a) Schematic representation of the assembled components of the chip. (b and c) Mixing test on PDMS replica of the chip using fluorescein and water under a fluorescence microscope. (d and e) Raman map at 593  $\text{cm}^{-1}$  with 250  $\mu\text{m}$  resolution. The red arrows in (c) and (e) conceptually represent the progression of the diffusion of the species through the channel section.<sup>161</sup> (D). Femtosecond laser implantation of nanoparticle array on a flexible substrate. (a) Experimental device and (b) schematic of the laser-induced forward transfer. (c) Preparation process and (d) SEM image of patterned Au islands on glass. NPAs fabricated under a vertically (e) and (f) diagonally polarized laser pulse. (g) NPAs fabricated using a diagonally polarized laser pulse with different pulse energies.<sup>163</sup> Reproduced from ref. 157, 159, 161 and 163 with permission from Wiley-VCH, American Chemical Society, Elsevier, and IOP Publishing, respectively; copyright 2023, 2023, 2025, and 2024.

**Table 3** Summary of representative microfluidic-SERS applications in liquid biopsy

Category	Detection strategy	System design/key technique	Key performance/feature	Ref.
CTCs	Label-based/single-cell Raman profiling	Single-cell trapping platform + tumor-targeted Ag nanopropes + tapered multimode optical fibers	Enhanced Raman intensity and reduced optical loss; precise single-cell analysis for pancreatic cancer	128
CTCs	Label-based	Spiral inertial separation chip + SERS-active bioprobes	>90% accuracy in distinguishing three cancer cell types from WBCs	38
CTCs	Label-based (immunoassay)	Multifunctional microfluidic device for parallel CTC and PSA detection	87% CTC capture efficiency with simultaneous PSA analysis	129
CTCs	Label-free/dual-mode recognition	Coordinated microfluidic device (CMD) + nanowire forest trapping substrate (NFTS)	Real-time phenotypic profiling of CTCs from whole blood	130
CTCs	Label-based	Mesoporous gold biosensor for ICP heterogeneity analysis	High-specificity detection of PD-L1, B7H4, CD276, CD80 in individual CTCs	131
CTCs	Label-based/multiplex Raman	High-throughput microfluidic manipulation system + multiplex Raman analysis	Suitable for <i>in vitro</i> cancer diagnostics and parallel CTC analysis	132
CTCs	Label-free	PMMA-TCNA chip with Au film substrate	Enrichment and sensitive Raman identification of PC3 cells	133
RNA detection	Label-based/hybridization	Continuous-flow microfluidic LSPR monitoring of oligonucleotide-sensor interactions	Real-time observation of probe hybridization dynamics	134
RNA detection	Label-based	Automated multi-chamber microfluidic chip + portable Raman for miR-214	Portable miRNA detection platform	135
RNA detection	Label-based	MCASS microchip for miR-141 detection	Enhanced Raman sensitivity and larger probe-modification area	136
RNA detection	Label-based/multiplex imaging	Barcoded microfluidic SERS chip + encoded nanorod aggregates + micromixer	Multiplex miRNA imaging with enhanced hybridization efficiency	137
RNA detection	Label-based/amplification-assisted	RCA + microdroplet-based SERS detection	Single-nucleotide resolution and improved reproducibility for miRNA-21/155	138
RNA detection	Label-based/LFA	LFA-based SERS test with DNA hairpin probes + SERS nanopropes	Sensitive hsa-miR-17-5p detection for early pregnancy biomarker screening	139
DNA detection	Label-based	DDHS-integrated microfluidic chip for CD63-mediated exosome capture	Ultra-low detection limit of 2.63 particles/ $\mu$ L	140
DNA detection	Label-based/amplification-assisted	High-throughput chip with EASA + CHA + hpDNA-modified Au nanocone arrays	Sensitive ctDNA detection in lung cancer mouse models	141
DNA detection	Label-free/direct detection	Finger-actuated chip with filtration grooves for ctDNA from whole blood	Amplification-free ctDNA analysis with high sensitivity	142
DNA detection	Label-based/isothermal amplification	Microdroplet SERS with enzymatic recycling (ER) reaction	Single-molecule sensitivity within 20 min	143
Exosome detection	Label-free/secretion profiling	SERS-integrated microfluidic chip for single-cell exosome secretion analysis	Distinguishes breast cancer subtypes and monitors drug response	144
Exosome detection	Label-based/multiplex glycoprofiling	EV-GLYPH microfluidic SERS platform	Differentiates malignant and benign lung nodules	145
Exosome detection	Label-based/multiplex tags	Serpentine-channel chip with multiplexed SERS tags	Automated profiling of multiple EV tumor biomarkers	146
Exosome detection	Label-based	Deep learning-assisted chip + PACD enrichment for NSCLC exosomes	Raman-based subtype analysis of NSCLC-derived exosomes	147
Exosome detection	Label-free/isolation + classification	Size-based chip + tangential flow filtration	82% recovery and >93% diagnostic accuracy for osteosarcoma exosomes	148
Exosome detection	Label-based	Cactus-like nanostructured SERS array	Enhanced sensitivity for prostate cancer-derived exosome detection	149
Exosome detection	Label-free/portable analysis	Digital microfluidics + Raman spectroscopy for serum exosomes	Portable and real-time serum exosome monitoring	150
Exosome detection	Label-based/multiplex	Seven-channel chip (S-MMEV) for simultaneous sEV biomarker analysis	Accurate differentiation of ovarian cancer <i>vs.</i> healthy controls	151
Exosome detection	Label-based/droplet aptasensor	Droplet microfluidic-SERS aptasensor for HER2-positive exosomes	High sensitivity <i>via</i> nanoparticle aggregation hotspots	152
Other biomarkers	Label-based	AuNP monolayer sensor + Fe(III) sensitizers	Dopamine detection at nanomolar levels	153
Other biomarkers	Label-based	AuNPs/MoS <sub>2</sub> composites <i>via</i> microfluidic-assisted growth	Sensitive adenine and cytosine detection	154
Other biomarkers	Label-based	AgNP-doped hydrogel microbeads <i>via in situ</i> polymerization	Selective ALP detection <i>via</i> small-molecule permeability	155
Other biomarkers	Label-free	Plasmonic polymer-embedded AuNP film	Stable amino acid analysis across broad pH and temperature ranges	156
Other biomarkers	Label-free/paper-based	Paper capillary pump-assisted SERS microfluidic system	Simplified analysis of cell secretions	157
Other biomarkers	Label-based/multiplex	Nanostructured SERS microfluidic biosensor	Simultaneous detection of serotonin, dopamine, and cortisol	158

Table 3 (continued)

Category	Detection strategy	System design/key technique	Key performance/feature	Ref.
Other biomarkers	Label-free	SERS-active cylindrical microgels <i>via</i> photo-crosslinking	Stable small-molecule detection without preprocessing	159
Other biomarkers	Label-free	Plasmonic cellulose microfilaments coated with AgNPs	Automated recognition for urea detection	160
Other biomarkers	Label-free/reaction monitoring	Inkjet-printed AuNP films on aluminum foil within chip	Monitoring of biomimetic reaction kinetics	161
Other biomarkers	Label-based	Magneto-plasmonic nanostirrers carrying Raman reporters	Improved reproducibility in IL-6 detection	162
Other biomarkers	Label-based/dual biomarker detection	3D AuNP hydrogel microparticles with hierarchical nanostructures	Simultaneous AFP and AFU detection	46
Other biomarkers	Label-free/online monitoring	Femtosecond laser-implanted Au nanostructures in flexible films	Online SERS monitoring of oxidation reactions	163

centrifugal microfluidic disc (CD-SERS) containing embedded SERS substrates. This configuration enabled uniform wetting, reproducible measurements, and label-free quantification of MTX and lamotrigine (LTG) in serum. Robust analysis was achieved using partial least squares regression (PLSR)<sup>171</sup> (Fig. 9B). Tania K. Naqvi *et al.* proposed a flexible, paper-based, pump-free microfluidic SERS device for cost-effective detection of triazolone, in which hydrophilic channels were engraved with wax molds and hot-pressing.<sup>172</sup>

Sebastian Fehse *et al.* presented a recyclable, chip-integrated SERS substrate fabricated by photochemical deposition of silver nanoparticles on TiO<sub>2</sub> films. The photocatalytic activity of TiO<sub>2</sub> allowed substrate reuse, enabling near real-time detection in an automated DMF-SERS system.<sup>173</sup> Junjie Chen *et al.* exploited an S-shaped microfluidic chip to synthesize monodispersed silver microparticles for ultrasensitive SERS applications.<sup>174</sup> Shuoyang Yan *et al.* developed a colloidal SERS platform based on cavity-like silver aggregates, offering stable flow-based detection windows for monitoring and identifying photochemical intermediates *in situ*<sup>175</sup> (Fig. 9C).

Additional contributions include Hongyu Li *et al.*, who fabricated a side-polished multimode fiber (SPMF) probe by depositing gold nanorods and embedding it within a microfluidic channel, forming a glass-based chip for detecting pesticide and antibiotic residues in tap water.<sup>176</sup> Wang Peng *et al.* demonstrated a porous SiC-Ag nanoparticle hybrid substrate integrated into a microfluidic chip for rapid trace substance detection.<sup>177</sup> Tongtong Zhang *et al.* applied direct laser writing to fabricate citric acid-modified silver aggregates inside microchannels, enabling quantitative SERS analysis of weakly interacting compounds such as the antidiabetic drug rosiglitazone.<sup>178</sup>

#### 4.5 Disease diagnosis

Ziting Qian *et al.* developed a three-dimensional organotypic microfluidic chip that incorporates SERS-based protein imprinting nanomaterials (SPINs) to investigate tumor cell extravasation *in vitro*. The platform integrates a collagen gel channel and a vascular channel sequentially seeded with

human umbilical vein endothelial cells (HUVECs) and breast cancer cells, enabling real-time observation of tumor cell extravasation. This model offers new opportunities for fundamental studies of cancer metastasis and for evaluating the efficacy of therapeutic interventions.<sup>179</sup>

Jianli Sun *et al.* fabricated a microfluidic biosensor consisting of a polystyrene/gold nanoparticle (PS/AuNP) microsphere array mounted on a quartz substrate. This lab-on-a-chip system demonstrated potential as a powerful platform for the early detection of circulating cancer biomarkers in blood samples.<sup>180</sup>

Xin Wang *et al.* integrated highly sensitive SERS detection into a microfluidic device to monitor VEGF secretion and pH fluctuations of the extracellular microenvironment during oxidative stress at the single-cell level. Magnetic bead-based capture probes formed immunosandwich complexes on the cell surface, significantly amplifying the SERS reporter signal and enhancing detection accuracy.<sup>181</sup> Wenwen Yuan *et al.* created a low-cost, paper-based nanocellulose analytical microfluidic device (NanoPAD) for SERS-based immunoassays of Alzheimer's disease biomarkers, successfully detecting glial fibrillary acidic protein (GFAP) in blood<sup>182</sup> (Fig. 9D).

In another study, Jianli Sun *et al.* designed a microfluidic system using PS microspheres coated with gold nanosheets to simultaneously detect A $\beta$ 1–42 and p-tau181 proteins at femtogram concentrations. Multiple test and control channels enabled ultrasensitive and quantitative detection of Alzheimer's disease biomarkers with a detection limit of 100 fg mL<sup>-1</sup> (ref. 183) (Fig. 10A). Qian Jin *et al.* developed a SERS-coupled SlipChip for single-cell metabolic profiling. This device compartmentalized individual cells and delivered saponins and nanoparticles in parallel to release metabolites, enabling multiplex SERS detection through a simple sliding motion. Tests on multiple cancer cell lines confirmed its sensitivity and high-throughput potential<sup>138</sup> (Fig. 10B).

Ankita Jaiswal *et al.* reported a PDMS-based microfluidic device for detecting  $\beta$ -amyloid peptide (A $\beta$ 1–42) in simulated cerebrospinal fluid. Using a purine-AgNP SERS substrate, the device produced strong hotspot signals and achieved excellent detection limits.<sup>184</sup> Xiaopeng Liu *et al.* introduced a SERS microfluidic chip designed for single-cell monitoring of

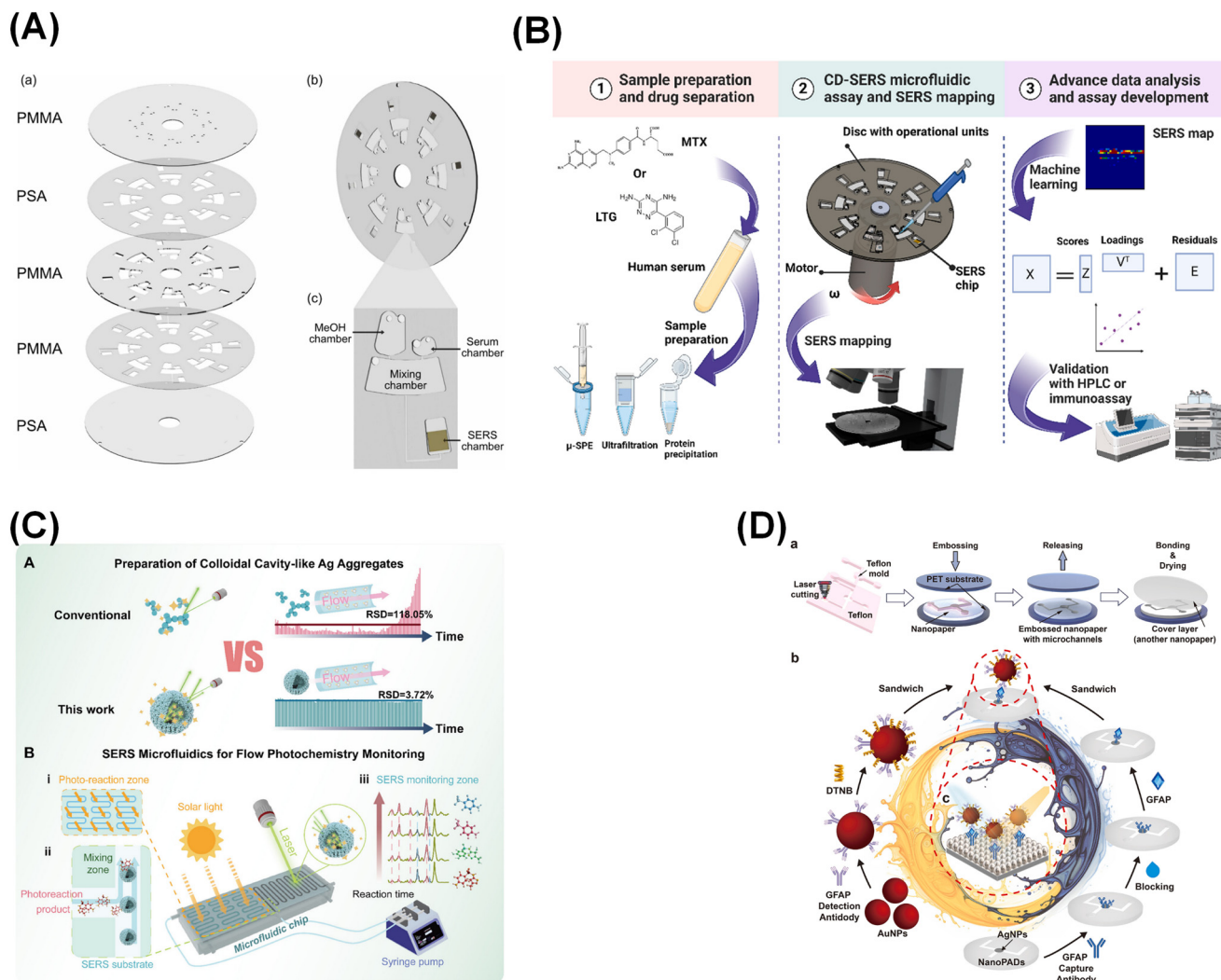


**Fig. 9** (A) The LoC cartridge is the centrifugal microfluidics design for nanopillar-assisted separation (NPAS) on disc. a) Explosion view of the disc with different layers. b) Prospective view of the design and close-up to a working unit and its specifications.<sup>170</sup> (B) Overall procedure of the drug quantification assay implemented in this work: 1) sample preparation, by spiking MTX and LTG in human serum, and drug separation performed by evaluating PP, UF and  $\mu$ -SPE. 2) The CD-SERS microfluidic assay design in which the separated drug is introduced on the disc; the disc is spun and centrifugal forces enable migration of the analyte on the SERS chip, placed in the sensing chamber; then the entire SERS chip is mapped. 3) Advanced data analysis of the SERS map with machine learning algorithms for drug quantification, and analytical validation with HPLC and immunoassay.<sup>171</sup> (C) A) Comparison of Ag cavity and conventional aggregates. B) Schematic diagram of the construction of the online SERS-microfluidics PAT platform and its use in monitoring flow photochemistry. i) Photodegradation zone; ii) mixing zone; iii) online SERS monitoring zone.<sup>175</sup> (D) Schematic of SERS detection. (a) Schematic of NanoPADs fabrication. (b) Preparatory illustration of SERS-based immunoassay for detecting the AD biomarker GFAP. (c) Schematic of SERS-based immunoassay.<sup>182</sup> Reproduced from ref. 170, 171, 175 and 182 with permission from Elsevier, Elsevier, Wiley-VCH, and Elsevier, respectively; copyright 2024, 2024, 2025, and 2024.

PTK7 receptor expression, enabling discrimination among colorectal cancer subtypes through migration assays in cell channel arrays.<sup>185</sup>

Kang Shen *et al.* proposed a pump-free LoC-SERS device based on D-amino acid oxidase (D-AAO)-mediated cascade reactions for quantifying D-proline and D-alanine, metabolites linked to gastric cancer<sup>186</sup> (Fig. 10C and D). Mengyue Wang *et al.* developed a SERS-enabled microfluidic immunoassay for the multiplexed quantification of acute ischemic stroke (AIS) biomarkers.<sup>187</sup> Dechun Zhang *et al.* combined 4D quantitative proteomics, a nano-hybrid-enhanced SERS chip, and machine learning to identify blood protein biomarkers related to

micropapillary (MPP) components in lung adenocarcinoma, aiding surgical decision-making<sup>188</sup> (Fig. 11A).

Kuo Yang *et al.* introduced a microfluidic SERS system coupled with machine learning to classify T-cell acute lymphoblastic leukemia (T-ALL) and chronic myeloid leukemia (CML), using ordered microchannel arrays for efficient tumor cell capture<sup>189</sup> (Fig. 11B). Jiahao Zhang *et al.* built an inertial microfluidic chip combined with label-free SERS probes for gastric cancer detection, successfully enriching tumor cells from gastric juice and ascites samples<sup>190</sup> (Fig. 11C). Mei-Chin Lien *et al.* presented a flexible plasmonic biosensor strip for SERS-based detection of uric acid in tears, achieving a detection limit

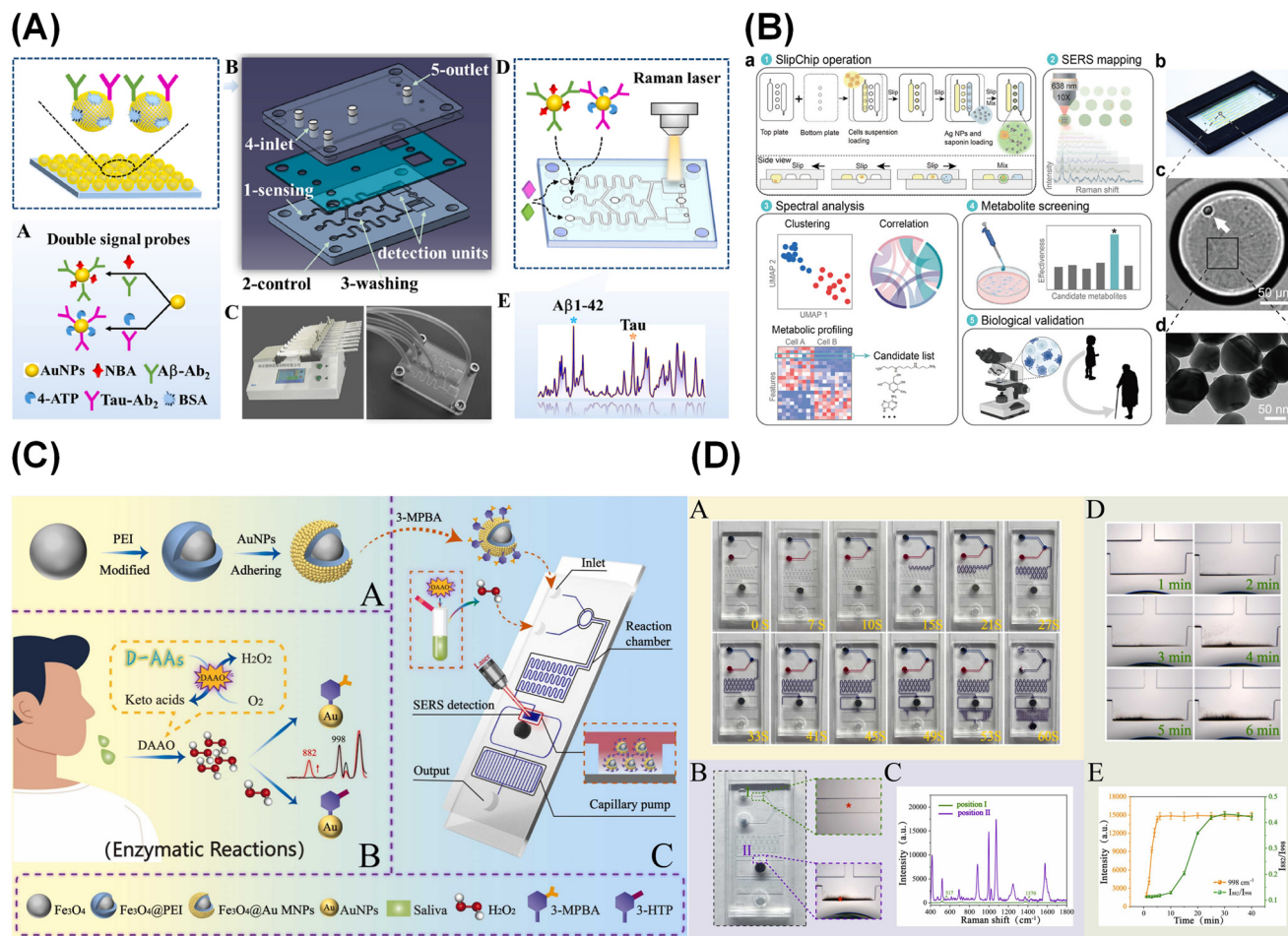


**Fig. 10** (A). Schematic illustrations of PS/Au-based SERS immunosensing chip for sensitive detection of Aβ<sub>1-42</sub> and tau protein.<sup>183</sup> (B). The detection of metabolic profiling at single-cell level via SlipChip-SERS microfluidic platform.<sup>138</sup> (C). (A) The procedure of synthesizing Fe<sub>3</sub>O<sub>4</sub>@Au MNPs. (B) Schematic diagram of the enzymatic reaction. (C) LoC-SERS device detects D-AAAs in saliva of GC patients.<sup>186</sup> (D). (A) Images of red-blue dye in LoC-SERS device channels flowing automatically by capillary force. (B) Two SERS detection sites (position I, position II) and (C) their corresponding SERS spectra of pump-free LoC-SERS device. (D) LoC-SERS device magnetic bead collection test and (E) corresponding time-obtained SERS intensity and 1882/1998 value.<sup>186</sup> Reproduced from ref. 138, 183 and 186 with permission from Elsevier, Elsevier, and Elsevier, respectively; copyright 2023, 2024, and 2024.

of ~10 μM, offering non-invasive diagnostics for gout.<sup>191</sup> Finally, Weian Wang *et al.* optimized photonic crystal structures with semi-coated gold nanospheres to enhance resonance efficiency, creating a SERS-based microfluidic biosensor for melanoma diagnosis<sup>192</sup> (Fig. 11D).

#### 4.6 Detection of environmental hazardous substances

Microplastic (MP) contamination poses growing risks to both ecosystems and human health, driving demand for rapid detection technologies. Ji Woo Jeon *et al.* introduced the MiDREAM system (microplastic detection in real-time via ML-integrated droplet analysis), which employs a peristaltic pump to generate high-throughput droplets encapsulating MPs, coupled with CMOS imaging and a YOLO v8 machine learning algorithm for real-time classification. This portable system enables efficient on-site environmental monitoring.<sup>193</sup>

Phenyl ether herbicides (PHs), widely used in agriculture, threaten ecological and human safety. Xu Wang *et al.* integrated microfluidic glass liquid chromatography (LC) with electrochemical detection (ECD) and SERS to analyze PH residues. The hybrid platform successfully achieved complete separation and quantitative analysis of three PH compounds.<sup>194</sup>

For detecting per- and polyfluoroalkyl substances (PFAS), Chunyu Li *et al.* functionalized microstructured optical fibers with β-cyclodextrin and silver nanoparticles, enabling direct SERS-based identification of PFAS with detection limits as low as 40 ng L<sup>-1</sup> for perfluorooctanoic acid.<sup>195</sup> Yiyue Yu *et al.* fabricated an anemone-like nanoarray substrate (ALAS) integrated into a pump-free microfluidic chip. The ordered plasmonic nanoantenna array enhanced light capture efficiency, enabling highly sensitive mercury ion detection<sup>196</sup> (Fig. 12A and B). Suyang Li *et al.* further synthesized uniform Ag@Au core-shell nanoparticles in microfluidic reactors, generating stable SERS substrates for pollutant detection.<sup>197</sup>

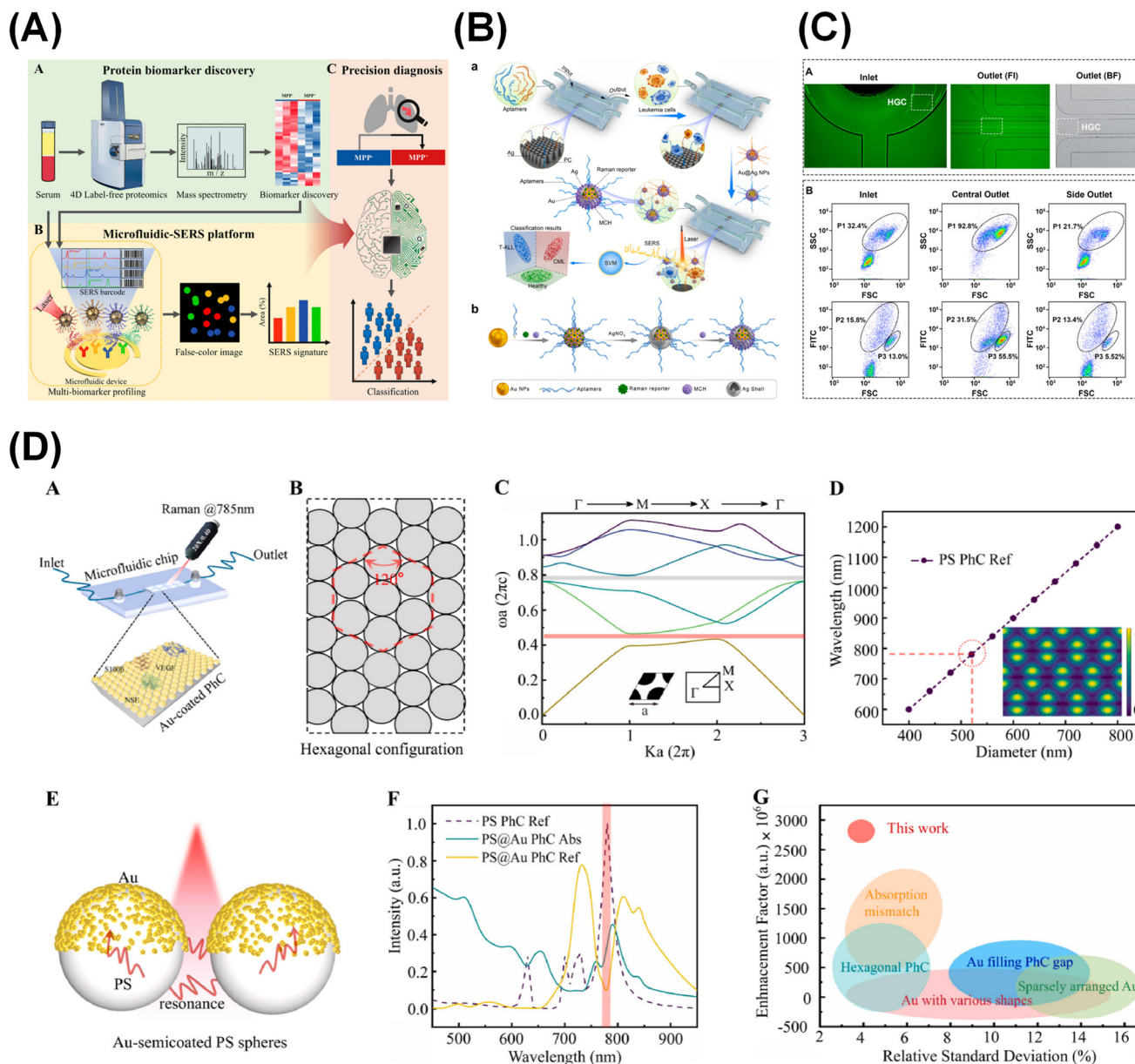


**Fig. 11** (A). Workflow from blood biomarker discovery to the development of a microfluidic-SERS immunoassay for MPP<sup>+</sup> LUAD detection.<sup>188</sup> (B). Schematic illustration of leukemia phenotyping.<sup>189</sup> (C). Cancer cells separation using an inertial microfluidic chip with periodic expansion structures.<sup>190</sup> (D). Design of Au-semicoated PhC for SERS.<sup>192</sup> Reproduced from ref. 188–190 and 192 with permission from Wiley-VCH, Elsevier, American Chemical Society, and Elsevier, respectively; copyright 2025, 2025, 2025, and 2025.

Mirkomil Sharipov *et al.* developed a paper-based microfluidic sensor decorated with molecularly imprinted nanogels and AgNPs for dual detection of bisphenol A (BPA) and bisphenol S (BPS) in plastics. The device supported both “drop-and-read” single-analyte detection and simultaneous BPA/BPS measurement using interconnected reservoirs<sup>198</sup> (Fig. 12C). Qian Ke *et al.* demonstrated a microfluidic SERS strategy for rapid detection of acetaminophen in tea. A dual-channel chip with multiple circular mixing units enabled efficient analyte–substrate interactions, providing a reliable method for pesticide residue analysis.<sup>199</sup>

Xing Wang *et al.* created a dual-function hydrogel-SERS microfluidic platform with four independent channels, each controlled by heat-activated hydrogel switches. The device simultaneously detected triazolone, pyrene, anthracene, and dibutyl phthalate, and incorporated deep learning algorithms for classification and prediction<sup>200</sup> (Fig. 12D).

SERS-based microfluidic approaches have also been applied to national security. Giulia Zappalà *et al.* coupled SERS with centrifugal microfluidics for real-time identification of chemical warfare agents (CWAs), enabling reliable on-site quantification<sup>201</sup> (Fig. 13A). Zihan Wang *et al.* fabricated structurally tunable silver aerogels combined with digital microfluidics (AgA-DMF) for

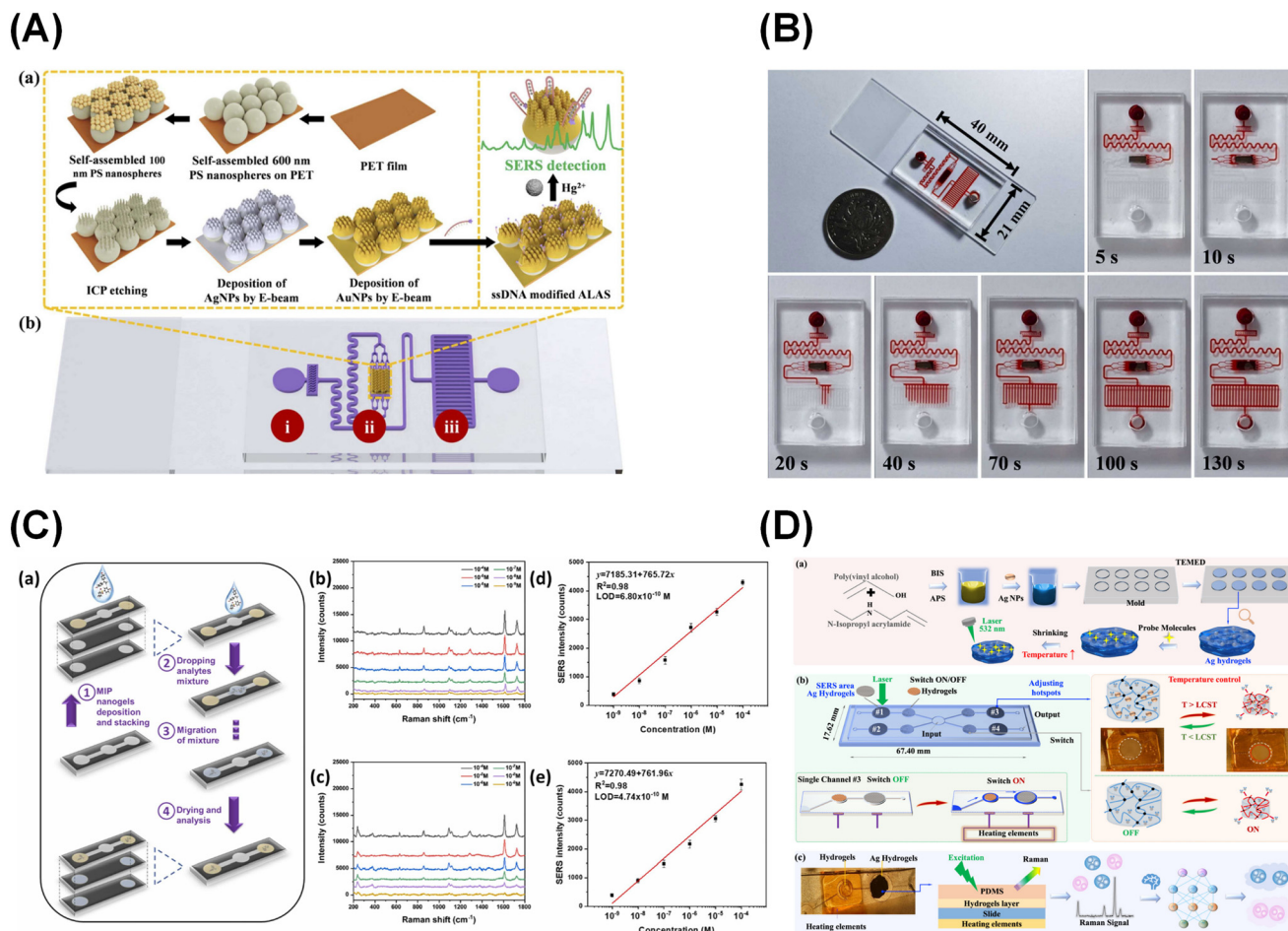


**Fig. 12** (A). (a) Schematic of the fabrication of anemone-like array substrate and  $\text{Hg}^{2+}$  detection, and (b) The pump-free microfluidic sensor contained three functional compartments: (i) sample injection section, (ii) SERS detection section, (iii) fluid driven section.<sup>196</sup> (B). The photograph of the microfluidic sensor and the capillary-driven flow process of red ink in the microfluidic channel over time.<sup>196</sup> (C). Analytical performance of the microfluidic SERS system. Schematic illustration of the microfluidic paper-based SERS device.<sup>198</sup> (D). Experimental flowchart. (a) Preparation process of Ag NPs-NIPAM/PVA hydrogel composite structure. (b) Dual-functional hydrogel-based microfluidic nanoplasmonic SERS sensing platform. (c) Actual image of one channel on the microfluidic SERS platform, and Raman measurement and deep learning assistant recognition verification.<sup>200</sup> Reproduced from ref. 196, 198 and 200 with permission from Elsevier, Elsevier, and American Chemical Society, respectively; copyright 2024, 2024, and 2025.

ultra-sensitive detection of hazardous substances such as TNT ( $10^{-8}$  M), NTO ( $10^{-9}$  M), and methylene blue ( $10^{-9}$  M)<sup>202</sup> (Fig. 13B). Wei Liu *et al.* further advanced SERS-DMF systems by integrating 40 driving and 8 storage electrodes into microfluidic chips, achieving automated high-throughput detection of explosives with improved reproducibility<sup>203</sup> (Fig. 13C). Finally, Caterina Credi *et al.* developed polymer-based fluidic platforms integrating optical functionalities using photopolymerizable PFPE materials, enabling scalable, anti-fouling, and fiber-compatible SERS chip fabrication for environmental and defense applications<sup>204</sup> (Fig. 13D).

Overall, the analysis of current applications suggests that the role of machine learning is highly context-dependent. In applications involving well-defined targets and strong reporter signals, such as nucleic acid detection or immunoassays, microfluidic-SERS systems can often achieve high analytical performance without complex data-driven models. In these cases, the primary advantages arise from improved fluid

control, enhanced signal reproducibility, and efficient multiplexing. However, in more complex scenarios, particularly those involving label-free detection of heterogeneous biological samples, the intrinsic limitations of SERS, including spectral overlap, noise, and variability, become more pronounced. Under these conditions, machine learning is not merely a supplementary tool but a necessary component for achieving clinically meaningful performance. It enables the extraction of subtle spectral features and supports robust classification in situations where traditional analysis would be insufficient. Therefore, the effectiveness of microfluidic-SERS systems should not be evaluated solely based on device performance or algorithm selection in isolation, but rather on the coordinated interaction between signal generation, sample control, and data interpretation strategies. This integrated perspective is essential for guiding future system design and for understanding the true capabilities and limitations of different application approaches.

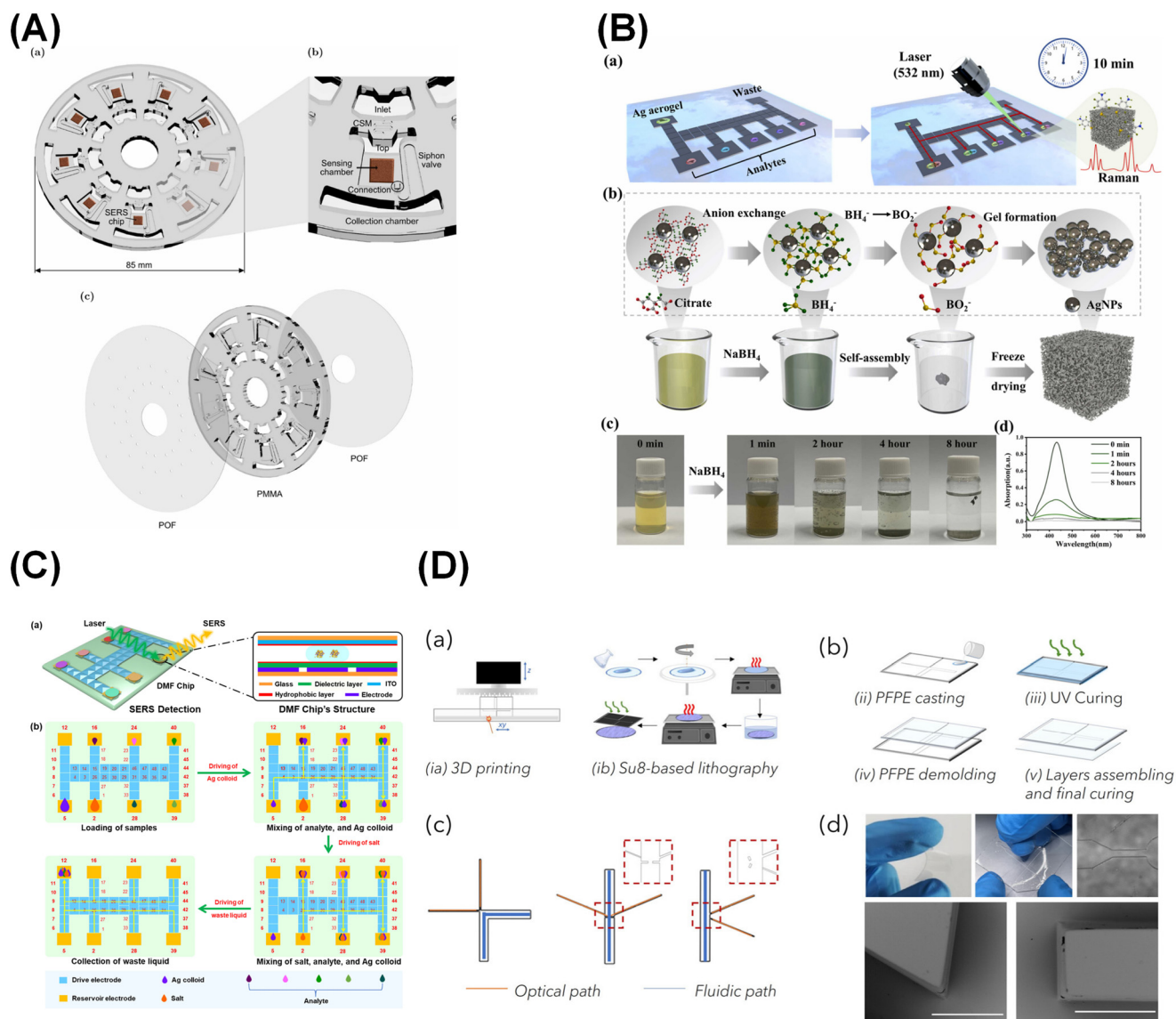


**Fig. 13** (A). (a) CM platform design rendering in perspective view. (b) Enlargement of one set of fluidic elements which enable fluidic unit operations. (c) Render of CM platform PMMA and POF layers. Top POF foil layer (100  $\mu\text{m}$  thick) for venting and loading holes. PMMA (3 mm thick) layer for chambers and SERS substrate integration. Bottom POF foil layer (100  $\mu\text{m}$  thick) to seal the device.<sup>201</sup> (B). (a) Detection schematic illustration based on AgA–DMF SERS platform. (b) The diagram of  $\text{NaBH}_4$  induced gelation mechanism. (c) Photographs of the fabrication process of the Ag aerogel. (d) The *in situ* UV-vis absorption spectra monitoring the gelation process.<sup>202</sup> (C). Schematic illustration of the SERS-based detection of trace explosives combined with digital microfluidics. (a) Illustration of the SERS–DMF platform and the structure of the DMF chip. (b) Working principle of the SERS–DMF platform for the high-throughput detection of explosives.<sup>203</sup> (D). (a) Fabrication of negative molds through (ia) laser-based 3D printing and (ib) Su8-based lithography. (b) Scheme depicting the REM fabrication of monolithic PFPE devices: (ii) pouring PFPE prepolymer–PI mixture onto the molds, (iii) UV-curing PFPE, (iv) peeling off the mold and (v) sealing with a flat layer of partially cured PFPE. (c) Designs of the optofluidic devices fabricated with different relative positions between the optical and fluidic paths. (d) Pictures (upper panel) and SEM images (lower panel) of monolithic PFPE microfluidic devices obtained by implementing the replica molding of 3D printed stamps (the scale bar for SEM images is 200  $\mu\text{m}$ ).<sup>204</sup> Reproduced from ref. 201–204 with permission from Elsevier, Elsevier, American Chemical Society, and MDPI, respectively; copyright 2025, 2024, 2023, and 2023.

## 5. Integration of microfluidic–SERS with wearable devices for dynamic and continuous monitoring

Yue Wang *et al.* presented a one-step fabrication strategy for a capillary-driven, point-of-care microfluidic chip created *via*

femtosecond laser direct writing. The device incorporates a catalytic system consisting of titanium dioxide nanoparticles with affinity for 5-aminosalicylic acid and potato root peroxidase, enabling intracellular  $\text{H}_2\text{O}_2$  detection. A semiconductor-based SERS quantification module was integrated, and the platform was successfully applied to the rapid measurement of hydrogen peroxide in MCF-7 breast

cancer cells.<sup>205</sup> Jingyu Xiao *et al.* designed a wearable plasmonic microneedle sensor for interstitial fluid (ISF) sampling and minimally invasive uric acid monitoring. The device employs negative pressure generated by finger pressing to extract ISF *via* a hollow microneedle array, which transports the fluid through microfluidic channels into the sensing chamber for SERS detection. This high-density array allowed label-free, ultrasensitive detection of uric acid.<sup>206</sup> Mengsu Hu *et al.* reported a silk fibroin-based sensing patch incorporating a self-assembled bimetallic inverse opal nanostructure, which provided uniform SERS hotspots for enhanced Raman signals. Integrated microfluidic channels enabled controlled, time-resolved sweat management, improving sample collection efficiency.<sup>207</sup>

Siyue Xiong *et al.* developed a flexible, portable microfluidic SERS device constructed from modified PDMS with self-adhesive properties. The chip contained densely distributed hotspots created using angled-deposition silver nanotriangles (AgNTs). Coupled with a one-dimensional convolutional neural network, the platform achieved high-accuracy, quantitative analysis of urea and glucose<sup>208</sup> (Fig. 14A). In another study, Mengsu Hu *et al.* created a silk fibroin-based binary nanosphere array SERS substrate and introduced a pseudoknot-assisted aptamer probe for cortisol detection. By combining epidermal microfluidics with a wearable patch, sweat could be collected without stimulation, enabling dynamic monitoring of cortisol and pH levels in real time<sup>209</sup> (Fig. 14B).

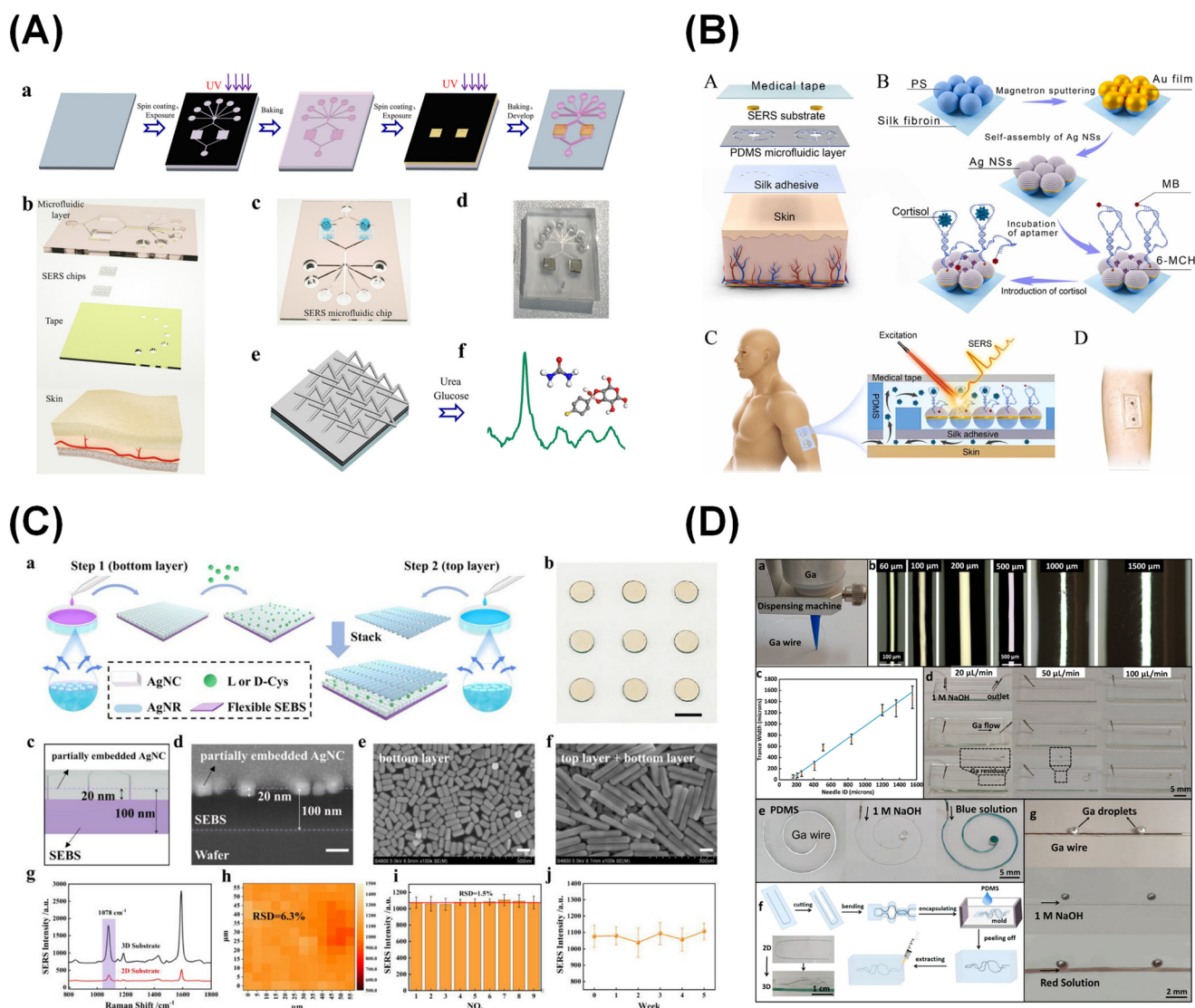


**Fig. 14** (A). Design of a portable, flexible SERS microfluidic chip.<sup>208</sup> (B). (A) Stacked view of the SF-based wearable microfluidic SERS biosensor. (B) The preparation process of SFOS/Au/Ag NSs substrate and cortisol measurement. (C) Conceptual diagram of the wearable sweat sensing patch and the cross-sectional view of the microfluidic SERS sensor. (D) Photograph of the microfluidic SERS sensing patch mounted on the forearm.<sup>209</sup> (C). Preparation and characterization of 3D chiral SERS flexible sensing element.<sup>210</sup> (D). Demonstration of microfluidic channel prepared by the direct-writing method.<sup>211</sup> Reproduced from ref. 208–211 with permission from American Chemical Society, Elsevier, Wiley-VCH, and American Chemical Society, respectively; copyright 2024, 2025, 2025, and 2023.

Shuang-Feng Pan *et al.* proposed a wearable patch combining microfluidics with three-dimensional chiral plasmonic nanostructures for SERS-based metabolic profiling of chiral molecules in sweat. The system enabled *in situ*, real-time collection and analysis of microliter-scale sweat samples<sup>210</sup> (Fig. 14C). Similarly, Qingwei Yuan *et al.* introduced a self-adhesive microfluidic chip integrating erasable liquid-metal plasmonic hotspots for glucose monitoring in sweat. Fabricated from modified PDMS with improved adhesion, the device closely conforms to the skin to collect, channel, and store sweat, enabling sensitive and accurate SERS detection of glucose<sup>211</sup> (Fig. 14D).

Kuo Yang *et al.* demonstrated a wearable SERS patch equipped with manually operated microfluidics for on-demand

detection of urea and uric acid. A liquid valve allowed users to direct sweat to distinct sensing zones, enabling up to five independent sampling events<sup>212</sup> (Fig. 15A). Yang Li *et al.* fabricated a flexible, paper-based wearable microfluidic SERS device integrated with a portable Raman spectrometer for continuous sweat monitoring. Its segmented microchannels allowed adjustable flow rates, facilitating rapid signal acquisition. The nanostructured paper sensor enabled molecular penetration and enrichment, allowing precise quantification of uric acid and pH<sup>213</sup> (Fig. 15B). Siyue Xiong *et al.* also used oblique angle deposition (OAD) to create ordered, high-density gold nanorod arrays (AuNRAs) on a digital microfluidic (DMF) chip. The AuNRA substrate, combined with the DMF system's low reagent consumption and automation,

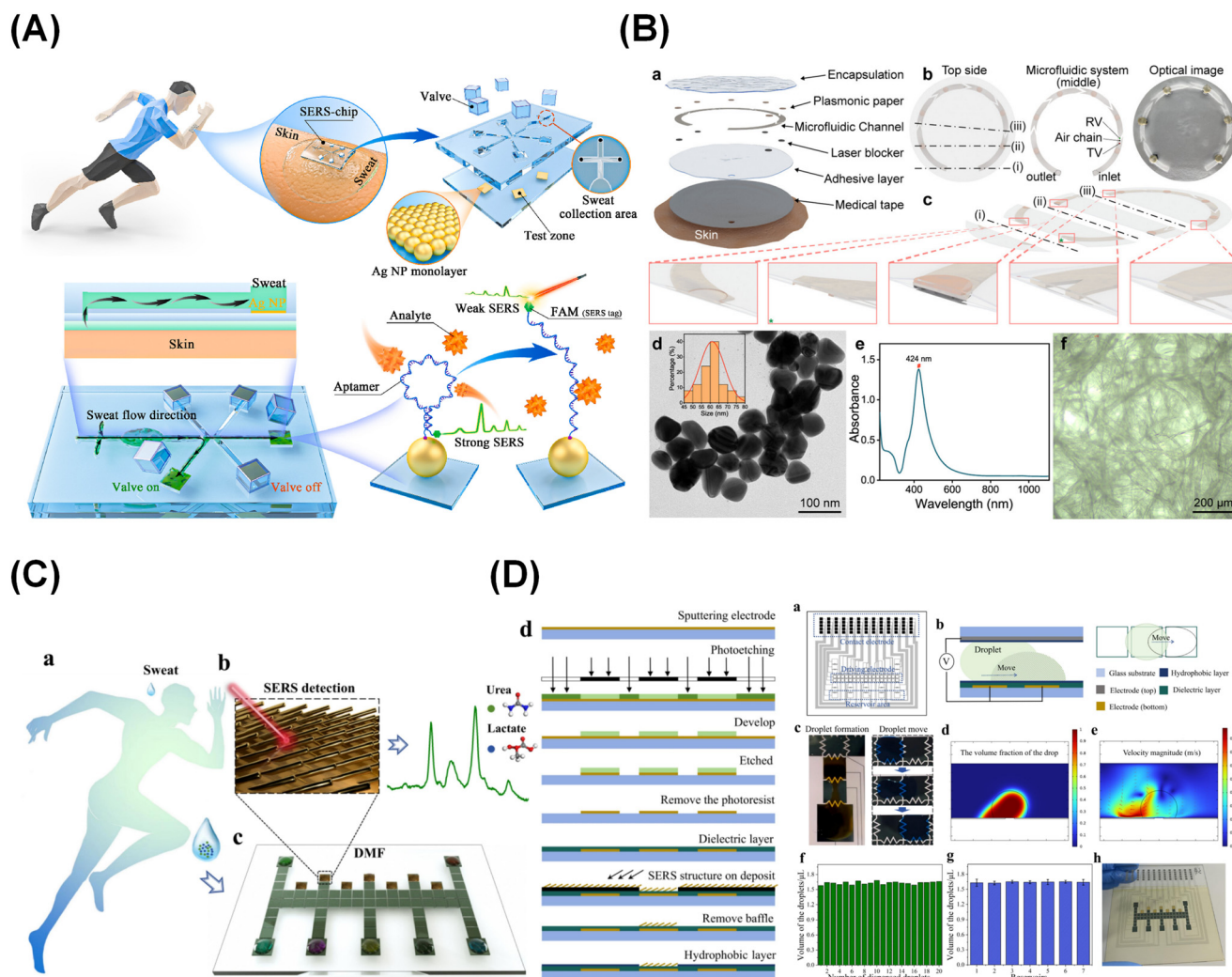


**Fig. 15** (A). Schematic diagram of the wearable SERS-microfluidic patch towards sweat-based on-demand kidney health monitoring.<sup>212</sup> (B). (a) Schematic diagram of an FWPPM sweat monitoring device. (b) Top, middle, and optical images of the device. (c) Cross-sectional views of the incisions defined by the dashed lines (i), (ii), and (iii) on the top side of (b), showing magnified sections corresponding to liquid outlet, inlet, detection site, air chain throttle valve (TV), and throttling rupture valve (RV), respectively. (d) Transmission electron microscopy (TEM) image with corresponding size distribution (inset) and (e) UV-vis-NIR absorbance spectrum of Ag NPs. (f) Spatial structural image of filter paper fibers.<sup>213</sup> (C). Design of the digital microfluidic chip. (a) Diagram illustrating sweat biomarkers. (b) SERS detection and AuNRAs diagram. (c) Diagram of the digital microfluidic chip. (d) Process flowchart for fabricating the DMF lower electrode plate.<sup>214</sup> (D). Fabrication of the digital microfluidic chip.<sup>214</sup> Reproduced from ref. 212–214 with permission from Elsevier, American Chemical Society, and Elsevier, respectively; copyright 2025, 2024, and 2025.

enabled fast, label-free SERS detection of sweat biomarkers, including urea and lactic acid, within 10 minutes<sup>214</sup> (Fig. 15C and D).

## 6. Challenges and future perspectives

This review has examined a wide range of microfluidic platforms combined with surface-enhanced Raman scattering (SERS) for disease diagnostics. By enabling precise fluid handling at nanoliter volumes, microfluidics offers high sensitivity and reproducibility, making it a promising approach for point-of-care (POC) testing, particularly in the rapid and accurate detection of infectious diseases. Conventional *in vitro* diagnostic tools, such as chemiluminescence and fluorescence assays, rely on photon emission processes and have long been applied to analyze biological fluids (*e.g.*, blood, urine, nasal secretions). However, these techniques are often limited by insufficient sensitivity and difficulties in real-time deployment. In this context, SERS has emerged as a strong candidate to overcome such barriers and is widely regarded as a next-generation POC diagnostic strategy.

Despite these advances, important challenges remain before SERS–microfluidic devices can be routinely implemented. Improving the sensitivity, reproducibility, and quantification accuracy of SERS signals, alongside robust calibration and multiplexing capabilities, will be crucial. The design of SERS tags is particularly complex, as no single strategy is universally applicable across the wide diversity of inorganic nanoparticles and biomolecules. The highly tunable physicochemical properties of nanomaterials including particle size, morphology, charge, and colloidal stability complicate their transferability across systems, hindering broad commercialization.

Future efforts should also focus on simplifying and modularizing analytical systems. This includes enhancing portability, integrating preprocessing units for on-chip reactions, and advancing droplet-based operations (*e.g.*, capture, sorting, mixing, splitting). Such modular systems could be incorporated into automated portable devices with greater commercial potential. Nonetheless, current microfluidic platforms face technical and manufacturing barriers, including limited lifespan (*e.g.*, channel clogging), low throughput from single-channel designs, fabrication complexity, and material-derived interference in Raman spectra. Cost and standardization are especially pressing issues. Fabrication of high-precision chips using methods such as photolithography, and materials like PDMS, silicon, or glass, remains expensive. More economical techniques such as hot embossing and injection molding are being developed to balance cost with precision. Hot embossing, in particular, enables submicron channel fabrication on thermoplastics (COP/COC, PMMA, PC), supporting medium-scale production with improved efficiency.<sup>215–217</sup>

Standardization is another bottleneck, as variations in fabrication and testing methods across laboratories reduce reproducibility and comparability. Initiatives such as the ISO 22916:2022 guideline aim to harmonize integration

requirements for microfluidic systems, providing a pathway toward universal platforms with consistent performance. Multiplexed detection is also essential, since complex diseases like cancer cannot be reliably diagnosed using a single biomarker. Encoded SERS tags, based on mixed suspensions, enable simultaneous detection of multiple targets with high sensitivity. However, spectral overlap among Raman reporters complicates decoding. Advanced curve fitting and machine learning strategies can mitigate these issues and help manage fluorescence background. Importantly, clinical translation requires rigorous cross-validation of SERS analyses against established diagnostic tools, with large-scale, statistically powered studies to ensure reproducibility.

Machine learning (ML) represents a particularly powerful approach for handling spectral complexity. Unlike traditional statistical techniques, ML can classify and predict outcomes in multi-analyte systems without explicit programming. To achieve widespread clinical adoption, several technical milestones must be addressed: (i) miniaturization of Raman spectrometers into handheld, touchscreen-enabled devices, (ii) development of compact fluid control systems suitable for POC integration, and (iii) creation of spectral databases from large clinical sample sets, combined with ML-driven analysis to improve accuracy.<sup>218,219</sup> Successful translation of SERS–microfluidic technologies from the laboratory to the clinic will require close collaboration among spectroscopists, engineers, software developers, and healthcare professionals, ensuring that these systems meet the stringent standards of real-world diagnostic practice.

Although microfluidic–SERS platforms have demonstrated considerable promise in sensitive, rapid, and multiplexed bioanalysis, their transition from laboratory prototypes to clinically deployable diagnostic systems remains challenging. To realize their full potential in point-of-care testing (POCT), several translational barriers must be addressed at the levels of standardization, validation, instrumentation, and regulatory acceptance. A major challenge lies in the standardization of SERS substrates and analytical workflows. The performance of SERS-based systems is highly dependent on nanostructure geometry, hotspot distribution, particle uniformity, and surface chemistry. Variability in substrate fabrication, sample preparation, and signal acquisition can significantly affect analytical reproducibility and limit inter-laboratory comparability. Therefore, robust manufacturing protocols, standardized operating procedures, and quality control benchmarks will be essential for enabling reproducible and clinically acceptable performance. Large-scale clinical validation is another critical requirement. While many published studies report excellent analytical sensitivity and classification accuracy, most remain based on proof-of-concept demonstrations using relatively small and highly controlled sample cohorts. For true clinical translation, microfluidic–SERS platforms must be evaluated using larger, multicenter, and demographically diverse patient populations, ideally with prospective study designs and comparisons against established gold-standard diagnostic methods. Such validation is necessary not only to

confirm analytical robustness, but also to establish clinical utility, sensitivity, specificity, and real-world applicability. Regulatory and translational considerations must also be taken into account. For clinical implementation, microfluidic-SERS systems will need to satisfy regulatory expectations regarding device reproducibility, analytical validation, biosafety, usability, and manufacturing consistency. In addition, the complexity of integrating nanomaterials, fluidic modules, spectral acquisition, and machine learning-based interpretation into a single diagnostic workflow presents unique translational challenges. Early consideration of regulatory requirements and translational design criteria may therefore accelerate the path toward commercialization and clinical adoption. The integration of portable Raman instrumentation represents another key factor for real-world deployment. Although benchtop Raman systems are commonly used in laboratory studies, clinically useful microfluidic-SERS devices will require compact, user-friendly, and robust portable readers that can operate outside specialized research settings. Advances in handheld Raman spectrometers, miniaturized optical components, smartphone-assisted interfaces, and automated data analysis pipelines are expected to play an important role in making these technologies more accessible for decentralized diagnostics. Taken together, the future success of microfluidic-SERS systems will depend not only on analytical innovation, but also on the establishment of clinically relevant, standardized, and scalable translational frameworks. Bridging the gap between proof-of-concept research and real-world implementation will require interdisciplinary collaboration among materials scientists, engineers, clinicians, regulatory experts, and industry partners.

Looking ahead, the future development of microfluidic-SERS systems is expected to be driven not only by incremental improvements in sensitivity and miniaturization, but also by deeper integration of spectroscopy, microfluidic engineering, artificial intelligence, and translational design. Several emerging research directions are likely to play a particularly important role in shaping the next generation of clinically relevant platforms. One important direction is the development of integrated optofluidic spectroscopy systems, in which fluid handling, optical excitation, signal collection, and spectral processing are co-designed within a single miniaturized architecture. Such systems may reduce optical loss, improve alignment stability, and enable more compact and automated diagnostic workflows. In particular, the integration of waveguides, on-chip optical components, and plasmonic sensing interfaces may significantly enhance the portability and scalability of microfluidic-SERS devices. A second major trend is the emergence of AI-driven automated sensing platforms. Future systems are likely to move beyond isolated machine learning models for offline spectral classification toward end-to-end intelligent diagnostic workflows, incorporating automated sample handling, real-time spectral preprocessing, feature extraction, classification, and decision support. Such closed-loop analytical systems may substantially improve robustness, reduce operator dependence, and enhance usability in decentralized or resource-limited settings. Standardized and

manufacturable SERS substrates will also be essential for the field to progress toward broader adoption. Although many proof-of-concept studies rely on highly specialized or laboratory-specific nanostructures, future efforts should increasingly focus on scalable, batch-consistent, and quality-controlled substrate fabrication strategies. Advances in template-assisted nanofabrication, nanoimprint lithography, roll-to-roll processing, and reproducible self-assembly may provide promising routes toward more reliable and commercially viable SERS platforms. Another important frontier is the construction of large, high-quality clinical spectral databases. For machine learning-assisted SERS to achieve robust and generalizable performance, future research must move beyond small, single-center datasets toward multicenter, longitudinal, and demographically diverse clinical cohorts. The establishment of standardized spectral repositories, together with harmonized metadata, annotation protocols, and benchmarking pipelines, will be crucial for enabling fair model comparison, reducing overfitting, and improving external validation. In addition, future progress will likely depend on the convergence of multimodal sensing and intelligent diagnostics. Combining SERS with complementary readout strategies such as fluorescence, electrochemistry, imaging, or digital microfluidics may enhance analytical confidence and broaden the scope of detectable biomarkers. Such hybrid platforms may be particularly valuable in complex clinical scenarios where single-modality readouts are insufficient. Overall, the next stage of microfluidic-SERS research is expected to move from isolated device innovation toward integrated, standardized, data-rich, and clinically deployable sensing ecosystems. Continued advances in these areas will be essential for transforming microfluidic-SERS from a promising analytical technology into a mature platform for precision diagnostics and point-of-care healthcare.

## 7. Conclusion

This review presents a broad summary of recent progress in surface-enhanced Raman scattering (SERS)-integrated microfluidic platforms. We outlined five major categories of these systems continuous-flow, microarray, droplet-based, digital microfluidic, and lateral flow assay (LFA) formats and discussed their applications in bioanalysis, particularly in biomolecule detection, cellular studies, and disease diagnostics. We also highlighted current challenges and future research directions that will shape the development of this emerging field.

The incorporation of microfluidics into SERS workflows has helped mitigate several persistent problems, including limited reproducibility, variable sensitivity, poor stability, memory effects, inefficient reactions, and low throughput. As a result, SERS-microfluidic platforms have become increasingly attractive tools for diverse applications ranging from molecular and single-cell investigations to chemical reaction monitoring and nanoparticle synthesis. Their versatility has enabled impact across multiple disciplines, including chemistry, biomedical

research, food safety testing, environmental surveillance, and industrial process monitoring. More broadly, the integration of microfluidics, SERS, and machine learning represents a shift from component-based biosensing toward intelligent analytical systems capable of closed-loop sample handling, molecular readout, and automated decision-making.

## Author contributions

All authors have read and approved the final manuscript and agreed to their individual contributions before submission. Biqing Chen: conceptualization, literature investigation, data curation, visualization, writing – original draft. Xiaohong Qiu: conceptualization, supervision, writing – review & editing. Yang Li: conceptualization, supervision, writing – review & editing.

## Conflicts of interest

The authors declare that they have no known competing financial interests or personal relationships that could have appeared to influence the work reported in this paper.

## Data availability

This article is a review paper and does not report any original data. No new data were generated or analyzed in this study. Therefore, data sharing is not applicable to this article.

## Acknowledgements

There was no financial support for this project. The authors sincerely thank their affiliated institutions for academic and administrative support during the preparation of this manuscript.

## References

- 1 Y. Yu, Y. Luan and W. Dai, Dynamic process, mechanisms, influencing factors and study methods of protein corona formation, *Int. J. Biol. Macromol.*, 2022, **205**, 731–739, DOI: [10.1016/j.ijbiomac.2022.03.105](https://doi.org/10.1016/j.ijbiomac.2022.03.105).
- 2 A. A. Smith, A. Vogel, O. Engberg, P. W. Hildebrand and D. Huster, A method to construct the dynamic landscape of a bio-membrane with experiment and simulation, *Nat. Commun.*, 2022, **13**(1), 108, DOI: [10.1038/s41467-021-27417-y](https://doi.org/10.1038/s41467-021-27417-y).
- 3 R. M. Lubken, A. M. de Jong and M. W. J. Prins, Real-Time Monitoring of Biomolecules: Dynamic Response Limits of Affinity-Based Sensors, *ACS Sens.*, 2022, **7**(1), 286–295, DOI: [10.1021/acssensors.1c02307](https://doi.org/10.1021/acssensors.1c02307).
- 4 L. Wen, G. Li, T. Huang, W. Geng, H. Pei and J. Yang, *et al.*, Single-cell technologies: From research to application, *Innovation*, 2022, **3**(6), 100342, DOI: [10.1016/j.xinn.2022.100342](https://doi.org/10.1016/j.xinn.2022.100342).
- 5 M. Shen, Y. Zhou, J. Ye, A. A. Abdullah Al-maskri, Y. Kang and S. Zeng, *et al.*, Recent advances and perspectives of nucleic acid detection for coronavirus, *J. Pharm. Anal.*, 2020, **10**(2), 97–101, DOI: [10.1016/j.jpha.2020.02.010](https://doi.org/10.1016/j.jpha.2020.02.010).
- 6 V. M. Corman, O. Landt, M. Kaiser, R. Molenkamp, A. Meijer and D. K. W. Chu, *et al.*, Detection of 2019 novel coronavirus(2019-nCoV) by real-time RT-PCR, *Eurosurveillance*, 2020, **25**(3), 2000045, DOI: [10.2807/1560-7917.Es.2020.25.3.2000045](https://doi.org/10.2807/1560-7917.Es.2020.25.3.2000045).
- 7 B. Guo, G. Liu, H. Wei, J. Qiu, J. Zhuang and X. Zhang, *et al.*, The role of fluorescent carbon dots in crops: Mechanism and applications, *SmartMat*, 2022, **3**(2), 208–225, DOI: [10.1002/smm2.1111](https://doi.org/10.1002/smm2.1111).
- 8 A.-I. Henry, B. Sharma, M. F. Cardinal, D. Kurouski and R. P. Van Duyne, Surface-Enhanced Raman Spectroscopy Biosensing: In Vivo Diagnostics and Multimodal Imaging, *Anal. Chem.*, 2016, **88**(13), 6638–6647, DOI: [10.1021/acs.analchem.6b01597](https://doi.org/10.1021/acs.analchem.6b01597).
- 9 L. Xie, K. Gong, Y. Liu and L. Zhang, Strategies and Challenges of Identifying Nanoplastics in Environment by Surface-Enhanced Raman Spectroscopy, *Environ. Sci. Technol.*, 2022, **57**(1), 25–43, DOI: [10.1021/acs.est.2c07416](https://doi.org/10.1021/acs.est.2c07416).
- 10 X. Meng, L. Qiu, G. Xi, X. Wang and L. Guo, Smart design of high-performance surface-enhanced Raman scattering substrates, *SmartMat*, 2021, **2**(4), 466–487, DOI: [10.1002/smm2.1058](https://doi.org/10.1002/smm2.1058).
- 11 X.-X. Wu, D.-H. Zhang, Y.-N. Ding, F. Cao, Y. Li and J.-L. Yao, *et al.*, Self-assembled co-delivery system of gold nanoparticles and paclitaxel based on in-situ dynamic covalent chemistry for synergistic chemo-photothermal therapy, *Rare Met.*, 2024, **44**(1), 417–429, DOI: [10.1007/s12598-024-03047-3](https://doi.org/10.1007/s12598-024-03047-3).
- 12 H. Ma, S.-Q. Pan, W.-L. Wang, X. Yue, X.-H. Xi and S. Yan, *et al.*, Surface-Enhanced Raman Spectroscopy: Current Understanding, Challenges, and Opportunities, *ACS Nano*, 2024, **18**(22), 14000–14019, DOI: [10.1021/acsnano.4c02670](https://doi.org/10.1021/acsnano.4c02670).
- 13 Y.-C. Ouyang, B.-J. Yeom, Y. Zhao and W. Ma, Progress and prospects of chiral nanomaterials for biosensing platforms, *Rare Met.*, 2024, **43**(6), 2469–2497, DOI: [10.1007/s12598-023-02602-8](https://doi.org/10.1007/s12598-023-02602-8).
- 14 M. Fleischmann, P. J. Hendra and A. J. McQuillan, Raman spectra of pyridine adsorbed at a silver electrode, *Chem. Phys. Lett.*, 1974, **26**(2), 163–166, DOI: [10.1016/0009-2614\(74\)85388-1](https://doi.org/10.1016/0009-2614(74)85388-1).
- 15 D. L. Jeanmaire and R. P. Van Duyne, Surface raman spectroelectrochemistry, *J. Electroanal. Chem. Interfacial Electrochem.*, 1977, **84**(1), 1–20, DOI: [10.1016/s0022-0728\(77\)80224-6](https://doi.org/10.1016/s0022-0728(77)80224-6).
- 16 M. G. Albrecht and J. A. Creighton, Anomalously intense Raman spectra of pyridine at a silver electrode, *J. Am. Chem. Soc.*, 2002, **99**(15), 5215–5217, DOI: [10.1021/ja00457a071](https://doi.org/10.1021/ja00457a071).
- 17 M. Fan, G. F. S. Andrade and A. G. Brolo, A review on recent advances in the applications of surface-enhanced Raman scattering in analytical chemistry, *Anal. Chim. Acta*, 2020, **1097**, 1–29, DOI: [10.1016/j.aca.2019.11.049](https://doi.org/10.1016/j.aca.2019.11.049).
- 18 R. Goel, S. Chakraborty, V. Awasthi, V. Bhardwaj and D. S. Kumar, Exploring the various aspects of Surface enhanced Raman spectroscopy(SERS) with focus on the recent progress: SERS-active substrate, SERS-instrumentation,

- SERS-application, *Sens. Actuators, A*, 2024, **376**, DOI: [10.1016/j.sna.2024.115555](https://doi.org/10.1016/j.sna.2024.115555).
- 19 M. Muhammad and Q. Huang, A review of aptamer-based SERS biosensors: Design strategies and applications, *Talanta*, 2021, **227**, 122188, DOI: [10.1016/j.talanta.2021.122188](https://doi.org/10.1016/j.talanta.2021.122188).
  - 20 T. Pan, D. Zhang, G. You, X. Wu, C. Zhang and X. Miao, *et al.*, PD-L1 targeted iron oxide SERS bioprobe for accurately detecting circulating tumor cells and delineating tumor boundary, *Chin. Chem. Lett.*, 2025, **36**(1), DOI: [10.1016/j.ccllet.2024.109857](https://doi.org/10.1016/j.ccllet.2024.109857).
  - 21 C. Zhang, L. Xu, X. Miao, D. Zhang, Y. Xie and Y. Hu, *et al.*, Machine learning assisted dual-modal SERS detection for circulating tumor cells, *Biosens. Bioelectron.*, 2025, **268**, 116897, DOI: [10.1016/j.bios.2024.116897](https://doi.org/10.1016/j.bios.2024.116897).
  - 22 J. Lin, X. Ma, A. Li, O. U. Akakuru, C. Pan and M. He, *et al.*, Multiple valence states of Fe boosting SERS activity of Fe<sub>3</sub>O<sub>4</sub> nanoparticles and enabling effective SERS-MRI bimodal cancer imaging, *Fundam. Res.*, 2024, **4**(4), 858–867, DOI: [10.1016/j.fmre.2022.04.018](https://doi.org/10.1016/j.fmre.2022.04.018).
  - 23 C. Zong, M. Xu, L.-J. Xu, T. Wei, X. Ma and X.-S. Zheng, *et al.*, Surface-Enhanced Raman Spectroscopy for Bioanalysis: Reliability and Challenges, *Chem. Rev.*, 2018, **118**(10), 4946–4980, DOI: [10.1021/acs.chemrev.7b00668](https://doi.org/10.1021/acs.chemrev.7b00668).
  - 24 Y. Wang, R. Gao, C. Zhan, H. Jia, X. Chen and Y. Lu, *et al.*, SERS-based microfluidic sensor for sensitive detection of circulating tumor markers: A critical review, *Coord. Chem. Rev.*, 2025, **523**, DOI: [10.1016/j.ccr.2024.216289](https://doi.org/10.1016/j.ccr.2024.216289).
  - 25 S. Han, J. Park, S. Moon, S. Eom, C. M. Jin and S. Kim, *et al.*, Label-free and liquid state SERS detection of multi-scaled bioanalytes via light-induced pinpoint colloidal assembly, *Biosens. Bioelectron.*, 2024, **264**, 116663, DOI: [10.1016/j.bios.2024.116663](https://doi.org/10.1016/j.bios.2024.116663).
  - 26 T. M. Cotton, S. G. Schultz and R. P. Van Duyne, Surface-enhanced resonance Raman scattering from cytochrome c and myoglobin adsorbed on a silver electrode, *J. Am. Chem. Soc.*, 2002, **102**(27), 7960–7962, DOI: [10.1021/ja00547a036](https://doi.org/10.1021/ja00547a036).
  - 27 Y. Xie, C. Chen, C. Zhang, L. Xu, Z. Li and W. Ren, *et al.*, Synergistic enhancement of ultrahigh SERS activity via Cu<sub>2</sub>O@Ag Core-Shell structure for accurate label-free identification of breast tumor subtypes, *Nano Today*, 2024, **54**, DOI: [10.1016/j.nantod.2023.102140](https://doi.org/10.1016/j.nantod.2023.102140).
  - 28 Y. Xie, X. Li, L. Xu, C. Zhang, Y. Ren and X. Shi, *et al.*, A cubic Cu<sub>2</sub>O@Ag bioprobe for label-free SERS classification of hepatic fibrosis and hepatocellular carcinoma, *Mater. Chem. Front.*, 2024, **8**(18), 2978–2988, DOI: [10.1039/d4qm00532e](https://doi.org/10.1039/d4qm00532e).
  - 29 Q. Yuan and Y. Wang, SERS Detection of Hydrophobic Molecules: Thio- $\beta$ -Cyclodextrin-Driven Rapid Self-Assembly of Uniform Silver Nanoparticle Monolayers and Analyte Trapping, *Biosensors*, 2025, **15**(1), 52, DOI: [10.3390/bios15010052](https://doi.org/10.3390/bios15010052).
  - 30 Y. Zhang, D. Jimenez de Aberasturi, M. Henriksen-Lacey, J. Langer and L. M. Liz-Marzán, Live-Cell Surface-Enhanced Raman Spectroscopy Imaging of Intracellular pH: From Two Dimensions to Three Dimensions, *ACS Sens.*, 2020, **5**(10), 3194–3206, DOI: [10.1021/acssensors.0c01487](https://doi.org/10.1021/acssensors.0c01487).
  - 31 L. Wu, A. Teixeira, A. Garrido-Maestu, L. Muinelo-Romay, L. Lima and L. L. Santos, *et al.*, Profiling DNA mutation patterns by SERS fingerprinting for supervised cancer classification, *Biosens. Bioelectron.*, 2020, **165**, 112392, DOI: [10.1016/j.bios.2020.112392](https://doi.org/10.1016/j.bios.2020.112392).
  - 32 M. He, J. Lin, O. U. Akakuru, X. Xu, Y. Li and Y. Cao, *et al.*, Octahedral silver oxide nanoparticles enabling remarkable SERS activity for detecting circulating tumor cells, *Sci. China: Life Sci.*, 2021, **65**(3), 561–571, DOI: [10.1007/s11427-020-1931-9](https://doi.org/10.1007/s11427-020-1931-9).
  - 33 S. Sloan-Dennison, G. Q. Wallace, W. A. Hassanain, S. Laing, K. Faulds and D. Graham, Advancing SERS as a quantitative technique: challenges, considerations, and correlative approaches to aid validation, *Nano Convergence*, 2024, **11**(1), 33, DOI: [10.1186/s40580-024-00443-4](https://doi.org/10.1186/s40580-024-00443-4).
  - 34 Y. Xu, G. Yu, R. Nie and Z. Wu, Microfluidic systems toward blood hemostasis monitoring and thrombosis diagnosis: From design principles to micro/nano fabrication technologies, *View*, 2022, **3**(1), DOI: [10.1002/viw.20200183](https://doi.org/10.1002/viw.20200183).
  - 35 X. Meng, J. Yu, W. Shi, L. Qiu, K. Qiu and A. Li, *et al.*, SERS Detection of Trace Carcinogenic Aromatic Amines Based on Amorphous MoO<sub>3</sub> Monolayers, *Angew. Chem., Int. Ed.*, 2024, **63**(33), e202407597, DOI: [10.1002/anie.202407597](https://doi.org/10.1002/anie.202407597).
  - 36 J. Lin, D. Zhang, J. Yu, T. Pan, X. Wu and T. Chen, *et al.*, Amorphous Nitrogen-Doped Carbon Nanocages with Excellent SERS Sensitivity and Stability for Accurate Identification of Tumor Cells, *Anal. Chem.*, 2023, **95**(10), 4671–4681, DOI: [10.1021/acs.analchem.2c05272](https://doi.org/10.1021/acs.analchem.2c05272).
  - 37 X. Cao, S. Ge, M. Chen, H. Mao and Y. Wang, LoC-SERS Platform Integrated with the Signal Amplification Strategy toward Parkinson's Disease Diagnosis, *ACS Appl. Mater. Interfaces*, 2023, **15**(18), 21830–21842, DOI: [10.1021/acscami.3c00103](https://doi.org/10.1021/acscami.3c00103).
  - 38 Y. Xie, L. Xu, J. Zhang, C. Zhang, Y. Hu and Z. Zhang, *et al.*, Precise diagnosis of tumor cells and hemocytes using ultrasensitive, stable, selective cuprous oxide composite SERS bioprobes assisted with high-efficiency separation microfluidic chips, *Mater. Horiz.*, 2024, **11**(22), 5752–5767, DOI: [10.1039/d4mh00791c](https://doi.org/10.1039/d4mh00791c).
  - 39 J. Zhuang, J. Yin, S. Lv, B. Wang and Y. Mu, Advanced “lab-on-a-chip” to detect viruses – Current challenges and future perspectives, *Biosens. Bioelectron.*, 2020, **163**, 112291, DOI: [10.1016/j.bios.2020.112291](https://doi.org/10.1016/j.bios.2020.112291).
  - 40 X. Xu, Q. Zhang, M. Li, S. Lin, S. Liang and L. Cai, *et al.*, Microfluidic single-cell multiomics analysis, *View*, 2022, **4**(1), DOI: [10.1002/viw.20220034](https://doi.org/10.1002/viw.20220034).
  - 41 X. Cao, Z. Liu, X. Qin, Y. Gu, Y. Huang and Y. Qian, *et al.*, LoC-SERS platform for rapid and sensitive detection of colorectal cancer protein biomarkers, *Talanta*, 2024, **270**, 125563, DOI: [10.1016/j.talanta.2023.125563](https://doi.org/10.1016/j.talanta.2023.125563).
  - 42 Y. Zhao, M. Guan, F. Mi, Y. Zhang, P. Geng and S. Zhang, *et al.*, A SERS/colorimetric biosensor based on AuNSs@Ag core-shell Prussian blue nanozyme for non-interference and rapid detection of *Staphylococcus aureus* in milk, *Microchim. Acta*, 2025, **192**(2), 83, DOI: [10.1007/s00604-024-06921-0](https://doi.org/10.1007/s00604-024-06921-0).

- 43 I. J. Jahn, O. Žukovskaja, X. S. Zheng, K. Weber, T. W. Bocklitz and D. Cialla-May, *et al.*, Surface-enhanced Raman spectroscopy and microfluidic platforms: challenges, solutions and potential applications, *Analyst*, 2017, **142**(7), 1022–1047, DOI: [10.1039/c7an00118e](https://doi.org/10.1039/c7an00118e).
- 44 Q. Zhou and T. Kim, Review of microfluidic approaches for surface-enhanced Raman scattering, *Sens. Actuators, B*, 2016, **227**, 504–514, DOI: [10.1016/j.snb.2015.12.069](https://doi.org/10.1016/j.snb.2015.12.069).
- 45 J. Lin, X. Meng, Y. Xie, Y. Peng, X. Fan and K. Liang, *et al.*, Selectivity and stability reshaping high-sensitivity detection boundaries: A technical leap and paradigm shift in semiconductor surface-enhanced Raman scattering, *Nano Res.*, 2026, **19**(3), DOI: [10.26599/nr.2026.94908347](https://doi.org/10.26599/nr.2026.94908347).
- 46 C. Zhan, Z. Guan, L. Yu, T. Jing, H. Jia and X. Chen, *et al.*, Microfluidics-aided fabrication of 3D micro-nano hierarchical SERS substrate for rapid detection of dual hepatocellular carcinoma biomarkers, *Lab Chip*, 2024, **24**(3), 528–536, DOI: [10.1039/d3lc00907f](https://doi.org/10.1039/d3lc00907f).
- 47 X. Y. Meng, Y. J. Xie, L. Sun, X. T. Wang, A. G. Wu and J. Lin, Electromagnetic field-charge transfer synergy boosted SERS in noble metal–semiconductor nanohybrids for environmental and bio-detection, *Rare Met.*, 2025, **44**(12), 9702–9725, DOI: [10.1007/s12598-025-03558-7](https://doi.org/10.1007/s12598-025-03558-7).
- 48 Y. Wang, X. Meng, W. Shi, Y. Xie, A. Liu and L. Xu, *et al.*, Single-Atom Cu Anchored on a UiO-66 Surface-Enhanced Raman Scattering Sensor for Trace and Rapid Detection of Volatile Organic Compounds, *Research*, 2025, **8**, 0841, DOI: [10.34133/research.0841](https://doi.org/10.34133/research.0841).
- 49 M. Moskovits, Surface-enhanced Raman spectroscopy: a brief retrospective, *J. Raman Spectrosc.*, 2005, **36**(6–7), 485–496, DOI: [10.1002/jrs.1362](https://doi.org/10.1002/jrs.1362).
- 50 J. Gopal, H. N. Abdelhamid, J.-H. Huang and H.-F. Wu, Nondestructive detection of the freshness of fruits and vegetables using gold and silver nanoparticle mediated graphene enhanced Raman spectroscopy, *Sens. Actuators, B*, 2016, **224**, 413–424, DOI: [10.1016/j.snb.2015.08.123](https://doi.org/10.1016/j.snb.2015.08.123).
- 51 C. Liu, C. Franceschini, S. Weber, T. Dib, P. Liu and L. Wu, *et al.*, SERS-based detection of the antibiotic ceftriaxone in spiked fresh plasma and microdialysate matrix by using silver-functionalized silicon nanowire substrates, *Talanta*, 2024, **271**, 125697, DOI: [10.1016/j.talanta.2024.125697](https://doi.org/10.1016/j.talanta.2024.125697).
- 52 J. Langer, D. Jimenez de Aberasturi, J. Aizpurua, R. A. Alvarez-Puebla, B. Auguie and J. J. Baumberg, *et al.*, Present and Future of Surface-Enhanced Raman Scattering, *ACS Nano*, 2019, **14**(1), 28–117, DOI: [10.1021/acsnano.9b04224](https://doi.org/10.1021/acsnano.9b04224).
- 53 S. E. J. Bell, G. Charron, E. Cortés, J. Kneipp, M. L. de la Chapelle and J. Langer, *et al.*, Towards Reliable and Quantitative Surface-Enhanced Raman Scattering (SERS): From Key Parameters to Good Analytical Practice, *Angew. Chem., Int. Ed.*, 2020, **59**(14), 5454–5462, DOI: [10.1002/anie.201908154](https://doi.org/10.1002/anie.201908154).
- 54 J. A. Huang, Y. L. Zhang, H. Ding and H. B. Sun, SERS-Enabled Lab-on-a-Chip Systems, *Adv. Opt. Mater.*, 2015, **3**(5), 618–633, DOI: [10.1002/adom.201400534](https://doi.org/10.1002/adom.201400534).
- 55 I. J. Hidi, M. Jahn, K. Weber, T. Bocklitz, M. W. Pletz and D. Cialla-May, *et al.*, Lab-on-a-Chip-Surface Enhanced Raman Scattering Combined with the Standard Addition Method: Toward the Quantification of Nitroxoline in Spiked Human Urine Samples, *Anal. Chem.*, 2016, **88**(18), 9173–9180, DOI: [10.1021/acs.analchem.6b02316](https://doi.org/10.1021/acs.analchem.6b02316).
- 56 C. Wang, G. Weng, J. Li, J. Zhu and J. Zhao, A review of SERS coupled microfluidic platforms: From configurations to applications, *Anal. Chim. Acta*, 2024, **1296**, 342291, DOI: [10.1016/j.aca.2024.342291](https://doi.org/10.1016/j.aca.2024.342291).
- 57 R. Burger, L. Amato and A. Boisen, Detection methods for centrifugal microfluidic platforms, *Biosens. Bioelectron.*, 2016, **76**, 54–67, DOI: [10.1016/j.bios.2015.06.075](https://doi.org/10.1016/j.bios.2015.06.075).
- 58 K. Sanger, O. Durucan, K. Wu, A. H. Thilsted, A. Heiskanen and T. Rindzevicius, *et al.*, Large-Scale, Lithography-Free Production of Transparent Nanostructured Surface for Dual-Functional Electrochemical and SERS Sensing, *ACS Sens.*, 2017, **2**(12), 1869–1875, DOI: [10.1021/acssensors.7b00783](https://doi.org/10.1021/acssensors.7b00783).
- 59 J. W. Martin, M. K. Nieuwoudt, M. J. T. Vargas, O. L. C. Bodley, T. S. Yohendiran and R. N. Oosterbeek, *et al.*, Raman on a disc: high-quality Raman spectroscopy in an open channel on a centrifugal microfluidic disc, *Analyst*, 2017, **142**(10), 1682–1688, DOI: [10.1039/c6an00874g](https://doi.org/10.1039/c6an00874g).
- 60 X. Su, Y. Xu, H. Zhao, S. Li and L. Chen, Design and preparation of centrifugal microfluidic chip integrated with SERS detection for rapid diagnostics, *Talanta*, 2019, **194**, 903–909, DOI: [10.1016/j.talanta.2018.11.014](https://doi.org/10.1016/j.talanta.2018.11.014).
- 61 O. Durucan, T. Rindzevicius, M. S. Schmidt, M. Matteucci and A. Boisen, Nanopillar Filters for Surface-Enhanced Raman Spectroscopy, *ACS Sens.*, 2017, **2**(10), 1400–1404, DOI: [10.1021/acssensors.7b00499](https://doi.org/10.1021/acssensors.7b00499).
- 62 L. Morelli, L. Seriola, F. A. Centorbi, C. B. Jendresen, M. Matteucci and O. Ilchenko, *et al.*, Injection molded lab-on-a-disc platform for screening of genetically modified E. coli using liquid–liquid extraction and surface enhanced Raman scattering, *Lab Chip*, 2018, **18**(6), 869–877, DOI: [10.1039/c7lc01217a](https://doi.org/10.1039/c7lc01217a).
- 63 P. He, E. Dumont, Y. Göksel, R. Slipets, K. Schmiegelow and Q. Chen, *et al.*, SERS mapping combined with chemometrics, for accurate quantification of methotrexate from patient samples, *Spectrochim. Acta, Part A*, 2024, **305**, 123536, DOI: [10.1016/j.saa.2023.123536](https://doi.org/10.1016/j.saa.2023.123536).
- 64 G. Soufi, E. Dumont, Y. Göksel, R. Slipets, R. A. Raja and K. Schmiegelow, *et al.*, Discrimination and quantification of methotrexate in the presence of its metabolites in patient serum using SERS mapping, assisted by multivariate spectral data analysis, *Biosens. Bioelectron.: X*, 2023, **14**, DOI: [10.1016/j.biosx.2023.100382](https://doi.org/10.1016/j.biosx.2023.100382).
- 65 A. Bonifacio, S. Cervo and V. Sergo, Label-free surface-enhanced Raman spectroscopy of biofluids: fundamental aspects and diagnostic applications, *Anal. Bioanal. Chem.*, 2015, **407**(27), 8265–8277, DOI: [10.1007/s00216-015-8697-z](https://doi.org/10.1007/s00216-015-8697-z).
- 66 N. E. Markina, A. V. Markin, A. M. Zakharevich and I. Y. Goryacheva, Calcium carbonate microparticles with embedded silver and magnetite nanoparticles as new SERS-active sorbent for solid phase extraction, *Microchim. Acta*, 2017, **184**(10), 3937–3944, DOI: [10.1007/s00604-017-2426-6](https://doi.org/10.1007/s00604-017-2426-6).

- 67 J. Jeon, N. Choi, H. Chen, J.-I. Moon, L. Chen and J. Choo, SERS-based droplet microfluidics for high-throughput gradient analysis, *Lab Chip*, 2019, **19**(4), 674–681, DOI: [10.1039/c8lc01180j](https://doi.org/10.1039/c8lc01180j).
- 68 Y. Li, Q. Chen, X. Xu, Y. Jin, Y. Wang and L. Zhang, *et al.*, Microarray surface enhanced Raman scattering based immunosensor for multiplexing detection of mycotoxin in foodstuff, *Sens. Actuators, B*, 2018, **266**, 115–123, DOI: [10.1016/j.snb.2018.03.040](https://doi.org/10.1016/j.snb.2018.03.040).
- 69 X. Xu, J. Lin, Y. Guo, X. Wu, Y. Xu and D. Zhang, *et al.*, TiO<sub>2</sub>-based Surface-Enhanced Raman Scattering bio-probe for efficient circulating tumor cell detection on microfilter, *Biosens. Bioelectron.*, 2022, **210**, 114305, DOI: [10.1016/j.bios.2022.114305](https://doi.org/10.1016/j.bios.2022.114305).
- 70 X. Yu, S. Park, S. Lee, S.-W. Joo and J. Choo, Microfluidics for disease diagnostics based on surface-enhanced raman scattering detection, *Nano Convergence*, 2024, **11**(1), 17, DOI: [10.1186/s40580-024-00424-7](https://doi.org/10.1186/s40580-024-00424-7).
- 71 S. Lee, H. Dang, J.-I. Moon, K. Kim, Y. Joung and S. Park, *et al.*, SERS-based microdevices for use as in vitro diagnostic biosensors, *Chem. Soc. Rev.*, 2024, **53**(11), 5394–5427, DOI: [10.1039/d3cs01055d](https://doi.org/10.1039/d3cs01055d).
- 72 J.-I. Moon, E. J. Choi, Y. Joung, J.-W. Oh, S.-W. Joo and J. Choo, Development of highly sensitive plasmonic biosensors encoded with gold nanoparticles on M13 bacteriophage networks, *Sens. Actuators, B*, 2024, **400**, DOI: [10.1016/j.snb.2023.134916](https://doi.org/10.1016/j.snb.2023.134916).
- 73 H. Chen, S.-G. Park, N. Choi, J.-I. Moon, H. Dang and A. Das, *et al.*, SERS imaging-based aptasensor for ultrasensitive and reproducible detection of influenza virus A, *Biosens. Bioelectron.*, 2020, **167**, 112496, DOI: [10.1016/j.bios.2020.112496](https://doi.org/10.1016/j.bios.2020.112496).
- 74 Z. Wang, S. Zong, L. Wu, D. Zhu and Y. Cui, SERS-Activated Platforms for Immunoassay: Probes, Encoding Methods, and Applications, *Chem. Rev.*, 2017, **117**(12), 7910–7963, DOI: [10.1021/acs.chemrev.7b00027](https://doi.org/10.1021/acs.chemrev.7b00027).
- 75 A. Walter, A. März, W. Schumacher, P. Rösch and J. Popp, Towards a fast, high specific and reliable discrimination of bacteria on strain level by means of SERS in a microfluidic device, *Lab Chip*, 2011, **11**(6), 1013–1021, DOI: [10.1039/c0lc00536c](https://doi.org/10.1039/c0lc00536c).
- 76 Y. S. Huh, A. J. Chung, B. Cordovez and D. Erickson, Enhanced on-chip SERS based biomolecular detection using electrokinetically active microwells, *Lab Chip*, 2009, **9**(3), 433–439, DOI: [10.1039/b809702j](https://doi.org/10.1039/b809702j).
- 77 B. D. Piorek, C. Andreou, M. Moskovits and C. D. Meinhart, Discrete Free-Surface Millifluidics for Rapid Capture and Analysis of Airborne Molecules Using Surface-Enhanced Raman Spectroscopy, *Anal. Chem.*, 2014, **86**(2), 1061–1066, DOI: [10.1021/ac402628t](https://doi.org/10.1021/ac402628t).
- 78 S. Park, C. Su Jeon, N. Choi, J.-I. Moon, K. Min Lee and S. Hyun Pyun, *et al.*, Sensitive and reproducible detection of SARS-CoV-2 using SERS-based microdroplet sensor, *Chem. Eng. J.*, 2022, **446**, 137085, DOI: [10.1016/j.cej.2022.137085](https://doi.org/10.1016/j.cej.2022.137085).
- 79 T. A. Meier, E. Poehler, F. Kemper, O. Pabst, H. G. Jahnke and E. Beckert, *et al.*, Fast electrically assisted regeneration of on-chip SERS substrates, *Lab Chip*, 2015, **15**(14), 2923–2927, DOI: [10.1039/c5lc00397k](https://doi.org/10.1039/c5lc00397k).
- 80 W. Yan, L. Yang, J. Chen, Y. Wu, P. Wang and Z. Li, In Situ Two-Step Photoreduced SERS Materials for On-Chip Single-Molecule Spectroscopy with High Reproducibility, *Adv. Mater.*, 2017, **29**(36), DOI: [10.1002/adma.201702893](https://doi.org/10.1002/adma.201702893).
- 81 J. Plou, M. Charconnet, I. García, J. Calvo and L. M. Liz-Marzán, Preventing Memory Effects in Surface-Enhanced Raman Scattering Substrates by Polymer Coating and Laser-Activated Deprotection, *ACS Nano*, 2021, **15**(5), 8984–8995, DOI: [10.1021/acsnano.1c01878](https://doi.org/10.1021/acsnano.1c01878).
- 82 R. Gao, N. Choi, S.-I. Chang, E. K. Lee and J. Choo, Real-time analysis of diaquat dibromide monohydrate in water with a SERS-based integrated microdroplet sensor, *Nanoscale*, 2014, **6**(15), 8781–8786, DOI: [10.1039/c4nr01269k](https://doi.org/10.1039/c4nr01269k).
- 83 E. Chung, R. Gao, J. Ko, N. Choi, D. W. Lim and E. K. Lee, *et al.*, Trace analysis of mercury(ii) ions using aptamer-modified Au/Ag core-shell nanoparticles and SERS spectroscopy in a microdroplet channel, *Lab Chip*, 2013, **13**(2), 260–266, DOI: [10.1039/c2lc41079f](https://doi.org/10.1039/c2lc41079f).
- 84 L. Ngo, L. Q. A. Pham, A. Tukova, A. Hassanzadeh-Barforoushi, W. Zhang and Y. Wang, Emerging integrated SERS-microfluidic devices for analysis of cancer-derived small extracellular vesicles, *Lab Chip*, 2023, **23**(13), 2899–2921, DOI: [10.1039/d3lc00156c](https://doi.org/10.1039/d3lc00156c).
- 85 H. Song, D. L. Chen and R. F. Ismagilov, Reactions in Droplets in Microfluidic Channels, *Angew. Chem., Int. Ed.*, 2006, **45**(44), 7336–7356, DOI: [10.1002/anie.200601554](https://doi.org/10.1002/anie.200601554).
- 86 X. Niu, S. Gulati, J. B. Edel and A. J. deMello, Pillar-induced droplet merging in microfluidic circuits, *Lab Chip*, 2008, **8**(11), 1837–1841, DOI: [10.1039/b813325e](https://doi.org/10.1039/b813325e).
- 87 S.-Y. Teh, R. Lin, L.-H. Hung and A. P. Lee, Droplet microfluidics, *Lab Chip*, 2008, **8**, 2, DOI: [10.1039/b715524g](https://doi.org/10.1039/b715524g).
- 88 Z. Xuan, J. Li, Q. Liu, F. Yi, S. Wang and W. Lu, Artificial Structural Colors and Applications, *Innovation*, 2021, **2**(1), 100081, DOI: [10.1016/j.xinn.2021.100081](https://doi.org/10.1016/j.xinn.2021.100081).
- 89 S.-J. Zhong, K.-Y. Chen, S.-L. Wang, F. Manshahi, N. Jing and K.-D. Wang, *et al.*, Metal-based nanowires in electrical biosensing, *Rare Met.*, 2024, **43**(12), 6233–6254, DOI: [10.1007/s12598-024-02821-7](https://doi.org/10.1007/s12598-024-02821-7).
- 90 K. Wu, T. Li, M. S. Schmidt, T. Rindzevicius, A. Boisen and S. Ndoni, Gold Nanoparticles Sliding on Recyclable Nanohoodoos Engineered for Surface-Enhanced Raman Spectroscopy, *Adv. Funct. Mater.*, 2017, **28**(2), DOI: [10.1002/adfm.201704818](https://doi.org/10.1002/adfm.201704818).
- 91 X. Zhang, X. Zhang, C. Luo, Z. Liu, Y. Chen and S. Dong, *et al.*, Volume-Enhanced Raman Scattering Detection of Viruses, *Small*, 2019, **15**(11), e1805516, DOI: [10.1002/smll.201805516](https://doi.org/10.1002/smll.201805516).
- 92 G. Cossio and E. T. Yu, Zeta Potential Dependent Self-Assembly for Very Large Area Nanosphere Lithography, *Nano Lett.*, 2020, **20**(7), 5090–5096, DOI: [10.1021/acs.nanolett.0c01277](https://doi.org/10.1021/acs.nanolett.0c01277).
- 93 L. Wu, Z. Wang, K. Fan, S. Zong and Y. Cui, A SERS-Assisted 3D Barcode Chip for High-Throughput Biosensing, *Small*, 2015, **11**(23), 2798–2806, DOI: [10.1002/smll.201403474](https://doi.org/10.1002/smll.201403474).

- 94 S. Kumar, S. Cherukulappurath, T. W. Johnson and S.-H. Oh, Millimeter-Sized Suspended Plasmonic Nanohole Arrays for Surface-Tension-Driven Flow-Through SERS, *Chem. Mater.*, 2014, **26**(22), 6523–6530, DOI: [10.1021/cm5031848](https://doi.org/10.1021/cm5031848).
- 95 S. Sevim, C. Franco, X. Z. Chen, A. Sorrenti, D. Rodríguez-San-Miguel and S. Pané, *et al.*, SERS Barcode Libraries: A Microfluidic Approach. *Advanced Science*, 2020, **7**(12), 1903172, DOI: [10.1002/advs.201903172](https://doi.org/10.1002/advs.201903172).
- 96 D. G. Rackus, M. H. Shamsi and A. R. Wheeler, Electrochemistry, biosensors and microfluidics: a convergence of fields, *Chem. Soc. Rev.*, 2015, **44**(15), 5320–5340, DOI: [10.1039/c4cs00369a](https://doi.org/10.1039/c4cs00369a).
- 97 R. A. Wallace, N. V. Lavrik and M. J. Sepaniak, Ultra-thin layer chromatography with integrated silver colloid-based SERS detection, *Electrophoresis*, 2016, **38**(2), 361–367, DOI: [10.1002/elps.201600319](https://doi.org/10.1002/elps.201600319).
- 98 I. Badillo-Ramírez, S. A. J. Janssen, G. Soufi, R. Slipets, K. Zór and A. Boisen, Label-free SERS assay combined with multivariate spectral data analysis for lamotrigine quantification in human serum, *Microchim. Acta*, 2023, **190**(12), 495, DOI: [10.1007/s00604-023-06085-3](https://doi.org/10.1007/s00604-023-06085-3).
- 99 X. Bi, L. Lin, Z. Chen and J. Ye, Artificial Intelligence for Surface-Enhanced Raman Spectroscopy. *Small Methods*, 2023, **8**(1), e2301243, DOI: [10.1002/smt.202301243](https://doi.org/10.1002/smt.202301243).
- 100 Y. Ding, Y. Sun, C. Liu, Q. Y. Jiang, F. Chen and Y. Cao, SERS-Based Biosensors Combined with Machine Learning for Medical Application\*\*, *ChemistryOpen*, 2023, **12**(1), e202200192, DOI: [10.1002/open.202200192](https://doi.org/10.1002/open.202200192).
- 101 E. A. Jensen, M. Serhatlioglu, C. Uyanik, A. T. Hansen, S. Puthusserypady and M. H. Dziegiel, *et al.*, Label-Free Blood Typing by Raman Spectroscopy and Artificial Intelligence, *Adv. Mater. Technol.*, 2023, **9**(2), DOI: [10.1002/admt.202301462](https://doi.org/10.1002/admt.202301462).
- 102 H. Qian, X. Shao, H. Zhang, Y. Wang, S. Liu and J. Pan, *et al.*, Diagnosis of urogenital cancer combining deep learning algorithms and surface-enhanced Raman spectroscopy based on small extracellular vesicles, *Spectrochim. Acta, Part A*, 2022, **281**, 121603, DOI: [10.1016/j.saa.2022.121603](https://doi.org/10.1016/j.saa.2022.121603).
- 103 H. Shin, B. H. Choi, O. Shim, J. Kim, Y. Park and S. K. Cho, *et al.*, Single test-based diagnosis of multiple cancer types using Exosome-SERS-AI for early stage cancers, *Nat. Commun.*, 2023, **14**(1), 1644, DOI: [10.1038/s41467-023-37403-1](https://doi.org/10.1038/s41467-023-37403-1).
- 104 L. Rolinger, M. Rüdter and J. Hubbuch, Comparison of UV- and Raman-based monitoring of the Protein A load phase and evaluation of data fusion by PLS models and CNNs, *Biotechnol. Bioeng.*, 2021, **118**(11), 4255–4268, DOI: [10.1002/bit.27894](https://doi.org/10.1002/bit.27894).
- 105 N. Ibtehaz, M. E. H. Chowdhury, A. Khandakar, S. Kiranyaz, M. S. Rahman and S. M. Zughaier, RamanNet: a generalized neural network architecture for Raman spectrum analysis, *Neural Comput. Appl.*, 2023, DOI: [10.1007/s00521-023-08700-z](https://doi.org/10.1007/s00521-023-08700-z).
- 106 M. Boodaghidzaji, S. Milind Athalye, S. Thakur, E. Esmaili, M. S. Verma and A. M. Ardekani, Characterizing viral samples using machine learning for Raman and absorption spectroscopy, *MicrobiologyOpen*, 2022, **11**(6), e1336, DOI: [10.1002/mbo3.1336](https://doi.org/10.1002/mbo3.1336).
- 107 B. Gardner, J. Haskell, P. Matousek and N. Stone, Guided principal component analysis(GPCA): a simple method for improving detection of a known analyte, *Analyst*, 2024, **149**(1), 205–211, DOI: [10.1039/d3an00820g](https://doi.org/10.1039/d3an00820g).
- 108 A. C. S. Talari, S. Rehman and I. U. Rehman, Advancing cancer diagnostics with artificial intelligence and spectroscopy: identifying chemical changes associated with breast cancer, *Expert Rev. Mol. Diagn.*, 2019, **19**(10), 929–940, DOI: [10.1080/14737159.2019.1659727](https://doi.org/10.1080/14737159.2019.1659727).
- 109 W. Liu, S. Sun, Y. Liu, H. Deng, F. Hong and C. Liu, *et al.*, Determination of benzo(a)pyrene in peanut oil based on Raman spectroscopy and machine learning methods, *Spectrochim. Acta, Part A*, 2023, **299**, 122806, DOI: [10.1016/j.saa.2023.122806](https://doi.org/10.1016/j.saa.2023.122806).
- 110 C.-C. Hsu, J. Xu, B. Brinkhof, H. Wang, Z. Cui and W. E. Huang, *et al.*, A single-cell Raman-based platform to identify developmental stages of human pluripotent stem cell-derived neurons, *Proc. Natl. Acad. Sci. U. S. A.*, 2020, **117**(31), 18412–18423, DOI: [10.1073/pnas.2001906117](https://doi.org/10.1073/pnas.2001906117).
- 111 R. Beeram, K. R. Vepa and V. R. Soma, Recent Trends in SERS-Based Plasmonic Sensors for Disease Diagnostics, Biomolecules Detection, and Machine Learning Techniques, *Biosensors*, 2023, **13**(3), 328, DOI: [10.3390/bios13030328](https://doi.org/10.3390/bios13030328).
- 112 N. Lyu, A. Hassanzadeh-Barforoushi, L. M. Rey Gomez, W. Zhang and Y. Wang, SERS biosensors for liquid biopsy towards cancer diagnosis by detection of various circulating biomarkers: current progress and perspectives, *Nano Convergence*, 2024, **11**(1), 22, DOI: [10.1186/s40580-024-00428-3](https://doi.org/10.1186/s40580-024-00428-3).
- 113 R. Pilot, R. Signorini, C. Durante, L. Orian, M. Bhamidipati and L. Fabris, A Review on Surface-Enhanced Raman Scattering, *Biosensors*, 2019, **9**(2), 57, DOI: [10.3390/bios9020057](https://doi.org/10.3390/bios9020057).
- 114 M. Nandipati, O. Fatoki and S. Desai, Bridging Nanomanufacturing and Artificial Intelligence A Comprehensive Review, *Materials*, 2024, **17**(7), 1621, DOI: [10.3390/ma17071621](https://doi.org/10.3390/ma17071621).
- 115 M. K. Masud, D. Natsuhara, Y. Dai, J. Bashir, A. S. Nugraha and S. M. Alshehri, *et al.*, A plasmonic mesoporous gold-based SERS-microfluidic platform for the detection of infectious diseases, *J. Mater. Chem. C*, 2024, **12**(44), 17977–17985, DOI: [10.1039/d4tc01638f](https://doi.org/10.1039/d4tc01638f).
- 116 J. Wang, Q. Zhou, K. Lowry, C. B. Howard and M. Trau, Development and application of multivalent nanobody-functionalized plasmonic probes in SERS sensing platforms, *Biosens. Bioelectron.*, 2025, **278**, 117292, DOI: [10.1016/j.bios.2025.117292](https://doi.org/10.1016/j.bios.2025.117292).
- 117 S. Park, K. Kim, A. Go, M.-H. Lee, L. Chen and J. Choo, Rapid and Sensitive Escherichia coli Detection: Integration of SERS and Acoustofluidics in a Lysis-Free Microfluidic Platform, *ACS Sens.*, 2025, **10**(2), 1217–1227, DOI: [10.1021/acssensors.4c03118](https://doi.org/10.1021/acssensors.4c03118).
- 118 H. Cortes-Cano, L. I. Olvera, E. M. Méndez-Aguilar, B. L. España-Sánchez, L. G. Arriaga and G. Oza, *et al.*, Surface Functionalization and Escherichia coli Detection Using

- Surface-Enhanced Raman Spectroscopy Driven by Functional Organic Polymer/Gold Nanofilm-Based Microfluidic Chip, *Biosensors*, 2023, **13**(12), 994, DOI: [10.3390/bios13120994](https://doi.org/10.3390/bios13120994).
- 119 H. Wang, C. Zheng, K. Li and Z. Jiang, Surface enhancement of Raman scattering of nanoparticles AuNPs, AuNRs and Au@AgNPs prepared by microfluidics, *Microchem. J.*, 2025, **213**, DOI: [10.1016/j.microc.2025.113831](https://doi.org/10.1016/j.microc.2025.113831).
- 120 Z. Dong, X. Liu, S. Zhou, Y. Zhu, J. Chen and Y. Liu, *et al.*, Microsphere lens array embedded microfluidic chip for SERS detection with simultaneous enhancement of sensitivity and stability, *Biosens. Bioelectron.*, 2024, **261**, 116505, DOI: [10.1016/j.bios.2024.116505](https://doi.org/10.1016/j.bios.2024.116505).
- 121 P. Wen, F. Yang, H. Zhao, Y. Xu, S. Li and L. Chen, Novel Digital SERS-Microfluidic Chip for Rapid and Accurate Quantification of Microorganisms, *Anal. Chem.*, 2024, **96**(4), 1454–1461, DOI: [10.1021/acs.analchem.3c03515](https://doi.org/10.1021/acs.analchem.3c03515).
- 122 Y. Liu, G. Su, W. Wang, H. Wei and L. Dang, A novel multifunctional SERS microfluidic sensor based on ZnO/Ag nanoflower arrays for label-free ultrasensitive detection of bacteria, *Anal. Methods*, 2024, **16**(14), 2085–2092, DOI: [10.1039/d4ay00018h](https://doi.org/10.1039/d4ay00018h).
- 123 L. Shang, P. Liang, L. Xu, Y. Xue, K. Liu and Y. Wang, *et al.*, Stable SERS Detection of *Lactobacillus fermentum* Using Optical Tweezers in a Microfluidic Environment, *Anal. Chem.*, 2023, **96**(1), 248–255, DOI: [10.1021/acs.analchem.3c03852](https://doi.org/10.1021/acs.analchem.3c03852).
- 124 C.-Y. Ku, Y.-W. Chiang, H.-Y. Hsu, H.-W. Cheng, K.-L. Chen and Y.-Y. Han, *et al.*, Air-liquid microfluidics-integrated surface-enhanced Raman spectroscopy for selective molecular adsorption and detection to achieve bacterial discrimination, *Biosens. Bioelectron.*, 2025, **285**, 117576, DOI: [10.1016/j.bios.2025.117576](https://doi.org/10.1016/j.bios.2025.117576).
- 125 M. Feizpour, H. Van den Bosche, L. Melikyan, T. Demuyser, P. Cools and H. Thienpont, *et al.*, Bacterial identification in SERS-integrated microfluidics using CNN-driven 2D classification of 1D spectra, *Talanta*, 2025, **295**, 128325, DOI: [10.1016/j.talanta.2025.128325](https://doi.org/10.1016/j.talanta.2025.128325).
- 126 B. Huo, L. Xia, Y. Hu and G. Li, Flexible microfluidic co-recognition coupled with magnetic enrichment and silent SERS sensing for simultaneous analysis of bacteria in food, *Biosens. Bioelectron.*, 2024, **255**, 116227, DOI: [10.1016/j.bios.2024.116227](https://doi.org/10.1016/j.bios.2024.116227).
- 127 H. Jayan, R. Zhou, Y. Zheng, S. Xue, L. Yin and H. R. El-Seedi, *et al.*, Microfluidic-SERS platform with in-situ nanoparticle synthesis for rapid *E. coli* detection in food, *Food Chem.*, 2025, **471**, 142800, DOI: [10.1016/j.foodchem.2025.142800](https://doi.org/10.1016/j.foodchem.2025.142800).
- 128 R. Ni, K. Ge, Y. Luo, T. Zhu, Z. Hu and M. Li, *et al.*, Highly sensitive microfluidic sensor using integrated optical fiber and real-time single-cell Raman spectroscopy for diagnosis of pancreatic cancer, *Biosens. Bioelectron.*, 2024, **264**, 116616, DOI: [10.1016/j.bios.2024.116616](https://doi.org/10.1016/j.bios.2024.116616).
- 129 Y. Zhuo, Y. Wang, R. Gao, C. Zhan, H. Liu and Y. Liu, *et al.*, Novel simultaneous separation and detection of CTCs and PSA on an integrated multistage microfluidic chip for early diagnosis of prostate cancer, *Microchem. J.*, 2025, **212**, DOI: [10.1016/j.microc.2025.113330](https://doi.org/10.1016/j.microc.2025.113330).
- 130 C. Zhan, R. Gao, Y. Wang, H. Tan, F. Wang and X. Chen, *et al.*, SERS-based microfluidic liquid biopsy of prostate cancer: New bioinspired dual recognition interface for single-cell detection, *Chem. Eng. J.*, 2025, **516**, DOI: [10.1016/j.cej.2025.164059](https://doi.org/10.1016/j.cej.2025.164059).
- 131 E. Ahmed, M. K. Masud, P. Komatineni, S. Dey, R. Lobb and M. S. A. Hossain, *et al.*, A mesoporous gold biosensor to investigate immune checkpoint protein heterogeneity in single lung cancer cells, *Biosens. Bioelectron.*, 2024, **249**, 115984, DOI: [10.1016/j.bios.2023.115984](https://doi.org/10.1016/j.bios.2023.115984).
- 132 A. Hassanzadeh-Barforoushi, A. Tukova, A. Nadalini, D. W. Inglis, S. Chang-Hao Tsao and Y. Wang, Microfluidic-SERS Technologies for CTC: A Perspective on Clinical Translation, *ACS Appl. Mater. Interfaces*, 2024, 22761–22775, DOI: [10.1021/acsami.4c01158](https://doi.org/10.1021/acsami.4c01158).
- 133 Y. Zhou, H. Cong, R. Gao, H. Zhu, Y. Liu and B. Li, *et al.*, A novel triangular nanocolumn array substrate integrated microfluidic chip for prostate cancer CTCs capture and SERS detection, *Microchem. J.*, 2025, **209**, DOI: [10.1016/j.microc.2024.112613](https://doi.org/10.1016/j.microc.2024.112613).
- 134 D. Costa, P. Pereira-Silva, P. Sousa, V. Pinto, J. Borges and F. Vaz, *et al.*, Critical Issues on the Surface Functionalization of Plasmonic Au-Ag/TiO<sub>2</sub> Thin Films with Thiolated Oligonucleotide-Based Biorecognition Elements, *Biosensors*, 2024, **14**(4), 159, DOI: [10.3390/bios14040159](https://doi.org/10.3390/bios14040159).
- 135 A. Foti, D. Montesi, S. Bertone, P. Rivolo, F. Geobaldo and F. Giorgis, *et al.*, Towards a portable setup for the on-site SERS detection of miRNAs, *J. Eur. Opt. Soc. Rapid Publ.*, 2024, **20**(1), DOI: [10.1051/jeos/2024028](https://doi.org/10.1051/jeos/2024028).
- 136 Y. Lu, Y. Yu, Y. Wang, W. Zhou, Z. Cheng and L. Yu, *et al.*, A micro-nano interface integrated SERS-based microfluidic sensor for miRNA detection using DNzyme walker amplification, *Anal. Chim. Acta*, 2023, **1283**, 341957, DOI: [10.1016/j.aca.2023.341957](https://doi.org/10.1016/j.aca.2023.341957).
- 137 X. Lu, D. Zhang, X. Chen, C. Yao and Z. Li, Interfacial Profiling of MicroRNAs at Patterned Nanogaps for an Integrated Microfluidic-SERS Liquid Biopsy, *Anal. Chem.*, 2023, **95**(44), 16049–16053, DOI: [10.1021/acs.analchem.3c02945](https://doi.org/10.1021/acs.analchem.3c02945).
- 138 J. Qian, L. Zhao, Y. Huang, C. Zhao, H. Liu and X. Liu, *et al.*, A microdroplet SERS-RCA biosensor with enhanced specificity and reproducibility for profiling dual miRNAs in idiopathic pulmonary fibrosis diagnosis and monitoring, *Chem. Eng. J.*, 2024, **482**, DOI: [10.1016/j.cej.2024.149012](https://doi.org/10.1016/j.cej.2024.149012).
- 139 K. W. Ng, S. Jaitpal, N. N. Vu, A. M. T. San Juan, S. Tripathy and R. S. Kodam, *et al.*, Lateral Flow Assay for Preeclampsia Screening Using DNA Hairpins and Surface-Enhanced Raman-Active Nanoprobes Targeting hsa-miR-17-5p, *Biosensors*, 2024, **14**(11), 535, DOI: [10.3390/bios14110535](https://doi.org/10.3390/bios14110535).
- 140 Y. Wang, R. Gao, C. Ma, H. Liu, H. Zhu and H. Jin, *et al.*, Dynamically controllable hot spots in DNA-derived hydrogel scaffold SERS substrate for exosome recognition using DNA self-assembly amplification, *Chem. Eng. J.*, 2024, **496**, DOI: [10.1016/j.cej.2024.154270](https://doi.org/10.1016/j.cej.2024.154270).
- 141 Y. Qian, Y. Gu, J. Deng, Z. Cai, Y. Wang and R. Zhou, *et al.*, Combined SERS Microfluidic Chip with Gold Nanocone Array for Effective Early Lung Cancer Prognosis in Mice

- Model, *Int. J. Nanomed.*, 2023, **18**, 3429–3442, DOI: [10.2147/ijn.S411395](https://doi.org/10.2147/ijn.S411395).
- 142 L. Wu, X. Liu, Y. Zhang, Z. Yang, L. Chen and S. Zong, *et al.*, A hand-powered SERS-microfluidic chip for circulating tumor DNA detection from whole blood, *Sens. Actuators, B*, 2024, **401**, DOI: [10.1016/j.snb.2023.135081](https://doi.org/10.1016/j.snb.2023.135081).
- 143 Y. Su, X. Wu, X. Sun, Q. Hu, J. Jiao and J. Ma, *et al.*, Droplet Digital Enzymatic Recycling for Single-Molecule Homogeneous Immunoassay, *Small*, 2025, **21**(35), e2503786, DOI: [10.1002/smll.202503786](https://doi.org/10.1002/smll.202503786).
- 144 X. Wang, J. Wang and S. Xu, Single-cell immunoassay of breast cancers based on their exosomal receptor expression profiles, *Chem. Eng. J.*, 2025, **506**, DOI: [10.1016/j.cej.2025.159904](https://doi.org/10.1016/j.cej.2025.159904).
- 145 Q. Zhou, X. Niu, Z. Zhang, K. O'Byrne, A. Kulasinghe and D. Fielding, *et al.*, Glycan Profiling in Small Extracellular Vesicles with a SERS Microfluidic Biosensor Identifies Early Malignant Development in Lung Cancer. Advanced, *Science*, 2024, **11**(33), e2401818, DOI: [10.1002/adv.202401818](https://doi.org/10.1002/adv.202401818).
- 146 W. Lin, L. Yuan, Z. Gao, G. Cai, C. Liang and M. Fan, *et al.*, An integrated sample-to-answer SERS platform for multiplex phenotyping of extracellular vesicles, *Sens. Actuators, B*, 2023, **394**, DOI: [10.1016/j.snb.2023.134355](https://doi.org/10.1016/j.snb.2023.134355).
- 147 H. Chen, H. Liu, L. Xing, D. Fan, N. Chen and P. Ma, *et al.*, Deep Learning-driven Microfluidic-SERS to Characterize the Heterogeneity in Exosomes for Classifying Non-Small Cell Lung Cancer Subtypes, *ACS Sens.*, 2025, **10**(4), 2872–2882, DOI: [10.1021/acssensors.4c03621](https://doi.org/10.1021/acssensors.4c03621).
- 148 Y. Jin, J. Zhang, X. Wu, C. Qu, X. Fang and Y. Yang, *et al.*, Microfluidics-based label-free SERS profiling of exosomes with machine learning for osteosarcoma diagnosis, *Talanta*, 2025, **294**, 128276, DOI: [10.1016/j.talanta.2025.128276](https://doi.org/10.1016/j.talanta.2025.128276).
- 149 H. Jia, W. Meng, R. Gao, Y. Wang, C. Zhan and Y. Yu, *et al.*, Integrated SERS-Microfluidic Sensor Based on Nano-Micro Hierarchical Cactus-like Array Substrates for the Early Diagnosis of Prostate Cancer, *Biosensors*, 2024, **14**(12), 579, DOI: [10.3390/bios14120579](https://doi.org/10.3390/bios14120579).
- 150 W. Dong, R. Fu, N. Zhang, J. Zhao, Y. Ma and H. Cui, *et al.*, Digital microfluidics with integrated Raman sensor for high-sensitivity in-situ bioanalysis, *Biosens. Bioelectron.*, 2025, **271**, 117036, DOI: [10.1016/j.bios.2024.117036](https://doi.org/10.1016/j.bios.2024.117036).
- 151 X. Chen, J. Tang, Y. Zhao, R. Wang, S. Sang and F. Yu, *et al.*, Sensitive phenotyping of serum extracellular vesicles on a SERS-microfluidic platform for early-stage clinical diagnosis of ovarian carcinoma, *Biosens. Bioelectron.*, 2025, **267**, 116724, DOI: [10.1016/j.bios.2024.116724](https://doi.org/10.1016/j.bios.2024.116724).
- 152 K. H. W. Ho, H. Lai, R. Zhang, H. Chen, W. Yin and X. Yan, *et al.*, SERS-Based Droplet Microfluidic Platform for Sensitive and High-Throughput Detection of Cancer Exosomes, *ACS Sens.*, 2024, **9**(9), 4860–4869, DOI: [10.1021/acssensors.4c01357](https://doi.org/10.1021/acssensors.4c01357).
- 153 M. Niihori, T. Földes, C. A. Readman, R. Arul, D. B. Grys and B. Nijs, *et al.*, SERS Sensing of Dopamine with Fe(III)-Sensitized Nanogaps in Recleanable AuNP Monolayer Films, *Small*, 2023, **19**(48), e2302531, DOI: [10.1002/smll.202302531](https://doi.org/10.1002/smll.202302531).
- 154 X. Xue, J. Yang, L. Xia and G. Li, Microfluidic-assisted synthesis of AuNPs/MoS<sub>2</sub> substrate for surface-enhanced Raman scattering detection of adenine and cytosine in chicken, *Spectrochim. Acta, Part A*, 2025, **338**, 126161, DOI: [10.1016/j.saa.2025.126161](https://doi.org/10.1016/j.saa.2025.126161).
- 155 L. Cong, X. Wang, J. Wang, W. Liu, W. Xu and S. Zhang, *et al.*, Three-Dimensional SERS-Active Hydrogel Microbeads Enable Highly Sensitive Homogeneous Phase Detection of Alkaline Phosphatase in Biosystems, *ACS Appl. Mater. Interfaces*, 2025, **17**(4), 5933–5941, DOI: [10.1021/acsaami.4c18139](https://doi.org/10.1021/acsaami.4c18139).
- 156 K. Maleeva, D. Dadadzhyanov, A. Palekhova, I. Kaliya, A. Tkach and A. Baranov, *et al.*, SERS substrates based on polymer-protected self-assembled plasmonic films with gold nanoparticles as enhancing element of a microfluidic sensor, *Opt. Mater.*, 2023, **146**, DOI: [10.1016/j.optmat.2023.114581](https://doi.org/10.1016/j.optmat.2023.114581).
- 157 J. Plou, P. S. Valera, I. García, D. Vila-Liarte, C. Renero-Lecuna and J. Ruiz-Cabello, *et al.*, Machine Learning-Assisted High-Throughput SERS Classification of Cell Secretomes, *Small*, 2023, **19**(51), e2207658, DOI: [10.1002/smll.202207658](https://doi.org/10.1002/smll.202207658).
- 158 Z. Zhang, Q. Dong, M. Xu, K. Yang and Z. Wang, An ultrasensitive SERS sensing chip for the serum screening of psychiatric disorders, *J. Mater. Chem. C*, 2024, **12**(4), 1485–1491, DOI: [10.1039/d3tc03688j](https://doi.org/10.1039/d3tc03688j).
- 159 J. Yoon, D.-H. Kim, S.-G. Park and S.-H. Kim, Micromolding-Assisted Production of SERS-Active Microcylinders for Size- and Charge-Selective Molecular Detection, *ACS Appl. Mater. Interfaces*, 2023, **15**(49), 57556–57568, DOI: [10.1021/acsaami.3c11627](https://doi.org/10.1021/acsaami.3c11627).
- 160 K. Yao, X. Xie, J. Jiao, A. Liu and Y. Huang, Plasmonic cellulose microfilament assisted SERS detection in microfluidics, *Spectrochim. Acta, Part A*, 2024, **308**, 123631, DOI: [10.1016/j.saa.2023.123631](https://doi.org/10.1016/j.saa.2023.123631).
- 161 F. Toffanello, F. Cardoni, A. Mercedi, T. Marchetti, A. Meggiolaro and D. Filippi, *et al.*, Microfluidics integrated with inkjet-printed SERS substrate for in-operando reaction kinetic monitoring, *Sens. Actuators, B*, 2025, **440**, DOI: [10.1016/j.snb.2025.137950](https://doi.org/10.1016/j.snb.2025.137950).
- 162 B. Zou, S. Lou, J. Duan, S. Zhou and Y. Wang, Design of Raman reporter-embedded magnetic/plasmonic hybrid nanostirrers for reliable microfluidic SERS biosensors, *Nanoscale*, 2023, **15**(18), 8424–8431, DOI: [10.1039/d3nr00303e](https://doi.org/10.1039/d3nr00303e).
- 163 Y. Hu, Y. Zhou, G. Luo, D. Li and M. Qu, Femtosecond laser-induced nanoparticle implantation into flexible substrate for sensitive and reusable microfluidics SERS detection, *Int. J. Extreme Manuf.*, 2024, **6**(4), DOI: [10.1088/2631-7990/ad48e9](https://doi.org/10.1088/2631-7990/ad48e9).
- 164 M. Lafuente, F. Almazán, E. Bernad, I. Florea, R. Arenal and M. A. Urbiztondo, *et al.*, On-chip monitoring of toxic gases: capture and label-free SERS detection with plasmonic mesoporous sorbents, *Lab Chip*, 2023, **23**(14), 3160–3171, DOI: [10.1039/d3lc00136a](https://doi.org/10.1039/d3lc00136a).
- 165 Y. Lu, X. Yuan, C. Jia, B. Lei, H. Zhang and Z. Zhao, *et al.*, Self-Assembled Bifunctional Copper Hydroxide/Gold-Ordered Nanoarray Composites for Fast, Sensitive, and Recyclable SERS Detection of Hazardous Benzene Vapors,

- Nanomaterials*, 2023, 13(13), 2016, DOI: [10.3390/nano13132016](https://doi.org/10.3390/nano13132016).
- 166 N. La Tran Ngoc, D. Van Hoang, A. Tuan Thanh Pham, N. Tran Truc Phuong, N. Xuan Dat Mai and T. T. K. Chi, *et al.*, Novel composites of nano-metal–organic frameworks (IRMOF-3) and silver nanoparticles for the ultra-sensitive performance of SERS sensing and optical fiber modes, *J. Sci.: Adv. Mater. Devic*, 2023, 8(3), DOI: [10.1016/j.jsamd.2023.100584](https://doi.org/10.1016/j.jsamd.2023.100584).
- 167 S. Xiong, C. Zhu, C. Wang, P. Dong and X. Wu, SERS-based pump-free microfluidic chip sensor for highly sensitive competitive immunoassay of cortisol in human sweat, *Lab Chip*, 2024, 24(24), 5384–5397, DOI: [10.1039/d4lc00858h](https://doi.org/10.1039/d4lc00858h).
- 168 F. Yao, J. Wang, W. Zhang, Z. Wang, Y. Li and H. Sun, *et al.*, A microfluidic platform for minute-scale synthesizing Au@Ag nanocubes. *Materials Today, Chemistry*, 2023, 34, DOI: [10.1016/j.mtchem.2023.101825](https://doi.org/10.1016/j.mtchem.2023.101825).
- 169 J. Xiao, J. Wang, Y. Luo, T. Xu and X. Zhang, Wearable Plasmonic Sweat Biosensor for Acetaminophen Drug Monitoring, *ACS Sens.*, 2023, 8(4), 1766–1773, DOI: [10.1021/acssensors.3c00063](https://doi.org/10.1021/acssensors.3c00063).
- 170 L. Seriola, G. Soufi, G. Zappalà, R. Slipets, T. Rindzevicius and K. Zor, *et al.*, Compact SERS detection system enabling automated assay on disc combined with advanced data analysis – A case study of methotrexate, *Sens. Actuators, B*, 2024, 419, DOI: [10.1016/j.snb.2024.136375](https://doi.org/10.1016/j.snb.2024.136375).
- 171 G. Soufi, I. Badillo-Ramírez, L. Seriola, R. Altaf Raja, K. Schmiegelow and K. Zor, *et al.*, Solid-phase extraction coupled to automated centrifugal microfluidics SERS: Improving quantification of therapeutic drugs in human serum, *Biosens. Bioelectron.*, 2024, 266, 116725, DOI: [10.1016/j.bios.2024.116725](https://doi.org/10.1016/j.bios.2024.116725).
- 172 T. K. Naqvi, A. Bajpai, S. Dwivedi, M. Bhaiyya, S. Goel and P. K. Dwivedi, Flexible, label free and low-cost paper based microfluidic SERS substrates for thiram detection, *Sens. Actuators, A*, 2023, 356, DOI: [10.1016/j.sna.2023.114341](https://doi.org/10.1016/j.sna.2023.114341).
- 173 S. Fehse, A. Das and D. Belder, Integration of a recyclable silver substrate for in situ surface-enhanced Raman spectroscopy in digital microfluidics, *Chem. Commun.*, 2024, 60(63), 8252–8255, DOI: [10.1039/d4cc01552e](https://doi.org/10.1039/d4cc01552e).
- 174 J. Chen, S. Li, F. Yao, W. Xu, Y. Li and Q. Chen, *et al.*, Rapid Fabrication of Homogeneous Submicron Silver Particles via a Microfluidic Chip and Use as a SERS Detection Substrate, *Chem*, 2023, 11(4), DOI: [10.3390/chemosensors11040232](https://doi.org/10.3390/chemosensors11040232).
- 175 S. Yan, Z. Zhang, J. Chen, Q. Wang, Y. Wu and Y. Sui, *et al.*, Cavity-Like Silver Aggregates-Based Colloidal SERS Microfluidic Platform for Highly Reproducible Online Reaction Process Analysis, *Small*, 2025, 21(30), e2501338, DOI: [10.1002/smll.202501338](https://doi.org/10.1002/smll.202501338).
- 176 H. Li, R. Chu, J. Cao, F. Zhou, K. Guo and Q. Zhang, *et al.*, Sensitive and reproducible on-chip SERS detection by side-polished fiber probes integrated with microfluidic chips, *Measurement*, 2023, 218, DOI: [10.1016/j.measurement.2023.113203](https://doi.org/10.1016/j.measurement.2023.113203).
- 177 W. Peng, C. Yi, L. Wang, Y. Zhang and Q. Liao, 3D Porous Silicon Carbide SERS Microfluidic Chip for Pesticide Residue Detection, *ACS Agric. Sci. Technol.*, 2024, 4(8), 818–826, DOI: [10.1021/acscagritech.4c00153](https://doi.org/10.1021/acscagritech.4c00153).
- 178 T. Zhang, Y. Yang, Y. Zhou, Y. Lu, M. Zhang and P. Liu, *et al.*, Microfluidic SERS chip for quantitative detection of weak surficial affinity molecules, *Appl. Surf. Sci.*, 2024, 654, DOI: [10.1016/j.apsusc.2024.159476](https://doi.org/10.1016/j.apsusc.2024.159476).
- 179 Z. Qian, Z. Wang, K. Zhu, K. Yang, L. Wu and S. Zong, *et al.*, A SERS-assisted 3D organotypic microfluidic chip for in-situ visualization and monitoring breast cancer extravasation process, *Talanta*, 2024, 270, 125633, DOI: [10.1016/j.talanta.2024.125633](https://doi.org/10.1016/j.talanta.2024.125633).
- 180 J. Sun, R. Wang, L. Wang, X. Wang, J. Wang and Z. Shi, *et al.*, Visual/quantitative SERS biosensing chip based on Au-decorated polystyrene sphere microcavity arrays, *Sens. Actuators, B*, 2023, 388, DOI: [10.1016/j.snb.2023.133869](https://doi.org/10.1016/j.snb.2023.133869).
- 181 X. Wang, J. Wang and S. Xu, Microdroplet-SERS platform for single cell-secreted VEGF and extracellular pH analysis in oxidative stress event, *Sens. Actuators, B*, 2025, 422, DOI: [10.1016/j.snb.2024.136545](https://doi.org/10.1016/j.snb.2024.136545).
- 182 W. Yuan, H. Yuan, R. Li, R. Yong, I. Mitrovic and E. G. Lim, *et al.*, A SERS nanocellulose-paper-based analytical device for ultrasensitive detection of Alzheimer's disease, *Anal. Chim. Acta*, 2024, 1301, 342447, DOI: [10.1016/j.aca.2024.342447](https://doi.org/10.1016/j.aca.2024.342447).
- 183 J. Sun, Z. Shi, L. Wang, X. Zhang, C. Luo and J. Hua, *et al.*, Construction of a microcavity-based microfluidic chip with simultaneous SERS quantification of dual biomarkers for early diagnosis of Alzheimer's disease, *Talanta*, 2023, 261, 124677, DOI: [10.1016/j.talanta.2023.124677](https://doi.org/10.1016/j.talanta.2023.124677).
- 184 A. Jaiswal, S. Mishra, P. K. Dwivedi and S. Verma, SERS-Based Microfluidic Bioscreening Platform for Selective Detection of  $\beta$ -Amyloid Peptides, *Langmuir*, 2024, 40(46), 24463–24470, DOI: [10.1021/acs.langmuir.4c03042](https://doi.org/10.1021/acs.langmuir.4c03042).
- 185 X. Liu, J. Wang, W. Zhang, Z. Ding, J. Gu and Y. Wang, *et al.*, In-situ SERS monitoring of membrane receptor PTK7 for assessing cancer cell migration at single-cell level on a microfluidic chip, *Sens. Actuators, B*, 2024, 404, DOI: [10.1016/j.snb.2024.135298](https://doi.org/10.1016/j.snb.2024.135298).
- 186 K. Shen, D. Zhang, H. Yin, B. Lu, Z. Hua and M. Tan, *et al.*, A magnetically embedded pump-free LoC-SERS device based on enzyme-mediated cascade reaction for gastric cancer-related D-amino acids detection, *Sens. Actuators, B*, 2024, 409, DOI: [10.1016/j.snb.2024.135615](https://doi.org/10.1016/j.snb.2024.135615).
- 187 M. Wang, H. Wan, Y. Wang, H. Yuan, Q. Ni and B. Sun, *et al.*, A Microfluidics-Based Multiplex SERS Immunoassay Device for Analysis of Acute Ischemic Stroke Biomarkers, *Transl. Stroke Res.*, 2023, 16(2), 217–226, DOI: [10.1007/s12975-023-01204-x](https://doi.org/10.1007/s12975-023-01204-x).
- 188 D. Zhang, K. Peng, H. Xu, Y. Chen and J. Wang, Proteomics-Empowered Microfluidic-SERS Immunoassay for Identifying and Detecting Biomarkers of Micropapillary Lung Adenocarcinoma. *Advanced, Science*, 2025, 12(25), DOI: [10.1002/advs.202501336](https://doi.org/10.1002/advs.202501336).
- 189 K. Yang, J. Zhao, Y. Huang, H. Sheng and Z. Wang, Combining array-assisted SERS microfluidic chips and machine learning algorithms for clinical leukemia

- phenotyping, *Talanta*, 2025, **283**, 127148, DOI: [10.1016/j.talanta.2024.127148](https://doi.org/10.1016/j.talanta.2024.127148).
- 190 J. Zhang, L. Xu, Y. Hu, L. Sun, Y. Xie and X. Miao, *et al.*, Integrating Inertial Microfluidics with SERS Bioprobe for Efficient Enrichment and Accurate Identification of Tumor Cells in Gastric Fluid and Ascites, *Anal. Chem.*, 2025, **97**(26), 13901–13911, DOI: [10.1021/acs.analchem.5c01428](https://doi.org/10.1021/acs.analchem.5c01428).
- 191 M.-C. Lien, I. H. Yeh, Y.-C. Lu and K.-K. Liu, Plasmonic nanomaterials-based flexible strips for the SERS detection of gouty arthritis, *Analyst*, 2023, **148**(17), 4109–4115, DOI: [10.1039/d3an01130e](https://doi.org/10.1039/d3an01130e).
- 192 W. Wang, W. Mao, H. Sun, F. Hou, W. Wang and W. Liu, *et al.*, Microfluidic SERS biosensor based on Au-semicoated photonic crystals for melanoma diagnosis, *Biosens. Bioelectron.*, 2025, **271**, 116983, DOI: [10.1016/j.bios.2024.116983](https://doi.org/10.1016/j.bios.2024.116983).
- 193 J. W. Jeon, J. W. Choi, Y. Shin, T. Kang and B. G. Chung, Machine learning-integrated droplet microfluidic system for accurate quantification and classification of microplastics, *Water Res.*, 2025, **274**, 123161, DOI: [10.1016/j.watres.2025.123161](https://doi.org/10.1016/j.watres.2025.123161).
- 194 X. Wang, Z. Guo, D. Zhang, Y. Yan, Y. Yu and B. Du, *et al.*, Integrating liquid chromatography-electrochemical detection-surface Enhanced Raman Spectroscopy on microfluidic chip for phenylurea herbicides analysis, *Sens. Actuators, B*, 2024, **407**, DOI: [10.1016/j.snb.2024.135436](https://doi.org/10.1016/j.snb.2024.135436).
- 195 C. Li, X. Fang, H. Li and X. Zhang, Direct and Rapid Sensing of Per- and Polyfluoroalkyl Substances Using SERS-Active Optical Fibers, *ACS Appl. Opt. Mater.*, 2024, **2**(4), 610–616, DOI: [10.1021/acsaom.4c00023](https://doi.org/10.1021/acsaom.4c00023).
- 196 Y. Yu, R. Gao, C. Zhan, Y. Wang, W. Zhou and X. Chen, *et al.*, Multi-dimensional synergistically coupled signal enhancement on nano-micro hierarchical anemone-like substrates integrated SERS-based microfluidic sensor, *Sens. Actuators, B*, 2024, **417**, DOI: [10.1016/j.snb.2024.136176](https://doi.org/10.1016/j.snb.2024.136176).
- 197 S. Li, J. Chen, W. Xu, B. Sun, J. Wu and Q. Chen, *et al.*, Highly homogeneous bimetallic core-shell Au@Ag nanoparticles with embedded internal standard fabrication using a microreactor for reliable quantitative SERS detection, *Mater. Chem. Front.*, 2023, **7**(6), 1100–1109, DOI: [10.1039/d2qm01202b](https://doi.org/10.1039/d2qm01202b).
- 198 M. Sharipov, T. J. Ju, S. Azizov, A. Turaev and Y.-I. Lee, Novel molecularly imprinted nanogel modified microfluidic paper-based SERS substrate for simultaneous detection of bisphenol A and bisphenol S traces in plastics, *J. Hazard. Mater.*, 2024, **461**, 132561, DOI: [10.1016/j.jhazmat.2023.132561](https://doi.org/10.1016/j.jhazmat.2023.132561).
- 199 Q. Ke, L. Yin, H. Jayan, H. R. El-Seedi, X. Zou and Z. Guo, Ag-coated tetrapod gold nanostars(Au@AgNSs) for acetamiprid determination in tea using SERS combined with microfluidics, *Anal. Methods*, 2024, **16**(17), 2721–2731, DOI: [10.1039/d4ay00297k](https://doi.org/10.1039/d4ay00297k).
- 200 X. Wang, S. Shen, N. Sun, Y. Zhu and J. Zhang, Neural Network-Assisted Dual-Functional Hydrogel-Based Microfluidic SERS Sensing for Divisional Recognition of Multimolecule Fingerprint, *ACS Sens.*, 2025, **10**(2), 1197–1205, DOI: [10.1021/acssensors.4c03096](https://doi.org/10.1021/acssensors.4c03096).
- 201 G. Zappalà, G. Soufi, E. Dumont, N. Molander, R. Slipets and L. H. E. Thamdrup, *et al.*, SERS-integrated centrifugal microfluidic platform for the detection and quantification of Chemical Warfare Agents in single-component solution and mixtures, *Sens. Actuators, B*, 2025, **422**, DOI: [10.1016/j.snb.2024.136698](https://doi.org/10.1016/j.snb.2024.136698).
- 202 Z. Wang, W. Liu, J. Wang, L. Huang, S. Cui and X. He, Structure-controllable Ag aerogel optimized SERS-digital microfluidic platform for ultrasensitive and high-throughput detection of harmful substances, *Sens. Actuators, B*, 2024, **401**, DOI: [10.1016/j.snb.2023.134934](https://doi.org/10.1016/j.snb.2023.134934).
- 203 W. Liu, Z. Wang, Z. Liu, J. Chen, L. Shi and L. Huang, *et al.*, Utilizing an Automated SERS-Digital Microfluidic System for High-Throughput Detection of Explosives, *ACS Sens.*, 2023, **8**(4), 1733–1741, DOI: [10.1021/acssensors.3c00012](https://doi.org/10.1021/acssensors.3c00012).
- 204 C. Credi, C. Dallari, S. Nocentini, G. Gatta, E. Bianchi and D. S. Wiersma, *et al.*, Fiber-Based SERS-Fluidic Polymeric Platforms for Improved Optical Analysis of Liquids, *Bioengineering*, 2023, **10**(6), 676, DOI: [10.3390/bioengineering10060676](https://doi.org/10.3390/bioengineering10060676).
- 205 Y. Wang, B. Lai, Z. Yu and Z. Xu, One-step fabrication of a self-driven point-of-care chip by femtosecond laser direct writing and its application in cancer cell H2O2 detection via semiconductor-based SERS, *Talanta*, 2024, **278**, 126483, DOI: [10.1016/j.talanta.2024.126483](https://doi.org/10.1016/j.talanta.2024.126483).
- 206 J. Xiao, S. Zhang, Q. Liu, T. Xu and X. Zhang, Microfluidic-based plasmonic microneedle biosensor for uric acid ultrasensitive monitoring, *Sens. Actuators, B*, 2024, **398**, DOI: [10.1016/j.snb.2023.134685](https://doi.org/10.1016/j.snb.2023.134685).
- 207 M. Hu, K. Zhu, J. Wei, K. Yang, L. Wu and S. Zong, *et al.*, Silk fibroin-based wearable SERS biosensor for simultaneous sweat monitoring of creatinine and uric acid, *Biosens. Bioelectron.*, 2024, **265**, 116662, DOI: [10.1016/j.bios.2024.116662](https://doi.org/10.1016/j.bios.2024.116662).
- 208 S. Xiong, C. Wang, C. Zhu, P. Dong and X. Wu, Dual Detection of Urea and Glucose in Sweat Using a Portable Microfluidic SERS Sensor with Silver Nano-Tripods and 1D-CNN Model Analysis, *ACS Appl. Mater. Interfaces*, 2024, **16**(48), 65918–65926, DOI: [10.1021/acsaomi.4c14962](https://doi.org/10.1021/acsaomi.4c14962).
- 209 M. Hu, K. Zhu, J. Wei, Z. Xu, K. Yang and L. Wu, *et al.*, Wearable microfluidic SERS patch based on silk fibroin for the non-invasive monitoring of sweat cortisol and pH, *Sens. Actuators, B*, 2025, **427**, DOI: [10.1016/j.snb.2024.137152](https://doi.org/10.1016/j.snb.2024.137152).
- 210 S. F. Pan, X. D. Tian, Y. Lu, Y. Q. Liao, M. Q. Liu and L. Y. Meng, *et al.*, Wearable SERS-Microfluidic Patch for Real-Time in Situ Monitoring of Chiral Metabolites in Sweat, *Small*, 2025, **21**(24), e2500770, DOI: [10.1002/smll.202500770](https://doi.org/10.1002/smll.202500770).
- 211 Q. Yuan, H. Fang, X. Wu, J. Wu, X. Luo and R. Peng, *et al.*, Self-Adhesive, Biocompatible, Wearable Microfluidics with Erasable Liquid Metal Plasmonic Hotspots for Glucose Detection in Sweat, *ACS Appl. Mater. Interfaces*, 2023, **16**(49), 66810–66818, DOI: [10.1021/acsaomi.3c11746](https://doi.org/10.1021/acsaomi.3c11746).
- 212 K. Yang, Z. Wang, K. Zhu, Y. Zhao, L. Wu and S. Zong, *et al.*, A wearable SERS-microfluidic patch for continuous monitoring of kidney health-related biomarkers in sweat, *Talanta*, 2025, **293**, 128039, DOI: [10.1016/j.talanta.2025.128039](https://doi.org/10.1016/j.talanta.2025.128039).

- 213 Y. Li, Y. Guo, H. Chen, X. Xiao, F. Long and H. Zhong, *et al.*, Flexible Wearable Plasmonic Paper-Based Microfluidics with Expandable Channel and Adjustable Flow Rate for Portable Surface-Enhanced Raman Scattering Sweat Sensing, *ACS Photonics*, 2024, **11**(2), 613–625, DOI: [10.1021/acsp Photonics.3c01490](https://doi.org/10.1021/acsp Photonics.3c01490).
- 214 S. Xiong, C. Wang, T. Wang, C. Zhu, P. Dong and X. Wu, Label-free detection of sweat biomarkers using AuNRAs-based SERS-digital microfluidic sensor, *Chem. Eng. J.*, 2025, **510**, DOI: [10.1016/j.ccej.2025.161849](https://doi.org/10.1016/j.ccej.2025.161849).
- 215 Z. Ye, H. Huang, F. Xu, P. Lu, Y. Chen and J. Shen, *et al.*, Thermal Annealing Effect on Surface-Enhanced Raman Scattering of Gold Films Deposited on Liquid Substrates, *Molecules*, 2023, **28**(3), 1472, DOI: [10.3390/molecules28031472](https://doi.org/10.3390/molecules28031472).
- 216 S. Abbasi, Q. Liu, D. Rosseel, H. Thienpont and H. Ottevaere, Enabling rapid parallel SERS detection with integrated microlens array. Sensing and Bio-Sensing, *Research*, 2025, **48**, DOI: [10.1016/j.sbsr.2025.100808](https://doi.org/10.1016/j.sbsr.2025.100808).
- 217 K. Ko, H. Yoo, S. Han, W. S. Chang and D. Kim, Surface-enhanced Raman spectroscopy with single cell manipulation by microfluidic dielectrophoresis, *Analyst*, 2024, **149**(23), 5649–5656, DOI: [10.1039/d4an00983e](https://doi.org/10.1039/d4an00983e).
- 218 M. Lu, Y. Joung, C. S. Jeon, S. Kim, D. Yong and H. Jang, *et al.*, Dual-mode SERS-based lateral flow assay strips for simultaneous diagnosis of SARS-CoV-2 and influenza a virus, *Nano Convergence.*, 2022, **9**(1), 39, DOI: [10.1186/s40580-022-00330-w](https://doi.org/10.1186/s40580-022-00330-w).
- 219 Y. Joung, K. Kim, S. Lee, B.-S. Chun, S. Lee and J. Hwang, *et al.*, Rapid and Accurate On-Site Immunodiagnoses of Highly Contagious Severe Acute Respiratory Syndrome Coronavirus 2 Using Portable Surface-Enhanced Raman Scattering-Lateral Flow Assay Reader, *ACS Sens.*, 2022, **7**(11), 3470–3480, DOI: [10.1021/acssensors.2c01808](https://doi.org/10.1021/acssensors.2c01808).